

University of Groningen

Eye movement behaviour of patients with visual field defects

Gestefeld, Birte

DOI:
[10.33612/diss.190470605](https://doi.org/10.33612/diss.190470605)

IMPORTANT NOTE: You are advised to consult the publisher's version (publisher's PDF) if you wish to cite from it. Please check the document version below.

Document Version
Publisher's PDF, also known as Version of record

Publication date:
2021

[Link to publication in University of Groningen/UMCG research database](#)

Citation for published version (APA):
Gestefeld, B. (2021). *Eye movement behaviour of patients with visual field defects*. University of Groningen. <https://doi.org/10.33612/diss.190470605>

Copyright

Other than for strictly personal use, it is not permitted to download or to forward/distribute the text or part of it without the consent of the author(s) and/or copyright holder(s), unless the work is under an open content license (like Creative Commons).

The publication may also be distributed here under the terms of Article 25fa of the Dutch Copyright Act, indicated by the "Taverne" license. More information can be found on the University of Groningen website: <https://www.rug.nl/library/open-access/self-archiving-pure/taverne-amendment>.

Take-down policy

If you believe that this document breaches copyright please contact us providing details, and we will remove access to the work immediately and investigate your claim.

Downloaded from the University of Groningen/UMCG research database (Pure): <http://www.rug.nl/research/portal>. For technical reasons the number of authors shown on this cover page is limited to 10 maximum.

Eye movement behaviour of patients with visual field defects

Birte Gestefeld

The research described in this thesis was supported by the European Union's Horizon 2020 research and innovation program under the Marie Skłodowska Curie grant agreement No 661883 (EGRET), the Laboratory of Experimental Ophthalmology, the University Groningen (RUG) and the Graduate School of Medical Sciences (GSMS).

Financial support for the publication of this thesis was kindly provided by the University of Groningen, BCN, GSMS and the Professor Mulder Stichting.



Manuscript:

Layout and cover: Birte Gestefeld
Cover image: gettyimages / Saul Herrera
Printed by: Proefschriftmaken
ISBN: 978-94-6423-475-6

Copyright © 2021 by Birte Gestefeld



university of
 groningen

Eye movement behaviour of patients with visual field defects

PhD thesis

to obtain the degree of PhD at the
 University of Groningen
 on the authority of the
 Rector Magnificus Prof. C. Wijmenga
 and in accordance with
 the decision by the College of Deans.

This thesis will be defended in public on

Wednesday 10 November 2021 at 11.00 hours

by

Birte Frederike Gestefeld

born on 10 December 1988
 in Bremen, Germany

Supervisors

Prof. F.W. Cornelissen
Prof. N.M. Jansonius

Co-supervisor

Dr. J.B.C. Marsman

Assessment Committee

Prof. J.H.C. Heutink
Prof. P. König
Prof. D. Crabb

Contents

1	Introduction	7
1.1	Thesis outline	10
1.2	Background	11
2	Using natural viewing behavior to screen for and reconstruct visual field defects	25
2.1	Abstract	26
2.2	Introduction	27
2.3	Methods	30
2.4	Results	38
2.5	Discussion	46
2.6	Supplementary Material	55
3	How free-viewing eye movements can be used to detect the presence of visual field defects in glaucoma patients	59
3.1	Abstract	60
3.2	Introduction	61
3.3	Experiment 1: Monocular eye movements under free-viewing conditions of glaucoma patients compared to those of normal sighted observers . .	65
3.4	Methods	65
3.5	Results	74
3.6	Experiment 2: binocular eye movements under free-viewing conditions of glaucoma patients compared to those of normal sighted observers . .	86
3.7	Methods	86

3.8	Results	91
3.9	Discussion	99
3.10	Supplementary Material	112
4	Eye tracking and virtual reality in the rehabilitation of mobility of hemi-anopia patients: a user experience study	115
4.1	Abstract	116
4.2	Introduction	117
4.3	Methods	119
4.4	Results	129
4.5	Discussion	137
4.6	Supplementary Material	143
5	General Discussion	145
5.1	Summary of the results	146
5.2	Discussion	148
5.3	Clinical applications	153
6	Thesis Summary	157
7	Samenvatting	159
8	Zusammenfassung	161
9	Acknowledgements	163

1

Introduction

We can see sharply only in the center of the visual field. To see details in our environment, we therefore need to continuously move our eyes so we can sample detailed information from different locations. These details are then integrated by our brain, which enables us to perceive our environment in a seemingly sharp and detailed way. Functional peripheral vision is necessary to guide our attention so we can turn our gaze towards relevant parts of our environment. To illustrate this process, consider the example of someone who wants to cross a road. When they perceive motion in the periphery of their visual field, they direct their gaze towards this area and see an approaching car. However, if their peripheral vision is impaired, they do not notice the approaching car until it is close to them, which can lead to dangerous situations.

Impaired vision in parts of the visual field, known more generally as visual field defects (VFD), leads to many problems with activities of daily living, and the risk of developing a VFD increases with age. There are many causes of damage in parts of the visual field. In the research reported in this thesis, I have focused on two very common causes: glaucoma and homonymous hemianopia (HH). Glaucoma is a neurodegenerative disease which usually starts with impaired peripheral vision. If left untreated, the VFD will increase and ultimately lead to blindness. HH is the loss of half of the visual field due to damage to the visual cortex caused by stroke or trauma.

The mentioned example of crossing a road shows that problems with activities of daily living in patients with VFD can be associated with their eye movements. Eye movements can fulfill two purposes in this context. Firstly, if the movements deviate from normal behaviour they can indicate the presence of a VFD. Secondly, eye movements can help patients with VFD cope with their visual defect and maintain a high quality of life. In the research reported here, I therefore focused on two main topics: using eye movements to screen for VFD in glaucoma and HH, and using eye tracking and virtual reality (VR) in vision rehabilitation therapy.

The current gold standard method to assess the state of the visual field is standard automated perimetry (SAP), where the subject sits with their head fixed in front of a hemispherical screen in which dots of different luminance intensities are displayed. The subject is then asked to press a button every time that they perceive a stimulus. During the test period they have to fix their gaze on a small spot at the center of the stimulus display. As this test requires a strong focus on the task at hand, it is difficult to perform,

especially for children and elderly people. In addition, it also has to be administered by trained medical personnel, which means that screening for VFD takes up a lot of time and resources at eye clinics. With a growing elderly population, which is at a high risk of developing a VFD and therefore needs regular screening, eye clinics will face a massive workload over the coming decades. If we could use eye movement behaviour, during a simple everyday life task such as watching videos to detect differences between patients with VFD and normal-sighted controls, this method could be used to screen for VFD. Such a method would be easier to administer, so it could be used outside specialized eye clinics, and it would also be more intuitive for the test subject. This would allow it to be used for testing groups, such as the very young and very old, who have difficulty completing the current perimetry test.

A major problem when dealing with glaucoma and HH is that the resulting VFD cannot be reversed. Currently, the only option to improve the quality of life of these patients is vision rehabilitation therapy, where they learn compensatory eye movement strategies for their VFD in various scenarios. In the research reported in my thesis, I focused on vision rehabilitation therapy for mobility-related tasks.

One of the shortcomings in the current approach is the lack of objective measurements of eye movements during the rehabilitation training. In addition, certain steps in the training procedure are too abrupt for some patients, and certain scenarios, like crossing a street, need to be practiced in a safer and more controlled way. If we could measure eye movements during vision rehabilitation and introduce a step in between very simple and very complex tasks that can be performed in a safe and controllable environment, we could improve the quality of vision rehabilitation training.

The first aim in my thesis research was to determine whether practitioners can use free-viewing eye movements to assess the condition of the visual field. My colleagues and I therefore designed a study in which individual participants watched movie clips and their eye-movement features were used to distinguish between patients with VFD and controls. In addition, we visualized the distribution of eye movement features in the visual field to determine if this distribution correlated with visual field damage of patients with glaucoma and HH. The second aim was to determine whether eye tracking and VR can be incorporated into the existing procedures of vision rehabilitation. More specifically, we tested which criteria need to be fulfilled to ensure that occupational ther-

apists can integrate eye tracking and VR into their current procedures while safeguarding patient safety.

1.1 Thesis outline

My thesis consists of three chapters containing experimental research. The studies in Chapters 2 and 3 focus on the first research topic: identifying eye movement features that differ between participants with simulated and real VFD and normal-sighted controls. Chapter 4 focuses on the second research topic: the usability of eye-tracking and VR in vision rehabilitation therapy.

Chapter 2 reports on a study based on free-viewing eye movement features collected while participants watched 90 short video clips. Using this data we determined whether we could predict the presence of different types of simulated VFD and reconstruct their locations. In this proof-of principle study we investigated whether we could use certain eye movement features and methods of analysis, such as the viewing priority (VP), which measures the similarity of scan paths, or the distribution of fixations across the visual field and machine learning approaches, to provide us with the necessary information to achieve our aims. In Chapter 3 we evaluated whether these methods of analysis could also be used to detect actual VFD.

Chapter 3 consists of our validation of two analysis pipelines on two patient data sets: the methods used in Chapter 2 and methods described in Crabb et al. (2014) on a data set collected by ourselves at the University Medical Center Groningen (UMCG) and a data set published by Asfaw et al. (2018). Both pipelines had previously shown that patients with VFD and controls could be separated based on free-viewing eye-movements. In the study reported in Chapter 3, we also tested the influence of experimental conditions on the separability of the two groups, more specifically the difference between monocular and binocular viewing behaviour and the content of the video clips. First, we used a subset of the movie clips from the study in Chapter 2 and showed them to patients with visual field defects and age-matched controls, who were watching these movies monocularly. Second, we used a data set published by (Asfaw et al., 2018). In their study, patients with glaucoma and age-matched controls watched three different movie clips of slightly longer duration (3, 5 and 7 minutes) with both eyes.

Chapter 4 describes a usability study. Because we wanted to introduce these technologies into vision rehabilitation therapy, as a first step we tested whether it would be possible to use the devices for patients and therapists and which criteria need to be fulfilled to

ensure trouble-free use. The introduction of these technologies should provide occupational therapists with an objective measure of the eye-movement behavior of their clients, which will make it easier to judge their progress and to provide more constructive feedback. VR technology will also make it possible to introduce new kinds of exercises into the current training programs. We assessed the user experiences of three groups: patients with HH, normal-sighted controls and occupational therapists. These participants tested a head-mounted eye tracker and a virtual reality headset during various exercises aimed at improving mobility.

1.2 Background

Eye movements and tracking eye movements

We can see sharply only in the center of the visual field at the fovea which subtends approximately 2 degrees of visual angle. The region subtending 4 to 5 degrees around the fovea is called the parafovea, where the accuracy drops to 50% at 5 degrees. Outside the parafovea our perception is blurry. To get a sharp image of our environment, we therefore need to move our eyes frequently and with high velocity. These movements are known as saccades, and occur up to three times per second. Between saccades we need to keep our eyes nearly stationary (fixated) to sample information in the foveal area of the visual field (Land and Furneaux, 1997). Besides saccades and fixations, there are smooth pursuit, vergence (to see in depth) and vestibular eye movements (Robinson, 1968).

Eye movement tracking is used in a variety of disciplines. Devices to track eye movements have been available for a number of years. The first eye movements were recorded by Delabarre and Huey, who used a very invasive eye tracking method by directly attaching a cup to the cornea to record eye movement during reading (Delabarre, 2013).

As attaching objects to the eye was not a practical way to record its movements, new devices were soon developed that did not touch the eye. The first photographic eye tracker was developed by Dodge and Cline to measure the angular velocity of eye movements. Since then, technical developments have led to more and more sophisticated eye trackers that have been used in a range of disciplines, most commonly visual perception, human-computer interaction, and computer graphics (Duchowski, 2017).

The most widely used type of eye tracker in current eye movement research is a video-based corneal reflection tracker, which captures an image of the eye with the corneal reflections of the light source. In this way, the eye movements can be registered as the

positional difference between the image of the pupil and the corneal reflection changes during eye movements (Duchowski, 2017). In order to calculate the location of gaze on the screen, almost all currently available eye trackers have to be calibrated. This is done by presenting several point stimuli on the screen, so that it is known where the participant is looking. Then, for each of these locations, the eye orientation can be mapped to the point of gaze. As this calibration procedure requires time and needs to be performed for every participant, there have been attempts to shorten this procedure. One promising approach is the stereoscopic eye tracker developed by Barsingerhorn et al. (2018), which consists of two cameras and two infra-red light sources. This makes it possible to calculate the optical axis and gaze direction using triangulation, which means that it does not need to be calibrated for each participant individually.

In the experiments described in the following chapters, my colleagues and I used two types of trackers: a remote eye tracker (Eyelink 1000 or Eyelink duo) and a head-mounted, video-based corneal reflection eye tracker (Pupil Labs Pupil Pro).

What guides visual attention?

Our visual system can only process a limited amount of information at the same time (Broadbent, 1958). When processing complex visual scenes, we therefore use cognitive operations to extract relevant information. This process is called visual attention, which is subdivided into covert and overt visual attention (McKains and Kastner, 2009). Overt visual attention involves directing the gaze towards the attended region. The studies reported in this thesis involved overt visual attention.

The initial research on this topic was performed by (Buswell, 1935) and (Yarbus, 1967), who studied which areas people focus their gaze on when looking at paintings. Their research showed that vision is an active process: the eye movements that observers make when looking at different parts of the painting are essential for them to grasp its content. Nowadays, there are several theories and models that aim to predict where an observer will direct their gaze in a scene, but none have been completely accurate. This is because visual attention is a complex activity. It is partly guided by bottom-up processes, which can be modelled by decomposing the visual scene into feature maps, where different locations compete for saliency (Itti et al., 1998). Saliency models extract lower-level visual features such as contrast, edge content, intensity bispectra, color, and symmetry, as well

as higher-level features such as faces and text. The models then construct a saliency map for each feature (Zhao and Koch, 2013). The saliency of the maps is added up and the model predicts that observers will look at the most salient location. The saliency model is biologically inspired by how the early visual cortex processes input. The most well-known implementation computes the centre-surround differences of three features: intensity, color and orientation.

After the first model for visual saliency was established, subsequent research showed that certain features are better predictors for eye movement features than others. Itti (2005) found that Bayesian surprise attracts the attention of observers the most, which means that they look at objects or regions in the scene which they did not expect to appear there. In dynamic scenes, motion and temporal change are very strong predictors of visual attention (Itti, 2005).

Models not only have different options to construct maps of a single feature, they also have different ways to combine the feature maps into a single model that will predict the gaze location. Engmann et al. (2009) linearly added the normalized maps of center-surround differences of the individual features. Instead of adding all features, other studies suggested selecting those with the maximal neural response (Koene and Zhaoping, 2007).

In recent years, saliency models have become more elaborate and their predictions have become more accurate. One example is the graph-based saliency model, which predicts fixation locations more reliably than the standard saliency model because it accounts for the tendency of observers to look towards the center of the screen (Harel et al., 2007).

On the other hand, the influence of top-down processes on guiding overt attention is too strong to be disregarded. Especially in free-viewing paradigms, saliency models that take only bottom-up information into account perform barely above chance level (Betz et al., 2010). Differences in task instructions can also change the viewing behavior of observers who are watching the same stimulus (Ballard et al., 1995). Depending on the task, the optimal point of gaze may not be the most salient one (Hayhoe and Ballard, 2005). Another factor that guides overt visual attention is experience or learned behavior. Eye movements are often anticipatory actions, rather than just reactions to stimuli. According to Friston et al. (2012), observers try to minimize surprise in their environment. To purposefully guide eye movements, the system that controls them needs to have an appropriate knowledge base, so observers know what to look for (Land and Furneaux,

1997). Other studies have shown that people fixate on objects rather than on salient regions that are not objects, and that emotional content positive or negative leads to longer dwelling times on the relevant part of the scene (Astudillo et al., 2018; Borji et al., 2013). Free-viewing eye movements are particularly difficult to predict because there are no task instructions which could reduce variance in the viewing behavior of different observers (Hayhoe and Ballard, 2005; Koehler et al., 2014). In free-viewing, two observers may be interested in different aspects of the same scene due to their personal preferences.

Visual field defects: Prevalence and causes

VFD can occur due to a variety of causes. They are particularly common in elderly people. In this demographic, the most common cause for a VFD is glaucoma followed by other optic nerve diseases and stroke (Ramrattan et al., 2001).

Glaucoma is characterized by slow degeneration to the optic nerve over time, which causes visual field loss. The visual field loss usually starts in the periphery and progressively shrinks the visual field to eventually cause complete blindness if left untreated. The most important risk factor for glaucoma is high intraocular pressure. Therefore, treatment aims at lowering intraocular pressure (IOP), usually by prescription eye drops (Peeters et al., 2010). As the visual field damage in glaucoma cannot be reversed, but only prevented from progressing, it is crucial to detect visual field loss at an early stage. However, this is difficult as it usually goes unnoticed by the patient until later stages, due to starting in the periphery and its slow progression. In addition, the visual system fills in missing parts in its perception with information from surrounding areas of the retina (Hoste, 2003). Another common type of visual field damage is HH or quadrantanopia, where a patient becomes blind in one half or one quadrant of the visual field due to damage in the visual system of the brain behind the optic chiasm. Approximately 20% of patients with acquired brain injuries due to stroke or accidents can develop HH (Kasten et al., 1999).

Elderly people are at a higher risk of developing VFDs because they are more likely to experience a stroke or a neurodegenerative disease, such as glaucoma. The Rotterdam study reported a fivefold increase in incidences of a VFD, irrespective of cause, between the ages of 55 and 80 years (Skenduli-Bala et al., 2005). Due to the increasing number of elderly people in the population, in the coming decades hospitals will have to diagnose,

treat and follow up on more people with VFDs (de Voogd et al., 2005).

Measuring visual field loss (Standard Automated Perimetry)

The current gold standard method to diagnose a VFD is Standard Automated Perimetry (SAP). To perform this test, the participant places their head in a headrest and fixates on a cross in a uniformly illuminated bowl. Light stimuli of varying luminance intensities are presented at different locations inside the bowl and the test subject is asked to press a button when they perceive the stimulus. In this way the luminance sensitivity thresholds of different locations on the retina are determined. Figure 1.1 shows an example of such a device and how it is operated. While SAP makes it possible to measure severity and



Figure 1.1: The test situation with Standard Automated Perimetry (SAP).

location of the VFD, it has several disadvantages. This test requires time and resources at eye clinics as it can only be administered by trained personnel and it takes up to 20

minutes to test both eyes. In addition, SAP is difficult for test subjects to perform, especially for elderly people the population with the highest risk of developing a VFD. This is because it requires the test subject to stay focused on the task and to keep their gaze steady on the fixation cross for the duration of the test. Loss of focus on the task often causes measurement errors in this test. Katz and Sommer (1990) found that 45% of visual field tests of glaucoma patients and 30% of visual field tests of normal-sighted controls using the Humphrey Field Analyzer (HFA) were not reliable according to the criteria of the manufacturer of the HFA. Most of the unreliable tests were caused by fixation errors, showing that the most difficult part for the test person is to keep their gaze fixed on one point. Due to the above-mentioned shortcomings of the HFA and the aging of the population, there is a need for simpler and faster screening tests for VFDs to reduce the workload at eye clinics and to increase the number of screening tests and follow-ups.

Impairments in daily life caused by VFDs

Many patients with VFD complain about difficulties with activities of daily living, such as reading or tasks involved with mobility (Lane, 2008). This is especially relevant for HH patients for whom a large part of the visual field disappears instantaneously. They often bump into obstacles or have difficulties in reading, driving, visual exploration, visual search and deficits of visuo-spatial orientation (Kasneci et al., 2014; Kerkhoff, 1992; Leff et al., 2000; Papageorgiou et al., 2007; Parker et al., 2011).

Glaucoma patients also report difficulties with activities of daily living, but due to their slowly progressing VFD and the variability in shape and location of the scotomas, this group is more heterogeneous (Ramulu, 2009). Many glaucoma patients have difficulties with glare and adaptation to different levels of lighting (Nelson et al., 2001). They also experience difficulties with activities such as climbing stairs or stepping over kerbs, reading, reaching for objects, shopping, crossing the road, using the bus or train, visiting friends and going to restaurants (Kotecha et al., 2009; Nelson et al., 2001).

Both patient groups thus experience similar difficulties. As a general rule, the larger and the more advanced the VFD, the more difficulties patients experience, which reduces their quality of life (Van Gestel et al., 2010). Glaucoma patients usually experience different visual field damage in each eye, and the state of the integrated visual field is more strongly determined by the better eye. Therefore, damage to the better eye usually has a

stronger impact on quality of life, and overlapping visual field damage may be a strong disabling factor (Ramulu, 2009; Van Gestel et al., 2010). Depending on which area of the visual field is impaired, they may have difficulties with different kinds of tasks. Reading and walking, for example, become difficult if the visual field along the horizontal meridian is impaired (Murata et al., 2013).

In HH, the VFD is the same in both eyes and all patients have an impairment of either the right or the left hemifield. Two factors have been shown to influence the perceived difficulty and the ability to perform certain tasks: foveal sparing and which hemifield is affected. Foveal sparing seems to have a positive effect on the quality of life (Leff et al., 2000; Papageorgiou et al., 2007) and HH patients with right-sided VFD have more difficulties when reading (Leff et al., 2000). Besides preventing further visual field loss, a major aim in the treatment of patients with VFDs is to realize a high health-related quality of life for each patient (Van Gestel et al., 2010). This can be achieved by developing coping mechanisms, but the ability to cope with VFDs differs between individual patients.

Vision rehabilitation therapy

Patients with VFDs who experience difficulties with activities of daily living can participate in vision rehabilitation therapy. For both patient groups, various treatment options are available including restoration training and substitution through optical aids (Lane, 2008).

While it is unclear whether vision restoration can actually be achieved in adults, learning a compensatory eye movement strategy for their specific VFD has been shown to help patients with activities of daily living. The objective of this method to maximize the functional field of view (Lane, 2008; Livengood and Baker, 2015). Participants in these programmes receive regular training sessions at vision rehabilitation centers, where occupational therapists use various exercises to teach them compensatory eye movement scanning patterns. These programmes are currently being offered to patients with HH. This group has a stereotypical VFD, which makes it more straightforward to determine a suitable compensatory strategy: making large saccades towards the blind hemifield. A common exercise in these training programmes is visual search or exploration, where patients practice these large saccades towards the blind hemifield while seated in front of

a screen and are tasked with searching for a stimulus (Kerkhoff, 1992). Compensatory scanning training has been improved and developed over the years. A study has also been performed about whether patients can learn compensatory eye-movements from home to reduce the necessary resources and costs for training (Aimola et al., 2014).

InSight-Hemianopia Compensatory Scanning Training (IH-CST) is an example of a successful training protocol. It was developed by Royal Dutch Visio and has been shown to improve mobility-related tasks (de Haan et al., 2015). This programme includes several exercises of varying difficulty. It is described in more detail in Chapter 4.

While there are standardized training procedures for HH patients, vision rehabilitation for glaucoma takes various approaches. When glaucoma patients enter occupational therapy, their limitations with certain tasks are assessed with a questionnaire and the therapists observe their performance on various tasks. Based on this assessment, the therapeutic interventions are planned. There is no equivalent of the IH-CST training for glaucoma patients. If we could better understand eye movements of glaucoma patients, this knowledge could be used to establish compensatory scanning training for glaucoma patients. Virtual reality is a promising approach for this research.

Virtual reality

A virtual environment is a computer-generated world with which the user can interact. In the first paper that described virtual reality, Sunderland wrote: The ultimate display would, of course, be a room within which the computer can control the existence of matter. (Sunderland, 1965). The idea behind virtual reality is to create an environment that is complex and immersive, but at the same time safe and controllable.

Two definitions of virtual reality (VR) are currently in use. One is technology-based and the other is experience-based. The technology-based definition states that VR enables the user to interact with a simulated, three-dimensional environment. This also includes the software that creates the virtual environment. The experience-based definition focuses more on the sense of immersion in the simulated environment Zhou and Deng (2009).

In 1929, Edward Link created the first flight simulator, and in 1960, the first head-mounted VR display was invented, which provided stereoscopic 3D and wide vision with stereo sound. Nowadays, VR systems have become very elaborate and user-friendly. Various companies produce devices that most commonly consist of head mounted displays,

which provide the user with an immersive visual and auditory experience. In many of these systems, the user can walk around in the virtual environment, as the position of the headset is tracked by motion sensors. They are used in a variety of areas such as education and clinical rehabilitation (Abulrub et al., 2011; Kawasaki and Yamaguchi, 2012; Li et al., 2017; Schultheis, 2001; Shim et al., 2003).

VR technology can be used to assist patients with VFD in different ways. One possibility is to use VR devices as visual aids. Younis et al. (2017) used a VR headset with a front camera to assist patients with peripheral VFD in scene perception by downscaling the captured scenery and presenting it in the central part of the visual field. Another option, which I focused on in this thesis, is to use it in vision rehabilitation training. It can for example be used to practice mobility related situations in a safe and controlled environment. Bowman and Liu (2017) found that training to cross a virtual street is as effective as training to cross a real street for individuals with low vision. In Chapter 4 we investigated if VR technology can be incorporated into already existing vision rehabilitation procedures.

References

- A. G. Abulrub, A. Attridge, and M. A. Williams. Virtual reality in engineering education: The future of creative learning. *International Journal of Emerging Technologies in Learning*, 6(4):411, 2011.
- L. Aimola, A. R. Lane, D. T. Smith, G. Kerkhoff, G. A. Ford, and Schenk T. Efficacy and feasibility of home-based training for individuals with homonymous visual field defects. *Neurorehabilitation and Neural Repair*, 28(3), 207218, 28(3):207218, 2014.
- D. S. Asfaw, P. R. Jones, N. D. Smith, and D. P Crabb. Data on eye movements in people with glaucoma and peers with normal vision. *Data in Brief*, 19, 12661273, 19, 2018.
- C. Astudillo, K. Munoz, and P. E. Maldonado. Emotional content modulates attentional visual orientation during free viewing of natural images. 2018.
- D. H. Ballard, M. M. Hayhoe, and J. B. Pelz. Memory representations in natural tasks. *Journal of Cognitive Neuroscience*, 7(1):6680, 1995.
- A. D. Barsingerhorn, F. N. Boonstra, and J. Goossens. Development and validation of a high-speed stereoscopic eyetracker. *Behavior Research Methods*, page 118, 2018.

- T. Betz, T. C. Kietzmann, N. Wilming, and P. König. Investigating task-dependent top-down effects on overt visual attention. *Journal of Vision*, 10(3):114, 2010.
- A. Borji, D. N. Sihite, and L. Itti. What stands out in a scene? a study of human explicit saliency judgment. *Vision Research*, (91):6277, 2013.
- E.L. Bowman and L. Liu. Individuals with severely impaired vision can learn useful orientation and mobility skills in virtual streets and can use them to improve real street safety. *PLoS One*, 2017.
- D. E. Broadbent. The effects of noise on behaviour. *Perception and communication*, page 81107, 1958.
- G. T. Buswell. How people look at pictures: A study of the psychology of perception in art. *University of Chicago Press*, 1935.
- D. P. Crabb, N. D. Smith, and H. Zhu. What's on tv? detecting age-related neurodegenerative eye disease using eye movement scanpaths. *Frontiers in Aging Neuroscience*, 6:312, 2014.
- G. A. de Haan, B. J. M. Melis-Dankers, W. H. Brouwer, and O. Tucha. The effects of compensatory scanning training on mobility in patients with homonymous visual field defects: A randomized controlled trial. *Plos One*, 2015.
- S. de Voogd, M. K. Ikram, R. C. W. Wolfs, Jansonius, A. N. M., Hofman, and P. T. V. M. De Jong. Incidence of open-angle glaucoma in a general elderly population: The rotterdam study. *Ophthalmology*, 112(9):14871493, 2005.
- E. B. Delabarre. A method of recording eye-movements. *The American Journal of Psychology*, 9(4):572–574, 2013.
- A. T. Duchowski. *Eye Tracking Methodology*. Springer, 2017.
- S. Engmann, B. t'Hart, T. Sieren, S. Onat, P. Koenig, and W. Einhauser. Saliency on a natural scene background: Effects of color and luminance contrast add linearly. *Attention, Perception and Psychophysics*, 71(7):14391459, 2009.
- K. Friston, R. A. Adams, L. Perrinet, and M. Breakspear. Perceptions as hypotheses: Saccades as experiments. *Frontiers in Psychology*, 3, 2012.

- J. Harel, C. Koch, and P. Perona. Graph-based visual saliency. In *NIPS Proceedings*, 2007.
- M. Hayhoe and D. Ballard. Eye movements in natural behavior. *Trends in Cognitive Sciences*, 9(4), 2005.
- A. M. Hoste. New insights into the subjective perception of visual field defects. *Bulletin de La Société Belge d'ophtalmologie*, (287):6571, 2003.
- L. Itti. Quantifying the contribution of low-level saliency to human eye movements in dynamic scenes. *Visual Cognition*, 12(6):10931123, 2005.
- L. Itti, C. Koch, and E. Niebur. A model of saliency-based visual attention for rapid scene analysis. *IEEE Transactions on Pattern Analysis and Machine Intelligence*, 1998.
- E. Kasneci, K. Sippel, M. Heister, K. Aehling, W. Rosenstiel, U. Schiefer, and E. Pappageorgiou. Homonymous visual field loss and its impact on visual exploration: A supermarket study. *Translational Vision Science and Technology*, 3(6), 2014.
- E. Kasten, D. Poggel, E. Müller-Oehring, J. Gothe, T. Schulte, and B. Sabel. Restoration of vision ii: Residual functions and training-induced visual field enlargement in brain-damaged patients. *Restorative neurology and neuroscience*, 1999.
- J. Katz and A. Sommer. Reliability of automated perimetric tests. *Archives of Ophthalmology*, 108(6), 1990.
- M. Kawasaki and Y. Yamaguchi. Effects of subjective preference of colors on attention-related occipital theta oscillations. *NeuroImage*, 59(1):808814, 2012.
- G. Kerkhoff. Rehabilitation of homonymous scotomata in patients with postgeniculate damage of the visual system: saccadic compensation training. *Restor Neurol Neurosci.*, 4(4):245–54, 1992.
- K. L. Koehler, F. Guo, S. Zhang, and M. P. Eckstein. What do saliency models predict? *Journal of Vision*, 14(3):127, 2014.
- A. R. Koene and L. Zhaoping. Feature-specific interactions in salience from combined feature contrasts: Evidence for a bottom-up saliency map in v1. *Journal of Vision*, 7(7):114, 2007.

- A. Kotecha, N. O’Leary, D. Melmoth, S. Grant, and D. P Crabb. The functional consequences of glaucoma for eye-hand coordination. *Investigative Ophthalmology and Visual Science*, 50(1):203213, 2009.
- M. F. Land and S. Furneaux. The knowledge base of the oculomotor system. *Philosophical Transactions of the Royal Society of London.*, Series B, Biological Sciences, 352(1358):12311239, 1997.
- A. Lane. Clinical treatment options for patients with homonymous visual field defects. *Clinical Ophthalmology*, 2(1)(93), 2008.
- A. P. Leff, S. K. Scott, H. Crewes, T. L. Hodgson, A. Cowey, D. Howard, and R. J. S. Wise. Impaired reading in patients with right hemianopia. *Annals of Neurology*, 47(2): 171178, 2000.
- L. Li, F. Yu, D. Shi, J. Shi, Z. Tian, J. Yang, and Q. Jiang. Application of virtual reality technology in clinical medicine. *American Journal of Translational Research*, 9(9): 38673880, 2017.
- H. M. Livengood and N. A. Baker. The role of occupational therapy in vision rehabilitation of individuals with glaucoma. *Disability and Rehabilitation*, 37(13):12021208, 2015.
- S. A. McKains and S. Kastner. *Encyclopedia of Neuroscience Visual Attention*, chapter Visual Attention. Springer, Berlin, Heidelberg, 2009.
- H. Murata, H. Hirasawa, Y. Aoyama, K. Sugisaki, M. Araie, C. Mayama, and R. Asaoka. Identifying areas of the visual field important for quality of life in patients with glaucoma. *PLoS ONE*, 8(3):1–7, 2013.
- P. Nelson, P. Aspinall, C. O’Brien, and I. U. Scott. Patients’ perception of visual impairment in glaucoma: A pilot study. *Evidence-Based Eye Care*, 2(2):114115, 2001.
- E. Papageorgiou, G. Hardiess, F. Schaeffel, H. Wiethoelter, H. O. Karnath, H. Mallot, and U. Schiefer. Assessment of vision-related quality of life in patients with homonymous visual field defects. *Graefes Archive for Clinical and Experimental Ophthalmology*, page 17491758, 2007.

- W. T. Parker, G. McGwin, J. M. Wood, J. Elgin, M. S. Vaphiades, L. B. Kline, and C. Owsley. Self-reported driving difficulty by persons with hemianopia and quadrantanopia. *Current Eye Research*, 36(3):270277, 2011.
- A. Peeters, C. A. B. Webers, M. H. Prins, M. P. Zeegers, F. Hendrikse, and J. S. A. G. Schouten. Quantifying the effect of intraocular pressure reduction on the occurrence of glaucoma. *Acta Ophthalmologica*, 88(1):511, 2010.
- R. S. Ramrattan, R. C. W. Wolfs, S. Panda-Jonas, J. B. Jonas, D. Bakker, H. A. Pols, and P. T. V. M. De Jong. Prevalence and causes of visual field loss in the elderly and associations with impairment in daily functioning: The rotterdam study. *Archives of Ophthalmology*, 119(12):17881794, 2001.
- P. Ramulu. Glaucoma and disability: Which tasks are affected, and at what stage of disease? *Current Opinion in Ophthalmology*, 20(2):9298, 2009.
- D. A. Robinson. The oculomotor control system: A review. *Proceedings of the IEEE*, 56(6):10321049, 1968.
- M. T. and Albert A. R. Schultheis. The application of virtual reality technology in rehabilitation. *Rehabilitation Psychology*, 2001.
- K. C. Shim, J. S. Park, H. S. Kim, J. H. Kim, Y. C. Park, and H. I. Ryu. Application of virtual reality technology in biology education. *Journal of Biological Education*, 37(2):7174, 2003.
- E. Skenduli-Bala, S. De Voogd, R. C. W. Wolfs, R. Van Leeuwen, M. K. Ikram, J. B. Jonas, and P. T. V. M. De Jong. Causes of incident visual field loss in a general elderly population: The rotterdam study. *Archives of Ophthalmology*, 123(2):233238, 2005.
- I. E. Sunderland. The ultimate display. In *Proceedings of IFIP Congress*, 1965.
- A. Van Gestel, C. A. B. Webers, H. J. M. Beckers, M. C. J. M. Van Dongen, J. L. Sevens, F. Hendrikse, and J. S. A. G. Schouten. The relationship between visual field loss in glaucoma and health-related quality-of-life. *Eye*, 24(12):17591769, 2010.
- A. Yarbus. Eye movements and vision,. *Plenum Press*, 1967.

- O. Younis, W. Al-Nuaimy, M. Al-Tae, and A. Al-Ataby. Augmented and virtual reality approaches to help with peripheral vision loss. *14th International Multi-Conference on Systems, Signals and Devices (SSD)*, pages 303–307, 2017.
- Q. Zhao and C. Koch. Learning saliency-based visual attention: A review. *Signal Processing*, 93(6):14011407, 2013.
- N. N. Zhou and Y. L. Deng. Virtual reality: A state-of-the-art survey. *International Journal of Automation and Computing*, 6(4):319325, 2009.

Using natural viewing behavior to screen for and reconstruct visual field defects

this chapter is based on: Gestefeld, B., Grillini, A., Marsman, J. B. C., and Cornelissen, F. W. (2020). Using natural viewing behavior to screen for and reconstruct visual field defects. *Journal of Vision*, 20(9):1-16.

2.1 Abstract

There is a need for simple and effective ways to screen for visual field defects (VFD). Watching a movie is a simple task most humans are familiar with. Therefore, we assessed whether it is possible to detect and reconstruct visual field defects based on free viewing eye movements, recorded while watching movie clips. Participants watched 90 movie clips of 1-minute, with and without simulated visual field defects (sVFD), while their eye movements were tracked. We simulated homonymous hemianopia (HH) (left and right sided) and glaucoma (small nasal arc, large nasal arc and tunnel vision). We generated fixation density maps of the visual field and trained a linear support vector machine to predict the viewing conditions of each trial of each participant based on these maps. To reconstruct the visual field defect, we computed viewing priority maps and maps of differences in fixation density of the visual field of each participant. We were able to classify the simulated visual field condition with over 85% accuracy. In simulated HH, the viewing priority distribution over the visual field indicated the location of the sVFD in the simulated HH condition. In simulated glaucoma the difference in fixation density to the control condition indicated the location of the sVFD. It is feasible to use natural viewing behavior to screen for and reconstruct (simulated) visual field defects. Movie clip viewing in combination with eye tracking may thus provide an alternative to or supplement standard automated perimetry, in particular in patients who cannot perform the latter technique.

2.2 Introduction

The most common way to establish the presence of a visual field defect is by means of standard automated perimetry (SAP), which assesses a person's luminance sensitivity across the visual field. With this test, clinicians can detect and localize visual field defects, already at an early stage of a disease (Wild, 1988). SAP is critical in the management and follow-up of ophthalmic disease. However, it has some requirements and instructions that make it less suitable for use in various groups, such as the very young or very old, or in people with a cognitive impairment. For example, SAP requires the tested person to fixate a small light spot over an extended period of time and to provide behavioral feedback. Both requirements can only be fulfilled if the tested person can remain focused on the task, which is often not achieved (Birt et al., 1997).

The Rotterdam study (Skenduli-Bala et al., 2005) found glaucoma to be the leading cause of visual field loss. Another common cause is stroke, which can lead to hemianopia or quadrantanopia, where people are blind in one half or one quadrant of their visual field. It also found that the occurrence of visual field defects increases 5-fold above the age of 55 years. With an increasing elderly population over the next decades, neurodegenerative eye diseases, such as glaucoma, as well as incidences of stroke, will become more and more common. Because both lead to visual field loss, there is a growing need for fast and easy to perform visual field tests.

A very simple and inexpensive method to assess the visual field is confrontational perimetry. In this method, the examiner presents both index fingers in opposing hemifields, while the patient is watching with one eye and fixating the doctor's opposite eye. The patient has to report which of the index fingers of the examiner wiggled. The sensitivity of this test, however, to detect certain VFDs is very low (Johnson and Baloh, 1991).

If we could find a method that is easier to perform than SAP and more accurate and reproducible than confrontational perimetry, it could open up regular screening to a larger group of patients. With the advances in eye tracking technology, a possible way to screen for VFDs would be to use eye movements. Eye movements are a spontaneous visual behavior and there is ample evidence that the presence of a VFD evokes eye movement behavior that is different from normal (Asfaw et al., 2018; Kanjee et al., 2012; Lamirel et al., 2014).

For patients with homonymous hemianopia (HH) or glaucoma, it has been shown that the presence of a visual field defect influences eye movement behavior during different

tasks. Patients with HH are usually aware of their VFD and many of them employ compensatory strategies in situations like driving or visual exploration during shopping, by making more saccades towards the blind hemifield (Bahnmann et al., 2015; de Haan et al., 2015; Kasneci et al., 2014). Differences in eye movement behavior between HH patients and healthy controls can also be observed during reading: patients with HH make more saccades and regressions per line (Trauzettel-Klosinski and Brendler, 1998).

Also, glaucoma patients show viewing behavior different from normal-sighted controls. For example, when glaucoma patients search for target objects in photographs, they make fewer saccades than healthy controls (Smith et al., 2012). As glaucoma patients can have defects in many different areas of the visual field and many of them also experience filling-in of their VFD and are not as aware of its location (Crabb et al., 2013), it is harder to define an appropriate compensatory eye movement strategy for glaucoma. However, (Kübler et al., 2015) found that some glaucoma patients were able to pass a simulated driving test and these patients showed increased visual exploration compared to the glaucoma patients who failed the test. The above-mentioned studies showed significant differences between groups, but a useful screening method needs to be able to distinguish between individual participants. That this is feasible was demonstrated by (Crabb et al., 2014), who used machine learning to classify observers as glaucoma patients or healthy controls and reached a sensitivity of 76% and a specificity of 90%. They used saccade maps, that were computed from eye movement data collected during free viewing of three different movie clips as an input to a naive Bayesian classifier.

While using machine-learning algorithms can be very successful in distinguishing between different viewing conditions, clinicians usually like to know which part of the visual field is still intact and which is not. The Humphrey Field Analyzer (HFA), therefore, computes a map of the visual field. An example of this can be seen in 2.1.

We chose to simulate different full VFDs which occur in HH and in glaucoma, rather than to assess this in actual patients. Simulating the VFDs has the advantage that we know exactly the 'ground truth', i.e. the part of the visual field that was masked. This means we can actually verify the quality of the reconstruction of the VFD. However, we simulated only absolute VFDs (no light sensitivity), which in the case of glaucoma usually occur only in later stages of the disease. This means that glaucoma patients usually get used to their loss of vision over time. More gradual visual field loss was not simulated in this study. We will therefore also not aim to compute a map that shows the severity

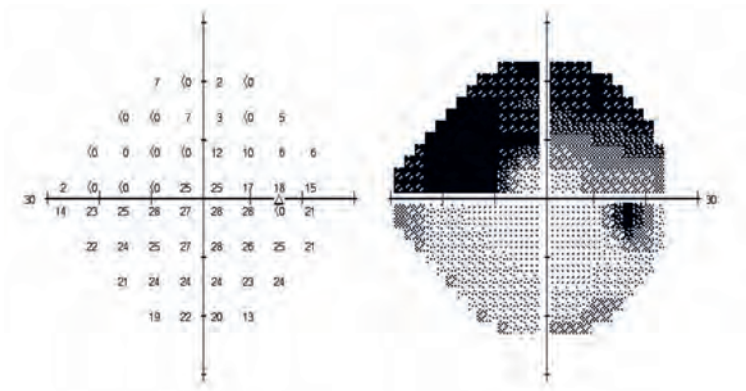


Figure 2.1: Example of a visual field map computed by the Humphrey Field Analyzer (HFA). The darker colors indicate a lower contrast sensitivity.

of the visual field loss, as shown in figure 1, but aim to approximately reconstruct the (simulated) blind area in the visual field.

We know from previous studies, that artificial scotomas have a strong impact on the eye movement behavior of normal-sighted participants, as was shown by (David et al., 2019). In their study participants freely explored static images of different scenes. They were able to identify different eye movement parameters based on which they were able to predict the viewing condition (simulated glaucoma, simulated macular degeneration or control) of the participant in a certain trial. Further evidence for this is that when performing a visual search task with artificial central and peripheral stimuli, normal-sighted participants showed increased fixation durations in comparison to performing the task without the artificial scotoma (Cornelissen et al., 2005). Tant et al. (2002) found that simulated HH elicits a similar scanning behavior as real HH in participants who performed a dot counting task. An obvious disadvantage of simulations is that they may not fully comprise the actual experience of people with an actual VFD (Crabb et al., 2013), and that the effects we measure are acute. Consequently, participants have relatively little time to adapt their behavior in response to the VFD. In our study, participants watched movie clips of 1 min duration, some clips with either simulated HH or simulated glaucoma and the rest of the clips in the control condition.

We asked two questions: 1.) can we predict the viewing condition of a specific trial

based on fovea-referenced differential fixation density maps and 2.) can we reconstruct the location of the sVFD for each participant?

Both questions should be answered affirmatively for the method to be potentially useful in clinical practice. We used machine learning to determine the accuracy with which we can predict the viewing condition. On top of that, we obtained maps of the visual field (in analogy to the one provided by Standard Automated Perimetry (SAP)) that locate the sVFD for each participant per scotoma archetype.

In addition to answering these two main research questions, we wanted to find out whether the content that was shown had an effect on the eye movement behavior, and more specifically, the possibility to reconstruct the sVFD. So, we obtained visual field maps for each movie clip per scotoma archetype, averaged across observers. We also aimed to understand the underlying eye movement strategy of the participants in the different sVFD conditions. We computed the average saccade amplitude in 18 different directions for each viewing condition to determine whether a certain scotoma archetype led to a characteristic pattern of saccade amplitudes, which could be an indicator for a compensatory strategy.

2.3 Methods

Participants/ Study Population

We tested 70 healthy participants (60 females, mean age: 20 years, standard deviation: 3.3 years) with normal or corrected to normal visual acuity and no visual field defect. The ethics committee of the Department of Psychology of the University of Groningen (RUG) approved the study protocol. Participants were psychology students who received study credits for their participation. All participants provided written informed consent. The study followed the tenets of the Declaration of Helsinki.

Materials

The data for this study was collected in two separate experiments, where the first experiment contained simulated HH trials and the second experiment contained simulated glaucoma trials. We analyzed the two resulting data sets separately using the same methods. The sets were collected on two different displays, because set 2 was collected at a later time point, when the equipment at the laboratory had been changed. In set 1, all

sVFD were HH (left and right sided). In set 2 all sVFD were glaucoma (small nasal arc, large nasal arc and tunnel vision). The first set was collected with 40 participants, who watched the clips with the simulated HH conditions. We presented movie clips on a 40 cm by 30 cm (1152 x 870 pixel) screen (LaCie CRT). This means that this screen covered a visual field of 36.9 x 28.1 deg (of visual angle). For set 2, 30 different participants watched movie clips on a 50 cm by 35 cm (1920 x 1080 pixel) screen (BenQ Zowie xl2540). The second screen thus covered a visual field of 45.2 x 32.5 deg.. For both sets, monocular eye movements were recorded with an Eyelink 1000 eye tracker (SR Research) at 1000 Hz, which was connected to a dedicated PC with an ethernet cable running Eyelink software. At the beginning of the experiment, we tested whether one eye calibrated more accurately or could be tracked more robustly. If this was the case, we chose to track this better eye. Otherwise we randomly chose the to be tracked eye. The host PC was connected to a laptop running MATLAB (Version 2016b, MathWorks, Natick, MA) with the Psychtoolbox (Brainard, 1997, Kleiner et al., 2007) and the Eye-linktoolbox (Cornelissen et al., 2002) via Ethernet. All participants were seated at 60 cm distance from the screen.

Stimuli

All movie clips were presented on the full screen. The sequences for both experiments were taken from 18 different movies, which could be grouped into the following categories: animations, cartoons, feature films (crime stories, dramas and comedies) and nature documentaries. The movie clips contained a wide range of different content. While some showed actors in different contexts others showed animated characters or landscapes and animals. For a complete list of movies from which we extracted the clips see the supplementary material. The original language of all movies was Dutch. Stimuli were presented using MATLAB with Psychtoolbox and gstreamer (<https://gstreamer.freedesktop.org>). Observers watched the clips without any task instructions, while their head was placed on a chin rest. The visual field defect was simulated by masking a part of the movie with gray bitmaps, which are shown in figure 1. For set 1 each participant watched 90 movie sequences in total. 30 or 60 movies were presented with simulated HH, either on the left or on the right side. For set 2, each participant watched 88 movie clips, 66 of these clips with a sVFD: a small nasal arc, a

large nasal arc and tunnel vision (22 clips each sVFD). All movie clips were presented for 1 minute. Auditory content was presented over headphones (Philips Ear clip headphones SHS4700/10). Volume was adjusted so that it was audible and comfortable for the participant.

Simulations

The sVFD were created as grayscale bitmaps in MATLAB (simulated HH) and GIMP (simulated glaucoma), which were overlaid over the current video frame. The simulations were coupled to the eye tracker and the mask moved along with the participants gaze, always covering the same part of the visual field. We presented the video frame as well as the mask as Psychtoolbox textures, which had the same refresh rate, namely 84 Hz for the simulated HH conditions and 60 Hz for the simulated glaucoma conditions. So, before each frame was drawn the program checked the gaze position and updated the location of the mask, accordingly. As the sampling rate of the eye tracker was higher than the refresh rate of the stimulus, the position of the mask could be updated in real time. If there was no sample available (e.g. because of a blink) the last available gaze position was used to position the mask. When participants gazed towards the center of the screen, the mask in the simulated HH conditions covered 50% of the screen horizontally and the entire screen vertically. In the glaucoma conditions, the small nasal arc covered 4% of the screen having a width of approximately 5 deg. and a length of about 15 deg. The large nasal arc covered about 15% of the screen having a width of 12 deg and a length of about 27 deg.. The tunnel vision simulation covered 86% of the screen masking everything outside the radius of the inner 15 deg..

Due to the gaze contingency of the simulations, depending on the momentary gaze direction of the participant, the masks could cover a larger or smaller part of the screen throughout a trial. In the simulated HH conditions, for example, up to 100% of the screen could be masked, if participants looked towards the non-masked side of the screen.

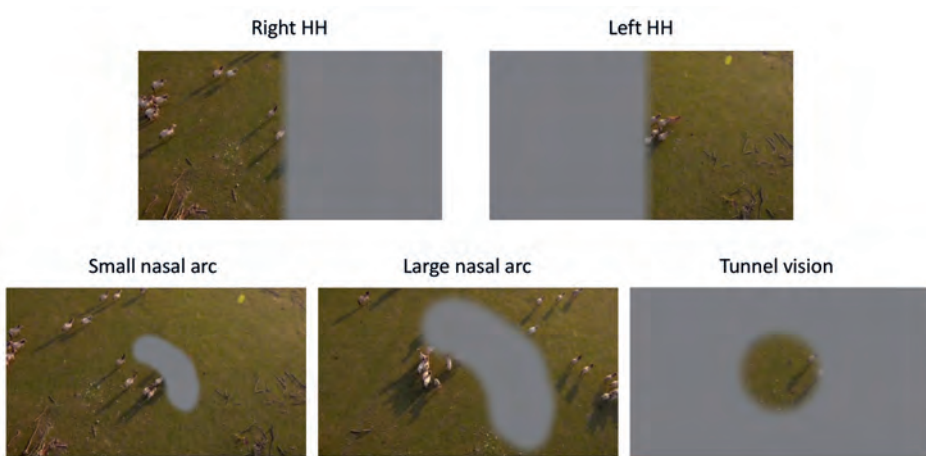


Figure 2.2: Illustration of the simulated VFDs overlaid over different scenes of the same movie.

Procedure

Participants were seated in front of a computer screen with their head fixed in a chin rest. We calibrated the eye tracker once before starting the experiment using the built-in calibration procedure of the Eyelink. Participants watched either 90 or 88 movie clips of 1-minute duration. As an initial goal of the first experiment was to test the influence of presenting audio content from different directions on the viewing behavior, the participants had to change the ear phones after each trial. The auditory condition was indicated on the screen before the experimenter started the trial. Sound was presented to the left or right or both ears, or muted. In addition, the screen showed information for the experimenter which keys should be pressed to continue or repeat the trial, or to exit the experiment. In both experiments, the next trial started if the experimenter pressed spacebar. Participants were informed that they could take a break in between trials if they felt tired. The experimenter also asked after 1/3 and 2/3 of the trials if the participant wanted to take a break. After breaks, we performed a drift correction. Moreover, if the participant changed their seating position or if we noticed that the eye tracker lost the gaze position frequently, we recalibrated the eye tracker. The order in which the movie

clips were presented was randomized for each participant.

Eye-movement analysis

The Eyelink 1000 gives an average eye position accuracy of better than 0.5 degrees. The average calibration error was <1 degree and the maximum calibration error <1.5 degrees. Participants who could not be calibrated accurately were not included. Data of three participants from the first set, and data of two participants from the second set, were excluded due to an inaccurate calibration (average calibration error above 1 degree and maximum calibration error above 1.5 degrees). Saccades and fixations were defined using the Eyelink's built-in algorithm. Fixations separated by a blink were concatenated.

Classification

Our first aim was to discriminate between viewing conditions based on the eye movement data. To do so, first, we extracted all fixations from the data. Next, we defined the center of the visual field to be the position of the first fixation. The position of the second fixation is defined with respect to that of the first fixation, and so on. In this way, we follow the visual field of the participant, always defining the position of a fixation with respect to the previous one.

We then defined grids over the visual field to compute the proportion of fixations that fell into each bin of the grid in one trial. As the two screens had different sizes, we based the size of the grid on the average saccade amplitudes of all participants in the control conditions of each screen. We computed the average saccade amplitude and added two standard deviations in 18 different directions (see 2.3). We then defined a rectangular grid that covered all fixations that fell into this area. For set 1 the grid covered an area of 30x28 deg. and for set 2 the grid covered 44x28 deg. In both sets the bin size was 2 deg. in horizontal and vertical direction, which is the same as the resolution of the grid used by Crabb et al. (2014). For each trial, we computed the sum of fixations per bin and z-normalized the resulting map (see figure 2.3 for examples).

The maps were vectorized and used to train a linear support vector machine to distinguish between the control and sVFD conditions, which were in set 1 control, right sided HH and left sided HH, and in set 2 control, small nasal arc, large nasal arc and tunnel vision. The classifier was trained and tested by means of a 10-fold cross validation,

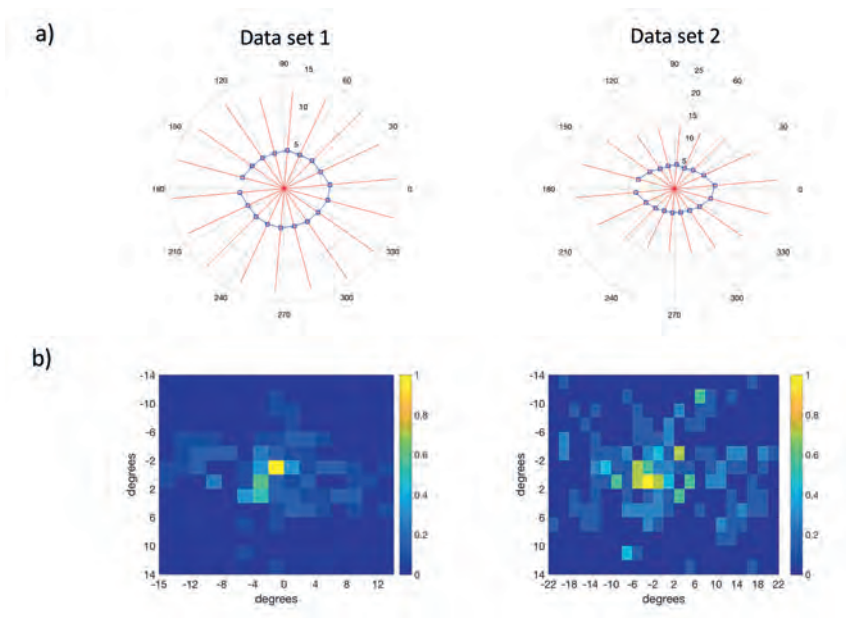


Figure 2.3: Figure 3: a) Saccade amplitudes averaged over all participants in the control condition. The blue squares show the mean saccade amplitudes per direction and the red lines are the corresponding error bars showing 2 standard deviations. b) Examples of fixation maps of one trial from each data set showing the proportion of fixations that fell into each bin.

with two thirds of the data used as training data. We firstly distinguished between the control condition and the presence of an sVFD (without making a distinction between different scotoma archetypes) to determine the sensitivity and specificity, which we visualized as an ROC curve. Secondly we determined the classification accuracy per sVFD archetype and visualized the results as confusion plots. As data set 1 contained different audio conditions, we wanted to exclude the possibility that there was an effect of the different auditory conditions on the viewing behavior of our participants. We, therefore, performed the same classification procedure as described above, but selecting trials from the (visual) control condition and distinguishing between the four different audio conditions (stereo, left ear, right ear and no sound). As the classification accuracy was chance

level, we concluded that different auditory conditions did not influence viewing behavior and did not distinguish between auditory conditions for our further analysis.

Reconstruction of the sVFD

For the reconstruction of the visual field, we collected all trials that were performed with the same sVFD by each participant. We then based the reconstruction of the respective sVFD on this set of trials.

We used two different approaches to reconstruct the simulated VFD on both data sets. In our first approach, we used the concept of viewing priority (Marsman et al., 2016). Viewing priority (VP) measures how consistent the viewing behavior of one observer is to that of other observers based on fuzzy c-means clustering. The value of VP is measured as the distance of a given fixation to a set of reference fixations, which are fixations made by other observers watching the same context (i.e. a movie scene in this experiment). These reference fixations usually cluster around the same aspect of the scene. To determine how closely clustered the reference fixations are, a set of random fixations is selected, which are fixations made by other observers watching different content (i.e. a different movie scene), and the distance of the reference fixations to the random fixations is computed. The height of the VP measure is dependent on the combination of the density of the reference fixation and the distance of the observers fixation to these clusters. For a detailed explanation of the calculation of VP, we refer to (Marsman et al., 2016). The VP for each fixation was computed by selecting reference and random sets from fixations made under normal viewing conditions for the same screen size. The size of the reference set and random set differed between fixations, as other observers may not make a fixation during a certain time interval. The set of reference fixations had a size of at least 10 fixations and the random set was 3 times the size of the reference set. We show how the VP is distributed across the visual field by first computing a heat map, where each fixation is represented as a Gaussian distribution with a width of 1 deg., weighted by its VP value. We then divide this map by the map that shows the distribution of fixations (without weights).

In our second approach, we used differences in fixation density between the control condition and the simulated VFDs followed by permutation statistics to test for significant differences. The following analysis steps were used to reconstruct the visual field defect:

1. Per participant, we calculated a reference map for the mean fixation density in the control condition by averaging across all other participants control condition trials.
2. Computation of a mean fixation density map for each viewing condition per participant (VFD map).
3. We calculated a difference map d by subtracting the reference map from each VFD map.
4. For each participant, compute the null distribution of differences by a) permuting n times across both control trials and simulated VFD trials and b) generating a set of random difference maps R , by drawing two random samples from the permuted sets of trials and subtracting the two.
5. The probability map is then calculated as follows: $P(x,y) = \text{sum}(d > R) / n$.

For each observer, we applied both approaches and computed the VP map and the differential fixation map for each condition. In addition, we also created average VP and differential fixation maps across all observers for each condition.

To calculate the performance for each approach, we calculated the correlations between both the VP map and the differential fixation map, and the binarized map of the visual field where the area of the defect is masked.

Both approaches were also used to compute maps for each condition and each film averaged over all participants, who had watched the same clip under the same viewing condition.

Eye movement strategies

As the last part of our data analysis, we investigated whether participants developed particular eye movement strategies when watching the movie clips with a certain sVFD archetype and whether they changed their behavior over time. We computed the average saccade amplitude in each viewing condition for each participant in 16 different directions, together spanning the full 360 degrees. In addition, to examine the possible presence of learning effects, we computed the average saccade amplitude and fixation duration of all participants per viewing condition over the first, middle and last tercile of all trials. To assess whether these eye movement features differed between these three sets, we performed a one-way ANOVA.

2.4 Results

We will first describe the results of the classification of each set into control and sVFD conditions, as well as into the sVFD archetypes using the distribution of fixations in the visual field as an input. Next, we show, how well the VP and the relative fixation density maps reconstructed the sVFD of each sVFD archetype. Finally, we will present the saccade amplitude per direction for each type of sVFD averaged across participants.

Classification based on the distribution of fixations

Assuming that this method will be used to screen for an underlying pathology, we first aimed to distinguish between the control condition and the presence of an sVFD. In addition, we wanted to find out whether it is also possible to distinguish between different sVFD archetypes within each data set to test the limitations of the method.

Figure 2.4b shows the ROC curve for both parts. The area under the curve for set 1 was 0.91. The area under the curve for set 2 was 0.87. Figure 2.4c shows the confusion plot with the mean percentages of trials labeled as each sVFD archetype. The overall average accuracy for archetype classification in set 1 was 85.55% (minimum: 83.93%, maximum 86.86%). The overall average classification accuracy for archetype classification in set 2 was 85.81% (minimum: 84.11%, maximum: 88.14%). The confusion plots show that the classification accuracy for the control condition is the highest with over 92% correctly classified trials. The lowest classification accuracy was achieved for the small nasal arc condition, for which 23.63% of trials get misclassified as being the control condition.

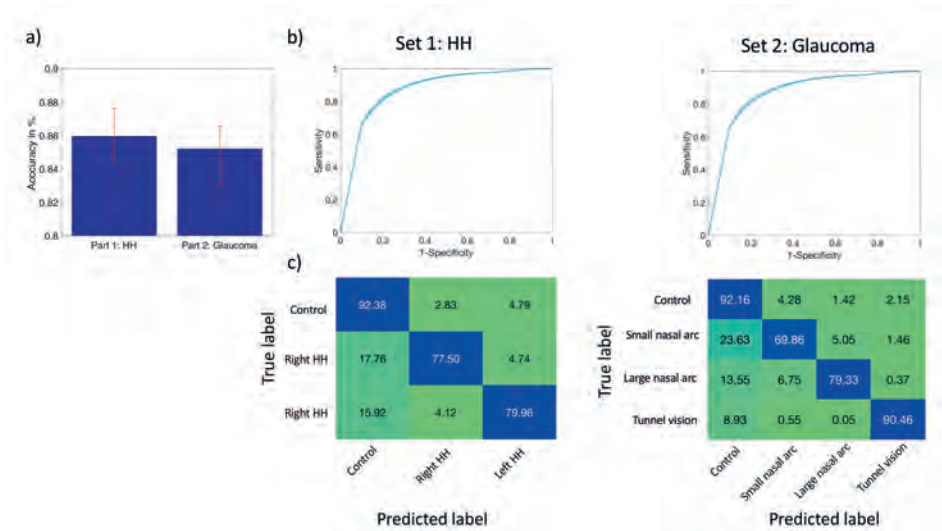


Figure 2.4: a) Overall classification accuracy of each part with error bars showing the minimum and maximum accuracy of the 10-fold cross validation. b) ROC curves for detecting the presence of an sVFD. The area under the curve for set 1 is 0.91 and for set 2 is 0.87. Error bars show the 95% confidence interval. c) The confusion plots when distinguishing between the different sVFD archetypes.

Reconstructing the sVFD

In the following two sections, we will show the results of the reconstruction of the sVFD using the distribution of VP and the comparisons of fixation density in the visual field per participant. We found that using the VP maps is our best approach to reconstruct the simulated HH archetypes, while the differential fixation maps are more closely correlated with the simulated glaucoma archetypes.

In the third section, we will show the results of the reconstruction based on both approaches for specific movie clips. The correlation of the reconstruction with the actual sVFD varies between movie clips.

1.) Reconstruction of the sVFD based on VP

Under normal viewing conditions, VP is high in all regions of the visual field, while in the simulated HH condition, the areas that are visible correspond to areas where fixations have a high VP (close to 1) and the masked areas correspond to areas with fixations that have on average a low VP (close to 0). The average correlation coefficient between the simulated right sided HH and its reconstruction was 0.38 (SD=0.23). The average correlation coefficient between the simulated left sided HH and its reconstruction was 0.24 (SD =0.31). Figure 2.5 shows the distribution of VP in the visual field averaged across all participants for each HH condition and some examples of the distribution of VP in the visual field of single observers. The different participants show some variance in the distribution of VP across the visual field. In the simulated glaucoma condition, it does not become clear where the sVFD was located when plotting the distribution of VP. It is simply high across the entire visual field in all conditions (see figure 2.6).

2.) Reconstruction of the VFD based on differential fixation density maps

In the differential fixation density maps, a lower p-value indicates a larger difference in the fixation density between the control condition and the simulated VFD conditions. In the simulated glaucoma conditions the distribution of p-values averaged across all observers showed that low p-values correspond mainly to the masked areas in the visual field. It is also possible to infer the location of the sVFD comparing fixation density of single participants to the average fixation density of all other participants in the control condition. There is some variance in the accuracy of the reconstruction between individual participants, as can be seen in figure 2.7. The average correlation coefficient of the small nasal arc was 0.26 (SD=0.1). The average correlation coefficient of the large nasal arc was 0.36 (SD=0.11) and the average correlation coefficient of the tunnel vision was 0.58 (SD=0.18).

In the simulated HH conditions high and low p-values are randomly distributed across the visual field and are therefore not useful to reconstruct the VFD, as shown in 2.8.

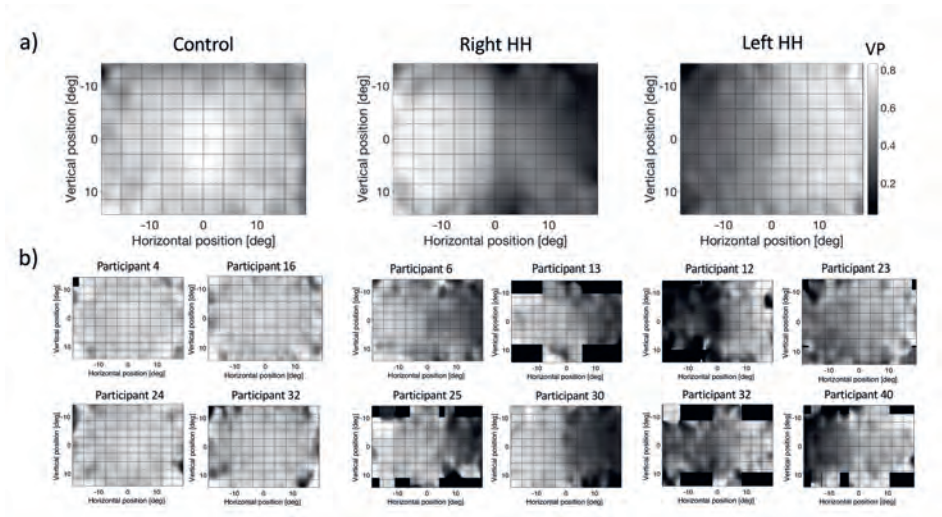


Figure 2.5: Distribution of VP in the visual field in the simulated HH conditions a) averaged over all observers b) examples of individual observers. A lower VP is indicated by a darker shade of gray, showing that the VP is lower in the areas of the sVFD. The grids were added on top of the maps to facilitate orientation for the viewer. The spatial distribution of VP is computed in a continuous manner.

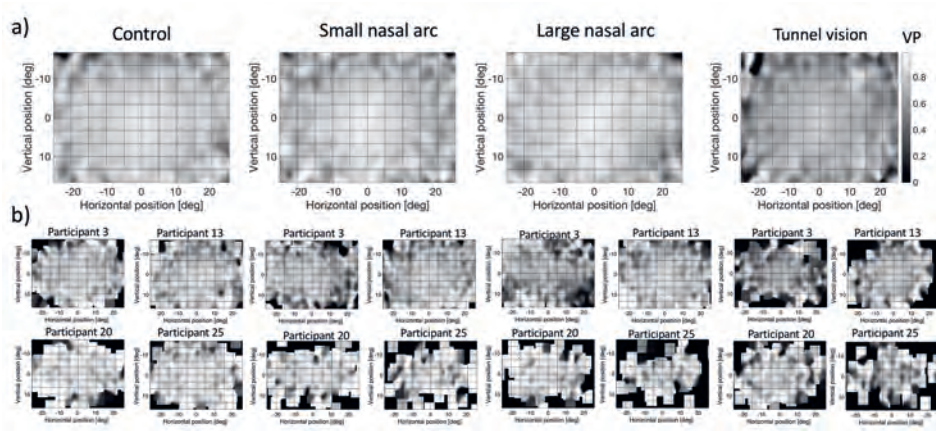


Figure 2.6: Distribution of VP in the visual field in the simulated glaucoma conditions a) averaged over all observers b) examples of individual observers.

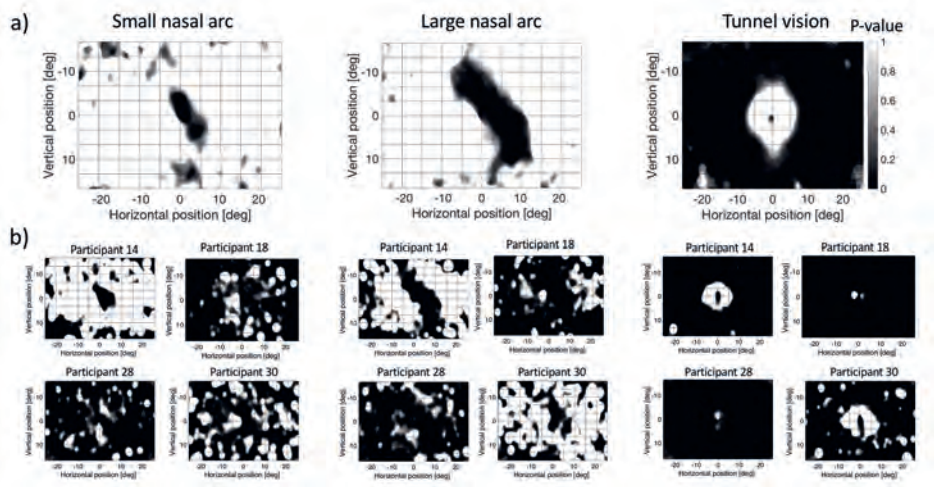


Figure 2.7: Differential fixation density maps, showing the distribution of p-values in the visual field in the simulated glaucoma condition a) averaged over all observers per condition b) examples of results obtained with different participants. A darker shade of gray represents a lower p-value showing that the fixation density in these areas is significantly different from the control condition.

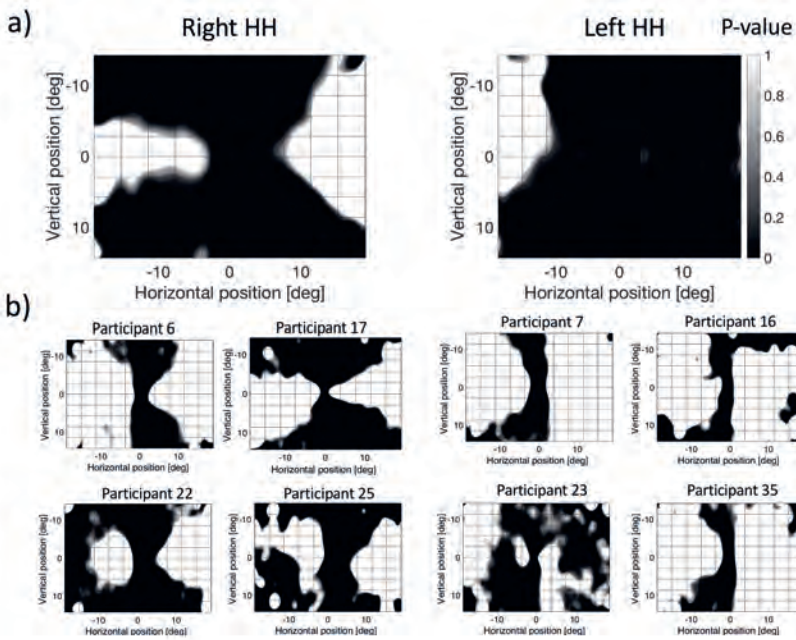


Figure 2.8: Differential fixation density maps, showing the distribution of p-values in the visual field in the simulated HH condition a) averaged over all observers per condition b) examples of different observers.

Saccade amplitudes and fixation duration

We computed the distributions of saccade amplitudes in 18 different directions to get a better understanding of how each sVFD influences the eye movements of the participants. In more concrete terms, we were interested in signs for potential compensatory strategies of our participants.

Figure 2.9 shows that in the two simulated HH conditions, participants made on average larger saccades towards the masked hemifield, especially in the horizontal direction. In the simulated glaucoma conditions, the saccade amplitude depends on the sVFD archetype. In both nasal arc conditions, our participants showed on average higher saccade amplitudes towards the masked parts of the visual field, with a bias for larger saccades in the horizontal direction. In the tunnel vision condition, saccade amplitudes in all directions were decreased compared to the control condition as measured with a two sample t-test ($p < 0.001$).

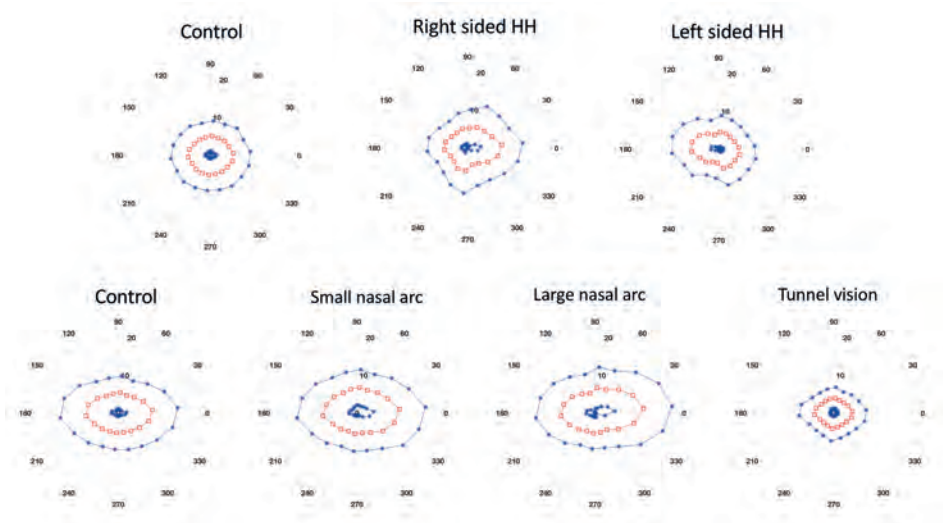


Figure 2.9: Average saccade length over all participants in the control condition and per sVFD archetype of both parts. The red squares show the mean saccade amplitude and the blue stars one standard deviation of each direction. Saccade amplitudes in degrees of visual angle.

In figure 2.10 we show the average saccade amplitudes and fixation durations of the first, middle and last tercile of the trials per viewing condition. We did not find significant differences between the three different groups with a one-way ANOVA, which we calculated for each part. Table 2.1 and 2.2 show the group means of each viewing condition and the F-values, degrees of freedom and p-values of the ANOVA.

Viewing condition	Fixation duration (ms.) group means: first, middle, and last tercile of trials	ANOVA results fixation duration	Saccade amplitude (deg.) group means: first, middle, and last tercile of trials	ANOVA results saccade amplitudes
Control	380; 398; 403	F= 0.56, df =2, p=0.58	8.0; 8.3; 8.1	F=1.05, df =2, p=0.36
Right sided HH	383;412; 383	F=0.51, df =2, p=0.61	8.9; 8.8; 9.3	F=0.48, df=2, p=0.62
Left sided HH	435; 428; 413	F= 0.48, df = 2, p=0.86	8.3; 8.1; 8.4	F=0.08, df = 2, p=0.92

Table 2.1: Group means and F-values, degrees of freedom and p-values as result of a one-way ANOVA of fixation duration and saccade amplitude of each viewing condition of the first, middle and last tercile of trials of dataset 1.

2.5 Discussion

Our main conclusion is that it is feasible to predict the presence and archetype of an sVFD with which an observer had been viewing a movie clip, based on the recorded eye movement data, for both simulated field defects that in some ways resemble those seen in HH and glaucoma. For single 1-min trials, this could be done with a mean accuracy of 85.6% (simulated HH) and a mean accuracy of 85.8% (simulated glaucoma). In addition, we were able to reconstruct the sVFD based on data from the same experiments, provided we integrated the data of at least several 1-min recordings. In fact, when combining the data of all participants that performed a specific simulation, visual field reconstructions

Viewing condition	Fixation duration (ms.) group means: first, middle, and last tercile of trials	ANOVA results fixation duration	Saccade amplitude (deg.) group means: first, middle, and last tercile of trials	ANOVA results saccade amplitudes
Control	354; 365; 357	F=0.18, df=2, p=0.83	10.0; 9.7; 9.7	F=0.34, df=2, p=0.71
Small nasal arc	360; 350; 340	F=0.8, df =2, p=0.45	10.7 deg, 10.7 deg, 10.8	F=0.05, df =2, p=0.95
Large nasal arc	354; 369; 350	F=0.8, df =2, p=0.62	11.2; 11.3; 11.3	F=0.08, df =2, p=0.92
Tunnel vision	318; 323; 315	F=0.18, df =2,p=0.83	5.6; 5.8; 5.7	F=0.25, df =2, p=0.78

Table 2.2: Group means and F-values, degrees of freedom and p-values as result of a one-way ANOVA of fixation duration and saccade amplitude of each viewing condition of the first, middle and last tercile of trials of dataset 2.

compared quite well to the simulated defects. Our results imply that the presence of a (simulated) visual field defect sufficiently changes viewing behavior (of normal-sighted controls) to use eye movement data as the basis for a clinically relevant screening on visual field defect, e.g. in patients unable to perform standard automated perimetry. In contexts in which the assessment time is not a limitation (e.g. at home), reconstructions may even become quite accurate.

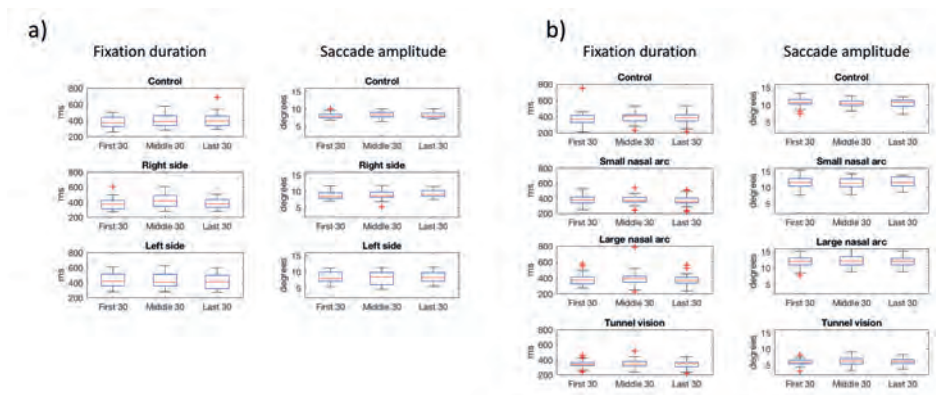


Figure 2.10: Box and whisker plots of fixation duration and saccade amplitude in each viewing condition a) of set 1 and b) of set 2 for the first, middle and last tercile of all trials. The red line indicates the median value per group, the box indicates the 25th and 75th percentile and the error bars show the most extreme values. Outliers are shown as red crosses.

Machine learning can predict the simulated visual field defect

In line with previous studies (Crabb et al., 2014; David et al., 2019), we found that machine learning is an effective way to separate sVFD from control conditions. We found that the spatial distribution of fixations in the visual field provides the necessary information to separate the sVFD and control conditions.

Based on the confusion plots, we found that the most difficult archetype to detect was the small nasal arc, which is not surprising, as it was the smallest sVFD. The identification of sVFD improved with size, with the tunnel vision condition being the most often correctly identified sVFD.

Especially in glaucoma, it is crucial to detect a VFD early on, when it is small to stop the progression of the disease early on. But it is the most challenging condition to detect. As the eye movement behavior is influenced, apart from the type of sVFD, by the content of the movie clip that is shown, we believe that classification accuracy could further improve if we could find the optimal content for the video clips.

Previous studies concluded that saccades are more informative than fixations when at-

tempting to classify eye movement behavior (Crabb et al., 2014; David et al., 2019). In our study, we use the relative distribution of fixations in space ('differential fixation maps'). By necessity, these are, however, closely related to saccade maps, such as used by Crabb et al. After all, participants must have made a saccade prior to a fixation. In contrast to saccade maps, the fixation maps also quantify any center bias of an observer, since we do not exclude the center of the visual field from the analysis. Saccade maps, on the other hand, may be more robust with respect to calibration errors as precise landing positions are less relevant.

The location of the sVFD can be reconstructed based on eye-movement behavior

In addition to classifying the viewing condition and sVFD type, we found that it was possible to reconstruct the VFD. Simulated HH could be reconstructed based on the distribution of VP, while the simulated glaucomatous VFD could be reconstructed based on differences in fixation density in the visual field of an observer. At present, reconstructions were made by combining the data of 22 (glaucoma) or 30 or 60 (HH) one-minute trials. As shown in figure S1 and S2, for some movies and simulations, it seems that when using one or two trials, the pattern of the sVFD already emerges.

Somewhat to our surprise, to reconstruct the VFD in the two different simulated pathologies required two rather different approaches. Presumably, this is the case because different types of visual field defects lead to fundamentally different viewing behavior, which we will discuss in detail in the following section.

Different sVFD result in different eye movement behavior and require different approaches for VFD reconstruction

We will now discuss a possible explanation for why the distribution of VP in the visual field is a good indicator for the location of the simulated HH but not for the simulated glaucoma conditions.

In HH, participants need to make many saccades into the masked part of the visual field. If they would not do this, they would end up looking at one side of the screen, with the mask entirely covering it. However, they are not able to direct their gaze towards an interesting part of the scene when saccading into the blind hemifield. Instead, they make

2

large horizontal saccades to swipe away the sVFD (see figure 2.9). However, these will be stereotypical and not driven by scene content, explaining the low VP. Making saccades into the blind hemifield is a viewing behavior that is also exhibited by (and taught to) hemianopia patients to improve their visual search performance (de Haan et al., 2015; Kennard, 2010). This strategy also explains why participants do not make fewer fixations in the complete area of the VFD in the simulated HH conditions than in the control condition. Observers have to direct the same number of fixations to each side of the visual field to not have the screen fully covered by the mask.

However, in the simulated glaucoma conditions, observers may not have an equally predictable viewing strategy to avoid blocking parts of the screen with the sVFD. In the two nasal arc conditions, the mask covers only a small part of the visual field, which makes it easier to predict whether there could be an interesting aspect of the scene covered by the mask. This would be most clearly the case in the small nasal arc condition. Additionally, when the mask covers relevant aspects of the movie scene, participants still have many options for directing their next saccade towards other visible parts of the scene. This may be a lowly prioritized part of the scene, which causes that their next fixation gets assigned a low VP. However, in the case of a small sVFD in particular an observer may still be able to predict, based on information surrounding the masked part, that the relevant part of the scene is hidden by the mask and thus direct their eyes towards it. In that case, the fixation would still be assigned a high VP.

In the simulated tunnel vision condition, the VP is on average lower in the entire visual field than in the other simulated glaucoma conditions, which may not be surprising as a large part of the visual field is masked, which makes it hard to follow the movie clip. Surprisingly, there is a less clear difference in VP between the (visible) center and (masked) periphery of the visual field as there is in the HH condition between the masked and unmasked part of the visual field. This may be due to an enhanced center bias and the short saccades in all directions in this condition. Participants do not seem to change their eye movement strategy over the time course of the experiment, while they get more used to the presence of the sVFD. At least this does not become apparent in basic eye movement features like fixation duration and saccade amplitude.

Stimuli used to evoke natural viewing behavior

Previous studies that investigated how VFDs influence natural viewing behavior have used static images (David et al., 2019) or longer movie clips Crabb et al. (2014). We decided to use movies to have movement as another salient feature that guides viewing behavior. Our movie clips are short, as the content of a movie clip can trigger a specific viewing behavior. By varying the content of our clips, we expected to obtain fixations that were more evenly distributed across the visual field. As figures 2.7 and 2.8 showed, not all movie clips are equally well suited to reconstruct the sVFD. Interestingly, for different archetypes of sVFD, different movie clips seem to be optimal. We conclude that a more variegated set of clips benefits visual field reconstruction.

Artificial scotomas

We simulated the VFD using gray masks to cover parts of the visual field, as is often done (e.g. David et al. (2019)). However, this is not how patients experience their VFD. Many patients experience filling-in of the missing parts of the visual field (Crabb et al., 2013). While in static conditions, healthy observers will also often fill-in such gray patches, the dynamic conditions and resulting jitter of the simulations in our experiment prevent this. Usually, patients gradually lose luminance sensitivity and this loss is different in both eyes. This means that they can adapt to a slow loss of vision over months and years. Healthy observers, being fully aware of which part of the visual field is masked, may therefore exhibit a different viewing behavior from patients. On the other hand, we know from previous studies that there are systematic differences in viewing behavior between patients and controls, and our methods are aimed at detecting those differences. For example, hemianopia patients make less regular and accurate saccades towards the affected side of their visual field during visual exploration of a scene (Zihl, 1995), which would arguably lead to a lower VP in the affected side of the visual field.

Future work

In future work, our approach needs to be tested with actual patients. Real VFDs are not perceived as grey areas in the field of view, but often are filled in with features from neighboring regions. Therefore, we need to test in patients whether our methods are

appropriate to detect actual VFDs (Crabb et al., 2013; Hoste, 2003). Moreover, there is still potential to optimize the selection of movie clips, as well as the methods for classification and reconstructing the VFD.

Conclusion

Our findings suggest that it is feasible to use natural viewing behavior recorded while participants view short movie clips to detect the presence of a sVFD. Moreover, it is possible to accurately reconstruct the sVFD. Movie clip viewing in combination with eye tracking may thus provide an alternative for or complement SAP, in particular for patients unable to perform SAP, such as young children, and vulnerable patients.

Acknowledgements

We want to thank Joost Heutink for mediating access to the Psychology student pool. Funding: This project has received funding from the European Unions Horizon 2020 research and innovation program under the Marie Skłodowska-Curie grant agreement No. 641805(EGRET) and No. 641805 (NextGenVis) and the Graduate School of Medical Sciences (GSMS), of the University Medical Center Groningen, University of Groningen. The funding organizations had no role in the design, conduct, analysis, or publication of this research.

References

- Asfaw, D. S., Jones, P. R., Smith, N. D., and Crabb, D. P. (2018). Data on eye movements in people with glaucoma and peers with normal vision. *Data in Brief*, 19:12661273.
- Bahnemann, M., Hamel, J., De Beukelaer, S., Ohl, S., Kehrer, S., Audebert, H., and Brandt, S. A. (2015). Compensatory eye and head movements of patients with homonymous hemianopia in the naturalistic setting of a driving simulation. *Journal of Neurology*, 262(2):316325.
- Birt, C. M., Shin, D. H., Samudrala, V., Hughes, B. A., Kim, C., and Lee, D. (1997). Analysis of reliability indices from humphrey visual field tests in an urban glaucoma population. *Ophthalmology*, 104(7):11261130.
- Cornelissen, F. W., Bruin, K. J., and Kooijman, A. C. (2005). The influence of artificial

- scotomas on eye movements during visual search. *Optometry and Vision Science: Official Publication of the American Academy of Optometry*, 82(1):2735.
- Cornelissen, F. W., Peters, E. M., and Palmer, J. (2002). The eyelink toolbox: Eye tracking with matlab and the psychophysics toolbox. *Behavior Research Methods, Instruments, and Computers*, 34(4):613617.
- Crabb, D. P., Smith, N. D., Glen, F. C., Burton, R., and Garway-Heath, D. F. (2013). How does glaucoma look? patient perception of visual field loss. *OPHTHA*, 120(6):11201126.
- Crabb, D. P., Smith, N. D., and Zhu, H. (2014). Whats on tv? detecting age-related neurodegenerative eye disease using eye movement scanpaths. *Frontiers in Aging Neuroscience*, 6(NOV):110.
- David, E. J., Lebranchu, P., Perreira Da Silva, M., and Le Callet, P. (2019). Predicting artificial visual field losses: A gaze-based inference study. *Journal of Vision*, 19(14):22.
- de Haan, G. A., Melis-Dankers, B. J. M., Brouwer, W. H., and Tucha, O. (2015). The effects of compensatory scanning training on mobility in patients with homonymous visual field defects: A randomized controlled trial. *Plos ONE*, page 129.
- Hoste, A. M. (2003). New insights into the subjective perception of visual field defects. *Bulletin de La Société Belge d'ophtalmologie*, 287:6571.
- Johnson, L. N. and Baloh, F. G. (1991). The accuracy of confrontation visual field test in comparison with automated perimetry. *Journal of the National Medical Association*, 83(10):895898.
- Kanjee, R., Yücel, Y. H., Steinbach, M. J., González, E. G., and Gupta, N. (2012). Delayed saccadic eye movements in glaucoma. *Eye and Brain*, 4:6368.
- Kasneji, E., Sippel, K., Heister, M., Aehling, K., Rosenstiel, W., Schiefer, U., and Pappageorgiou, E. (2014). Homonymous visual field loss and its impact on visual exploration: A supermarket study. *Translational Vision Science and Technology*, 3(6).
- Kennard, C. (2010). Compensatory strategies following visual search training in patients with homonymous hemianopia: an eye movement study. *Journal of Neurology*, page 18121821.

- 2
- Kübler, T. C., Kasneci, E., Rosenstiel, W., Heister, M., Aehling, K., Nagel, K., and Papa-georgiou, E. (2015). Driving with glaucoma: Task performance and gaze movements. *Optometry and Vision Science*.
- Lamirel, C., Milea, D., Cochereau, I., Duong, M. H., and Lorenceau, J. (2014). Impaired saccadic eye movement in primary open-angle glaucoma. *Journal of Glaucoma*, 23(1):2332.
- Marsman, J.-B. C., Cornelissen, F. W., Dorr, M., Vig, E., Barth, E., and Renken, R. J. (2016). A novel measure to determine viewing priority and its neural correlates in the human brain. *Journal of Vision*.
- Skenduli-Bala, E., De Voogd, S., Wolfs, R. C. W., Van Leeuwen, R., Ikram, M. K., Jonas, J. B., and De Jong, P. T. V. M. (2005). Causes of incident visual field loss in a general elderly population: The rotterdam study. *Archives of Ophthalmology*, 123(2):233238.
- Smith, N. D., Glen, F. C., and Crabb, D. P. (2012). Eye movements during visual search in patients with glaucoma. *BMC Ophthalmology*.
- Tant, M. L. M., Cornelissen, F. W., Kooijman, A. C., and Brouwer, W. H. (2002). Hemianopic visual field defects elicit hemianopic scanning. *Vision Research*, 42(10):13391348.
- Trauzettel-Klosinski, S. and Brendler, K. (1998). Eye movements in reading with hemianopic field defects: The significance of clinical parameters. *Graefes Archive for Clinical and Experimental Ophthalmology*, 236(2):91102.
- Wild, J. M. (1988). Techniques and developments in automated perimetry: A review. *Ophthalmic and Physiological Optics*, 8(3):295308.
- Zihl, J. (1995). Visual scanning behavior in patients with homonymous hemianopia. *Neuropsychologia*, 33(3):287303.

2.6 Supplementary Material

List of movies used

1. Haai Five
2. Beestenboot
3. Jets
4. Buurman en Buurman
5. Knabbel en Babbel
6. Donald Duck
7. Bambi
8. Beauty and the Beast
9. Jungle Book
10. Russen
11. Spangen
12. Baantjer
13. Dik Trom
14. Dansen op de vulkaan
15. 5 kinderen en it
16. Freek in het wild
17. Freek op safari
18. Nieuwe wildernis

Reconstruction of the sVFD based on data of single movie clips

We were interested in the effect of the content of a movie clip on the quality of the reconstruction of the sVFD. Therefore, we reconstructed them based on the data of each movie clip using both approaches (VP and differential fixation maps), combining the data of all participants who had watched the movie in the same condition. When reconstructing the VFD based on data of single movie clips, we observe some differences in the distribution of VP in the simulated HH conditions depending on which movie clip was presented, as shown in figure S1. The differential fixation maps computed from the simulated glaucoma conditions are much more variable than the VP maps from the HH condition. There are more archetypes in the glaucoma condition and therefore fewer trials of one movie clip with the same sVFD. Figure S2 shows the simulated glaucoma archetypes. We found that small or large nasal arcs can be reconstructed using nine or ten trials of, for example movie clip 10, 17 or 44. Using only four trials of movie clip 88 leads to a pretty good reconstruction of the large nasal arc.

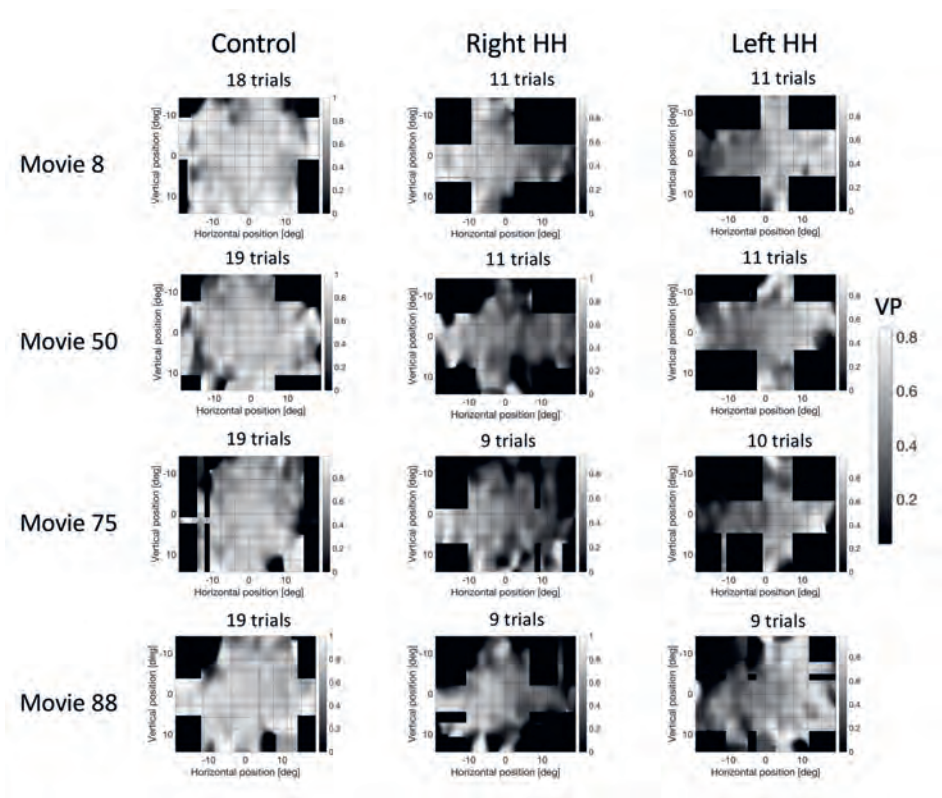


Figure 2.11: Examples of average VP maps obtained for participants viewing a particular movie clip with simulated HH.

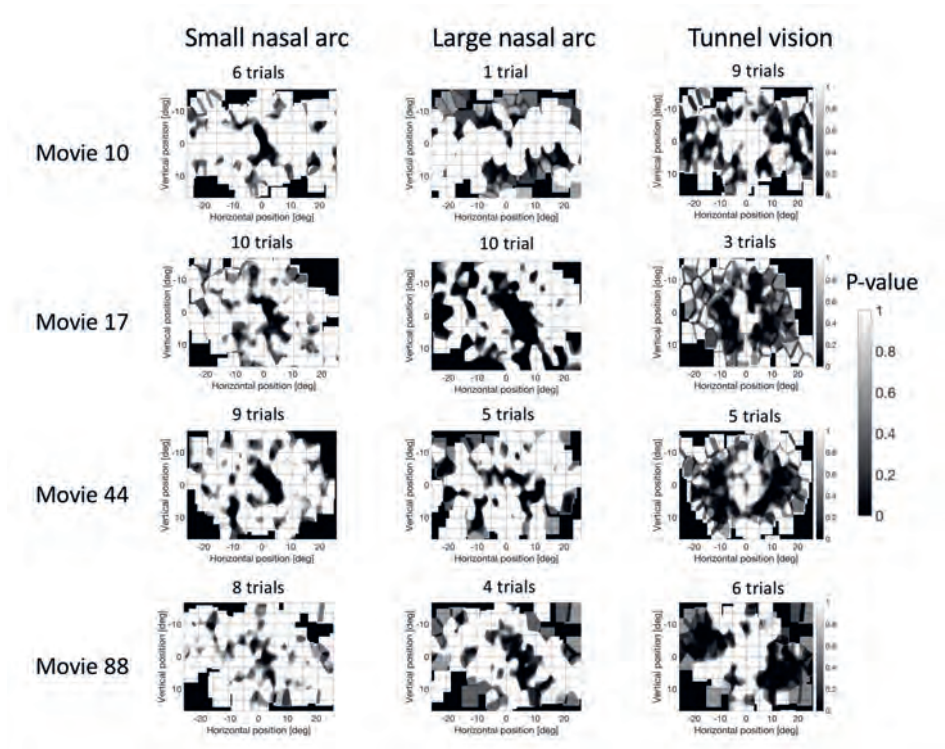


Figure 2.12: Examples of differential fixation maps averaged across participants for a particular movie clip watched with simulated glaucoma.

How free-viewing eye movements can be used to detect the presence of visual field defects in glaucoma patients

this chapter is based on: Gestefeld, B., Marsman, J. B. C., and Cornelissen, F. W. (2021). How free-viewing eye movements can be used to detect the presence of visual field defects in glaucoma patients. *Frontiers in Medicine, section Ophthalmology*, Accepted for Publication.

3.1 Abstract

Purpose: There is a need for more intuitive perimetric screening methods, which can also be performed by elderly people and children, currently unable to perform standard automated perimetry (SAP). Ideally, these methods should also be easier to administer, such that they may be used outside of a regular clinical environment. We evaluated the suitability of various methodological and analytical approaches for detecting and localizing VFD in glaucoma patients, based on eye movement recordings.

Methods: The present study consisted of two experiments. In experiment 1, we collected data from 20 glaucoma patients and 20 age-matched controls, who monocularly viewed 28 1-minute video clips while their eyes were being tracked. In experiment 2, we re-analyzed a published dataset (Asfaw et al., 2018), that contained data of 44 glaucoma patients and 32 age-matched controls who had binocularly viewed 3 longer-duration (3, 5 and 7 mins) video clips. For both experiments, we first examined if the two groups differed in the basic properties of their fixations and saccades. In addition, we computed the viewing priority (VP) of each participant. Following Crabb et al. (2014), for each participant, we mapped their fixation locations and used kernel Principal Component Analysis (kPCA) to distinguish patients from controls. Finally, we attempted to reconstruct the location of a patients VFD by mapping the relative fixation frequency and the VP across their visual field.

Results: We found direction dependent saccade amplitudes in glaucoma patients that often differed from those of the controls. Moreover, the kPCA indicated that the fixation maps of the two groups separated into two clusters based on the first two principal components. On average, glaucoma patients had a significantly lower VP than the controls, with this decrease depending on the specific video viewed.

Conclusions: It is possible to detect the presence of VFD in glaucoma patients based on their gaze behavior made during video viewing. While this corroborates earlier conclusions, we show that it requires participants to view the videos monocularly. Nevertheless, we could not reconstruct the VFD with any of the evaluated methods, possibly due to compensatory eye movements made by the glaucoma patients.

3.2 Introduction

Screening for visual field defects (VFD) as well as monitoring their progression is critical in the management of many ophthalmic diseases, such as glaucoma. The risk for developing a VFD increases with age. It is crucial to detect its presence early on, especially in glaucoma patients who, eventually, will become blind if disease progression is not halted through treatment. The current gold standard method for detecting visual field defects (VFD) is standard automated perimetry (SAP). It requires the tested person to fixate their gaze on a single point and to press a button every time that they perceive a stimulus in the periphery of their visual field. This means that they have to maintain a high level of attention over a prolonged period of time. It is also required that the participant correctly understands the task. As a consequence, SAP is rather difficult to perform for children under the age of seven years, many elderly people, and people with attentional problems (Morales and Brown, 2001; Mendieta et al., 2021; Wall M., 2004). This is problematic, as non-compliance will increase test duration and can negatively impact the precision of the measurement (Katz and Sommer, 1990). Therefore, there is a need for screening tests which are easier to perform and more engaging than the current ones.

Exploiting naturally occurring eye movements to monitor the occurrence of VFD

One of the most difficult aspects of SAP is that the patient needs to fixate a single point while attending to stimuli appearing in their visual periphery. Rather, ones natural tendency would be to make an eye movement to such suddenly appearing stimuli. In our view, rather than asking the patient to suppress such reflexive tendencies, one should try to exploit these tendencies when screening for the presence of a VFD. Previous studies have attempted to simplify the gold standard perimetric test by instructing participants to make saccades towards the target stimuli presented in the periphery, instead of pressing a button while maintaining fixation. Previous studies found that the saccadic reaction time of glaucoma patients is significantly lower than those of normal-sighted controls and concluded that this feature could be exploited in a new type of perimetric screening test (Mazumdar et al., 2014). In our current study, our specific goal was to avoid giving our participants a task on which they had to focus, and present stimulus material that is

naturally engaging for most people and that would evoke spontaneous viewing behavior. This is why we chose to show short video clips and simply asked our participants to just view and enjoy them, while we recorded their eye movements. If we could find differences in the free-viewing eye movement behavior of glaucoma patients and normal-sighted controls using this approach, this could result in a very intuitive way of screening for the presence of a VFD. Such an approach could potentially be more suitable for use in people that have trouble with performing SAP. However, such variegated target groups are less suitable for evaluating a new approach, which is why in the present study we focus on adult glaucoma patients.

VFD influence eye movements

Previous research has shown that patients with VFD differ from normal-sighted controls in various eye movement features. However, these differences are often subtle and the results of studies could differ depending on their experimental paradigm. Observers with simulated VFD showed longer fixation durations during visual search (Cornelissen et al., 2005). Moreover, Smith et al. (2011) found that glaucoma patients made fewer saccades during visual search than normal-sighted controls. In contrast, Wiecek et al. (2012) found no differences in participants with actual VFD, compared to controls, in search and fixation duration, saccade amplitude or the number of saccades made. These differences between visual search studies can be attributed to differences in experimental design and whether the VFD was real or simulated. While Cornelissen et al. (2005) used computer generated search displays containing Landolt-Cs and simulated the VFD, the other two studies used photographs of natural scenes, and included participants with actual VFD. However, the two latter studies differed in them recording binocular (Smith et al., 2011) or monocular (Wiecek et al., 2012) viewing behavior. These examples demonstrate how differences in experimental design may affect the outcome of studies on the influence of VFD on eye movements.

Cross validating previous methods of analysis

Previous studies have shown that it is possible to detect the presence of either real or simulated VFD based on free viewing eye movements (Crabb et al., 2014; David et al., 2019; Gestefeld et al., 2020). Moreover, simulated VFD could even be reconstructed based on

an analysis of these free viewing eye movements (Gestefeld et al., 2020). However, there have only been few studies on this topic and the methods that were used have not been cross-validated on different data sets. In addition, it is critical to verify whether results that have been achieved with simulated VFD can be replicated in participants with real VFD. It is known that patients experience their loss of sensitivity in the visual field differently from how VFD are simulated (Glen et al., 2013). Previously, we simulated the VFD by masking parts of the visual field with a gray-level bitmap, resulting in a VFD which was noticeable, instantaneous and blocked parts of the visual field completely (Gestefeld et al., 2020). A real glaucomatous VFD does not have any of these attributes. Often, glaucoma patients are not even aware of their VFD due to their brain filling-in the missing information (Carvalho et al., 2019). The consequence of filling-in on viewing behavior is unknown. Therefore, while it is obvious that simulated and real VFD differ in many ways, the consequences thereof, for our ability to use eye movements to detect VFD, is not. Consequently, it is critical to evaluate whether analysis methods are also suitable for detecting VFD in actual patients.

The present study consists of two experiments with slightly different paradigms. For our first experiment, we collected eye movement data from 20 glaucoma patients and 20 age-matched controls, who watched 28 video clips of one-minute length with one eye. In the second experiment, we reanalyzed a data set (Asfaw et al. (2018a) in which 44 glaucoma patients and 31 controls watched three different video clips of varying length with both eyes simultaneously. All glaucoma patients who participated in these two experiments had asymmetrical visual field loss, which meant that the state of their visual field changed depending on whether they viewed the stimulus with one or with both eyes. We hypothesized that the free-viewing eye movements of the glaucoma patients, made while viewing video clips, would differ from those of normal-sighted controls. More specifically, we tested whether we could detect and localize the VFD. Since our comparison will be to gold standard SAP, which is performed monocularly, in experiment 1 we choose to record viewing behavior monocularly. This will allow us to compare the VFD reconstruction based on viewing behavior to visual field sensitivity as determined by SAP. In contrast, the eye movement data of experiment 2 was recorded during binocular viewing. A comparison over studies may allow us to answer if using one or two eyes to view videos leads to different viewing behavior in patients and which approach

is most suitable for screening for VFD. We performed nearly identical analyses on both data sets. This way, we could determine which analyses, experimental conditions and video materials best separate patients and controls.

First, we compared the group medians of different basic eye movement features. We also compared the viewing priority (VP) of the two groups (Marsman et al., 2016). VP can be used to express the similarity in the viewing behavior of an individual to that of a peer-group of observers watching the same movie, while taking into account any inherent biases (e.g., center bias) in viewing behavior that may be present (e.g., induced by the use of a specific set-up, such as a screen). The VP algorithm takes the viewing behavior of a large group of observers, both made during a specific movie and during a number of other movies, as the starting point for its comparison. The VP of a given fixation is calculated using fuzzy c-means clustering. First, the distance to a set of reference fixations is measured. Reference fixations are fixations made by other observers during the same time interval, while watching the same video clip. This means that we compare the locations of fixations of one participant to those of other participants, while they are viewing the same content. In addition, the distance of the reference fixations to a set of random fixations are calculated. Random fixations are fixations made by other observers during the same time interval, while watching a different video clip. In summary, VP measures the similarity of the viewing behavior of a selected observer to and a reference group, while taking into account content independent biases.

In addition, we cross validated and replicated another method of analysis which had previously been used to separate glaucoma patients and controls, namely kernel principal component analysis (kPCA) in combination with naive Bayes classification (Crabb et al., 2014). In kPCA, the original data, in the case of this study the proportion of saccade end points in a grid across the visual field, is transformed into a higher dimensional space, where it can be linearly separated. For the purpose of this study, it would be ideal if the patients could be separated from the controls in this new space.

In addition to separating the two groups, we attempted to reconstruct the location of the VFD using two different methods. We computed the distribution of the VP and the distribution of fixation frequency over the visual field aiming at identifying damaged regions in the visual field based on a reduced VP or a deviating frequency of fixation from the control group. The underlying assumption of this analysis is that patients with VFD would systematically miss salient information in damaged parts of their visual field, due

to a reduction in the bottom-up information. As such, in the absence of any compensatory strategies, they would be expected to make fewer saccades towards the damaged part of their VF. Using a top-down strategy, patients may try to compensate for their VFD by frequently directing their gaze towards the damaged parts of the visual field. If successful, the distribution of fixations across the visual field would not differ between patients and controls. In fact, a patient may even fixate the damaged parts of the visual field more frequently than the controls. However, in such a case, the viewing priority in the damaged areas of the visual field of the patients would be lower, because such compensatory eye movements would not necessarily be directed at conspicuous events or parts in the scene.

Next, the methods and results for each of the two experiments will be described in separate sections. In the discussion, we will compare and discuss the results of the two experiments.

Experiment 1: Monocular eye movements under free-viewing conditions of glaucoma patients compared to those of normal sighted observers

Experiment 2: Binocular eye movements under free-viewing conditions of glaucoma patients compared to those of normal sighted observers

3.3 Experiment 1: Monocular eye movements under free-viewing conditions of glaucoma patients compared to those of normal sighted observers

3.4 Methods

Summary

In this experiment, we collected eye movement data of glaucoma patients and age matched controls, who each viewed a large number of short video clips. We occluded one eye, with the aim of eliminating any putative compensation of the VFD between the two eyes in the glaucoma patients, and obtaining results under similar conditions as in SAP. Showing short video clips also allowed us to analyze the eye movement features for each clip separately and investigate the influence of video content on eye movements.

Participants

We collected data from 31 glaucoma patients and 32 controls. The patients with VFD had a mean age of 64 years (range: 40-81 years) and the controls had a mean age of 60 years (range: 35-83). Details can be found in table 1. All participants had normal or corrected to normal visual acuity. We had to exclude the data of 11 glaucoma patients and 12 controls, due to an inability of the eye tracker to continuously measure the gaze position, due to a loss of the pupil or the corneal reflection. This was the case for participants (Glaucoma patients and controls) who wore multifocal glasses, participants with drooping eyelids or participants who had artificial lenses. As the eye tracker could not be used with multifocal glasses, we replaced them with a pair of trial lenses from the ophthalmology clinic, with the appropriate correction. However, this did not always enable the eye tracker to acquire data continuously. The ethics committee of the UMCG approved the study protocol. All participants provided written informed consent. The study followed the tenets of the Declaration of Helsinki.

Procedure

All participants watched 28 different video clips of one-minute length with one eye. The clips were taken from different types of videos, such as motion pictures, nature documentaries or comic films. The list of videos from which they were taken is provided in the supplementary material in table S1.

At the beginning of each session, we performed a standard 9-point calibration choose with which eye the participant would perform the experiment at random. Next, we performed a standard 9-point calibration using the built-in routines of the tracker and tested if we could obtain an accurate calibration. In case we could not obtain an accurate calibration, we also obtained the calibration accuracy for the other eye and performed the experiment with the most accurately calibrated eye. Details on the visual field of the glaucoma patients and on which eye was tracked in the experiment can be found in table 3.2. Participants were seated at 60 cm distance from the screen and were asked to place their head in a chin rest. They were asked to view the video clips as they would normally. We gave the participants the opportunity to take a break after each video clip.

The clinical data of the patients (visual fields and visual acuity) was obtained from their medical record at the UMCG. For the control group, either before or after they viewed

the video clips, we measured eye pressure, visual acuity, and used a frequency doubling technology (FDT) perimeter-based screening and an OCT image to rule out the presence of glaucoma and/or a VFD. In FDT, the participant has to fixate in the middle of the stimulus display, while flickering achromatic sinusoidal grating of low spatial frequency is presented. The participant has to press a button when they see a stimulus. A deviant FDT score is indicative of putative retinal ganglion cell damage associated with glaucoma (Cello et al., 2000). In addition, we performed a Montreal cognitive assessment test (Nasreddine et al., 2005) with all participants to rule out the presence of cognitive deficits.

Participant characteristics	Controls	Patients
Age range (in years)	35-83	40-81
Mean age (+SD)	60(10.39)	64(12.19)
Gender (in percentage)	male = 55%	male = 55%

Table 3.1: Characteristics of the participants

Patient ID	Age	Gender	eye tested	MD	IVF score
P003	70	male	left	-6.65/ -26.26	14
P004	73	male	right	-19.84/ -10.28	21
P008	64	male	left	-1.42/ -15.31	0
P009	66	female	right	-4.86/ -9.85	4
P010	69	female	right	-17.24/ -6.96	10
P013	41	male	right	-28.98/ -28.96	88
P014	72	female	left	-32.76/ -23.74	79

P016	69	male	left	-16.45/ -24.48	77
P021	78	male	right	-6/ 0.61	0
P022	65	female	left	-3.34/ -1.56	0
P023	47	female	left	-5.24/ -5.29	0
P025	78	male	left	-5.81/ -20.23	12
P026	81	male	right	-24.9/ -2.78	7
P027	67	male	left	-23.58/ -16.76	37
P028	60	male	left	-24.49/ -24.07	72
P029	64	male	right	only FDT available	n.a.
P030	77	male	left	-17.99/ -15.75	65
P031	63	female	right	-8.68/ -0.93	3
P032	68	female	right	-6.21/ -5.82	2

Table 3.2: This table shows the age, gender, with which eye they performed the experiment, the MD value of the tested and the covered eye and the IVF score of each glaucoma patient.

Stimulus presentation and eye tracking

We presented the video clips full-screen on a 50 cm by 35 cm (1920 x 1080 pixel) display (BenQ Zowie xl2540). Participants viewed the screen from a distance of 60 cm,

such that it covered a visual field of 45.2×32.5 deg (of visual angle). One eye of the participants was covered with a standard ophthalmic eye patch. Monocular eye movements were recorded with an Eyelink 1000 and an Eyelink duo eye tracker (SR Research) at 1000 Hz . The host PC was connected to a laptop running MATLAB (Version 2017b, MathWorks, Natick, MA) with the Psychtoolbox (Brainard, 1997; Kleiner et al., 2007) and the Eyelinktoolbox (Cornelissen et al., 2002) via Ethernet. All video clips were presented in the same order for each participant. The procedure was controlled by a custom Matlab script.

Selection of the video clips

We used a subset of the movies shown in Gestefeld et al. (2020). The movies were selected because, based on data recorded in the experiment of Gestefeld et al. (2020), they resulted in different viewing behavior in observers with and without various simulated VFD. The video clips we used for this study were selected based on the classification performance of a k-nearest neighbor (kNN) classifier distinguishing between four different classes (the three different simulated glaucoma archetypes and the control conditions) using data from each video clip. We then selected the video clips which showed a classification performance of $\geq 50\%$. This resulted in 28 1-minute video clips.

Data analysis

Fixations and saccades in visual field coordinates

The Eyelink 1000 processes the raw data using its built-in algorithms to define fixations and saccades. Saccades were defined using a velocity threshold of 30 deg./sec. and an acceleration threshold 8000 deg./sec.^2 . All other eye movement data was classified as a fixation. We used this pre-processed data for further analysis. The fixation location and saccade start and end points were provided as x-y coordinates on the screen, where the origin of the screen was the top left corner.

As the location of the visual field changes its location with every eye movement with respect to the scene, we define its origin at the starting point of each saccade. When analyzing fixations, we define the center of the visual field at the location of a fixation at a certain time point. The position of the next fixation was then determined with respect

to this fixation of which the location was the origin of the coordinate system. In terms of these visual field coordinates, eye movements to the left result in a negative coordinate along the x-axis and downward eye movements result in a negative coordinate along the y-axis.

Basic eye movement features

We first computed the mean fixation duration, the number of fixations, the mean saccade amplitude and the mean saccade velocity over all video clips for each subject and compared the two groups using a Wilcoxon-Mann-Whitney signed-rank test. A p-value of $p < 0.05$ was regarded as significant. As we compared 3 basic eye movement and, in a later analysis step, the VP of the two groups we corrected for 4 measurements. After Bonferroni correction for multiple comparisons a p-value of $p < 0.013$ was regarded as significant.

Comparison of directional saccade amplitudes of glaucoma patients and controls

Then we tested if the directional saccade amplitudes of individual glaucoma patients differed from those of the control group. We first estimated a normal range of median and maximum saccade amplitudes by computing them for all participants in the control group. We then determined whether the median and maximum saccade amplitude of each patient with VFD stayed within this normal range.

More precisely, we computed the median and maximum saccade amplitudes of each participant in 18 bins of 20 degrees of visual angle, spanning 360 degrees. For each of the glaucoma patients we computed the rank of the median and maximum saccade amplitude relative to those of the controls in the same directional bin. The rank order was normalized by dividing it by the number of controls, so that it ranged between 0 and 1. We then plotted the rank of the saccade amplitude in each direction and marked the upper and lower 2.5% of the normalized ranks with a dashed line (see figure 2).

To see if patients with similar types of VFD, in the eye that they used to watch the video clips, showed similar patterns in directional saccade amplitudes, we split our patients into six different groups according to the VFD in the tracked eye: peripheral VFD (scotoma outside the central 10 degrees), nasal arc, large peripheral VFD (tunnel vision), VFD

affecting the periphery and the central 10 degrees of the visual field, almost complete blindness and intact visual field. We did not perform any statistical inference tests, as we only had small groups of participants with a similar type of VFD.

Viewing priority

We calculated the viewing priority (VP) with the aim to determine whether the fixation locations of (individual) glaucoma patients differ systematically from those of the normal-sighted controls. We expect to find an overall lower VP in glaucoma patients, if they frequently fail to direct their gaze towards parts of the visual scene, which get fixated by the control group. In addition, we could use the VP to localize damaged parts of the visual field, if the VP of fixations after eye movements towards the damaged parts of the visual field was systematically decreased.

We extracted the fixations of each participant from the pre-processed data and computed the VP for each of them (Marsman et al., 2016; Gestefeld et al., 2020). To compute the VP of a fixation by one of our participants, we need a reference set of fixations and a random set of fixations, both consisting of fixations made by other participants. The more densely the reference fixations are clustered in the same region, compared to the random fixations, and the closer the fixation of interest is located to the reference fixations, the higher is the VP.

For both reference and random data set we used fixations made by the control group, because we know that the viewing behavior of normal-sighted observers during movie viewing is very consistent, with the fixations of most observers clustering in the same areas of a scene. Also, the aim of this study is to identify deviances of the glaucoma patients viewing behavior from normal viewing behavior. VP provides a very straightforward way to identify them.

We averaged the VP value from all fixations of each trial for each participant and used a Wilcoxon-Mann-Whitney test to compare the ranks of the two groups. After Bonferroni correction, a p-value <0.002 was regarded as significant. In addition, we computed the Pearson's correlation coefficient of the VP and the severity of the VFD. More precisely, we correlated the VP with the mean deviation (MD) of the luminance sensitivity (in dB) from normal as measured by SAP.

Firstly, we used the MD of the tracked eye. Secondly, we correlated the VP with the

MD of the two eyes combined. To calculate the severity of the two eyes combined, we used two different measures. The first one was simply the mean MD of both eyes and the second one the integrated visual field score (IVF score), as described in (Crabb and Viswanathan, 2005).

The IVF score is calculated by taking the maximum contrast sensitivity of each overlapping location in the visual field as the contrast sensitivity of that location. From this combined visual field, the 52 locations that make up the integrated visual field were considered in turn. A location got a score of 0 if it exhibited a measured threshold severity of ≥ 20 dB, scored one if it had a threshold between 10 dB and 19 dB, and scored 2 for a threshold below 10 dB.

Lastly, we compared the VP to the between eye difference in MD of the open and the close eye. If the difference is positive, it means that the patient watched the clips with their better eye.

Comparison of the spatial distribution of eye movement features in the visual field between groups

The method used in this section is a partial replication of Crabb et al. (2014), who previously used kernel principal component analysis (kPCA) in combination with a naive Bayes classifier to separate participants with and without VFD. As we did not have enough data to use machine learning, we only applied kPCA and visualized the results. First, we defined a grid spanning the part of the visual field in which most eye movements occurred, given that the observer has an intact visual field. This area was determined by computing the median saccade amplitudes of the control group in 18 bins of 20 degrees of visual angle, adding two standard deviations. To fit a rectangular grid over this area it needs to cover 21 degrees half angle in the horizontal directions and 11 degrees half angle in the vertical directions. The bin size was two degrees of visual angle, as this bin size had also been applied by Crabb et al. (2014). For each trial we counted the number of fixations that fell into each bin and divided the number by the maximum value of all bins so that the values range between zero and one. We then computed the Euclidean distances between the fixation maps coming from the same video clip of different observers. The mean (*meanDist*) and the maximum (*maxDist*) of these distances were then used to construct the kernel matrices to transform the data into the feature space. We constructed

one kernel of two participants i and j considering the data from all video clips using the following formula:

$$k_{ij} = \exp(-0.5(\text{meanDist} + \text{maxDist})^2/2^2) \quad (3.1)$$

In addition,, we computed one kernel per video clip of two participants i and j using the Euclidean distance (textitDist) between the fixation maps of the respective video clips. We used the following formula:

$$k_{ij} = \exp(-\text{Dist}) \quad (3.2)$$

considering data of one trial only. After transforming the data into feature space, we plotted the data along the first two feature axes to visualize the distances between the fixation maps of the different participants. If the spatial distribution of fixations between the two groups is different, the transformed data should form separable clusters in the new feature space.

Reconstructing the VFD based on the spatial distribution of eye movement features in the visual field

To test if we could reconstruct the location and shape of the VFD, we computed the average VP and the distribution of the relative fixation frequency across the visual field in a continuous manner.

To compute the distribution of VP across the visual field, we collected the fixation locations of all trials per participant and computed a fixation heat map, where each fixation was modelled as a Gaussian with a standard deviation of 1 degree. The standard deviation of the Gaussian reflects the accuracy of the eye movement data that measure the position of the eye with an error of up to 0.5 degree of visual angle. Hence, the Gaussian reflects the potential measurement error in each direction. It also reflects the size of the area in which the participants can see detail, as it is approximately the size of the foveal part of the visual field. We weighted this fixation heat map by the VP values, as well as a fixation map, where only the Gaussians were added up. We then divided the two maps, ending up with a map depicting the distribution of average VP values across the visual field.

To compute maps showing the relative frequency of fixations, with respect to the controls, we again computed heat maps of fixations as described above. We computed one

map for each participant, averaged over all trials and z-normalized the data. For each glaucoma patient we then counted how many controls had a smaller proportion of fixations in the same location of the visual field and divided this number by the number of control participants. This way, we obtained a map showing the distribution of fixations of each patient in relation to the control group as a normalized rank value, ranging between 0 and 1.

To be better able to relate the contrast sensitivity of the visual field, as measured with the HFA to the relative frequency of fixations in the visual field of the patients, we performed the same analysis as described above with the modification to compute the relative fixation frequency in discrete bins.

We defined a grid spanning 30 degrees of visual angle divided into bins of 6 degrees, analogous to the test locations of the HFA SITA 30-2 visual field test, which we obtained from the patients clinical dossier. We correlated the relative proportion of fixations in each bin with the contrast sensitivity values measured at the same location in the visual field. Then, we computed the proportion of fixations that fell into each bin averaged over all trials of each participant and compared the discrete fixation map of each patient to the fixation maps of the controls. We then obtained a relative fixation frequency map per bin. We plotted the sensitivity value against the proportion of fixations of each location and fit a regression line through the points.

3.5 Results

Basic eye movement features

The median fixation duration was 310.96 ms. (SD = 60.26 ms.) for the control group and 298.94 ms. (SD = 83.64 ms.) for the VFD group. The Wilcoxon-Mann-Whitney test showed no significant difference between the two groups for this feature ($p=0.694$, $z\text{-score}=0.39$). The median saccade amplitude was 5.42 deg. (SD=0.87 deg.) for the control group and 4.49 deg. (SD=1.63 deg.) for the VFD group. The p-value of the Wilcoxon-Mann-Whitney U-test was $p = 0.025$ ($z\text{-score}=2.25$), which was not significant after Bonferroni correction. The median saccade velocity was 75.14 deg./min. (SD=34.56 deg./min.) for the control group and 48.81deg./min. (SD=40.93 deg./min.) for the VFD group. The Wilcoxon-Mann-Whitney test showed no significant difference between the two groups for this feature ($p=0.081$, $z\text{-score}=1.74$). Figure 3.1 shows box and whisker plots for each of the three features for patients and controls, with circles

representing the values of individual participants.

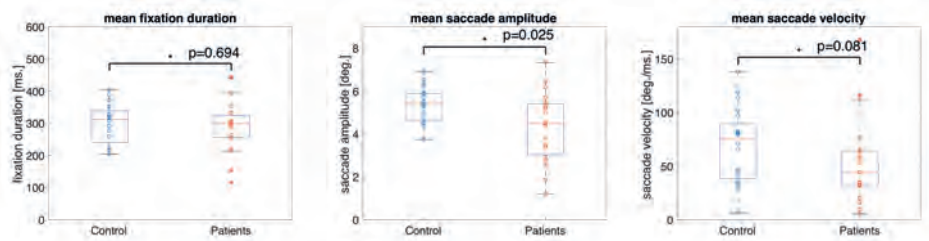


Figure 3.1: Box and whisker plots showing the means and 25-75 percentiles of four different eye movement features of glaucoma patients and controls. Circles represent the results of individual participants.

Comparison of directional saccade amplitudes between patients and controls

We tested whether the location of the VFD has an influence on saccade amplitudes by comparing the saccade amplitudes in 18 different directional bins of each patient and the control group. We hypothesized that the saccade amplitudes that patients made towards directions in which a VFD was located would differ from the saccade amplitudes of the control group towards the same location. We tested this hypothesis by computing the ranks of the directional saccade amplitudes of each patient with VFD compared to the control group. Figure 3.2 shows in which directions the median and maximum directional saccade amplitudes of representative glaucoma patients differ from those of the control group. It shows their ranks relative to the saccade amplitudes of the control group. As a reference, it also shows the average VP of this patient over all trials and the visual field sensitivity of both eyes.

Patients with peripheral VFD in the tracked eye, as shown in panel 2a, mostly showed similar saccade amplitudes to the control group. However, the second patient in panel 2a displayed lower median saccade amplitudes than the control group in several directions, with ranks of those saccade amplitudes being below the 5% lowest saccade amplitudes of the controls.

The first patient shown in panel 2b showed smaller median saccade amplitudes than the

control group, except in the directions where the VFD in the tracked eye was located. The second patient in panel 2b showed similar median saccade amplitudes to the control group, making the largest saccades towards the area of the nasal arc.

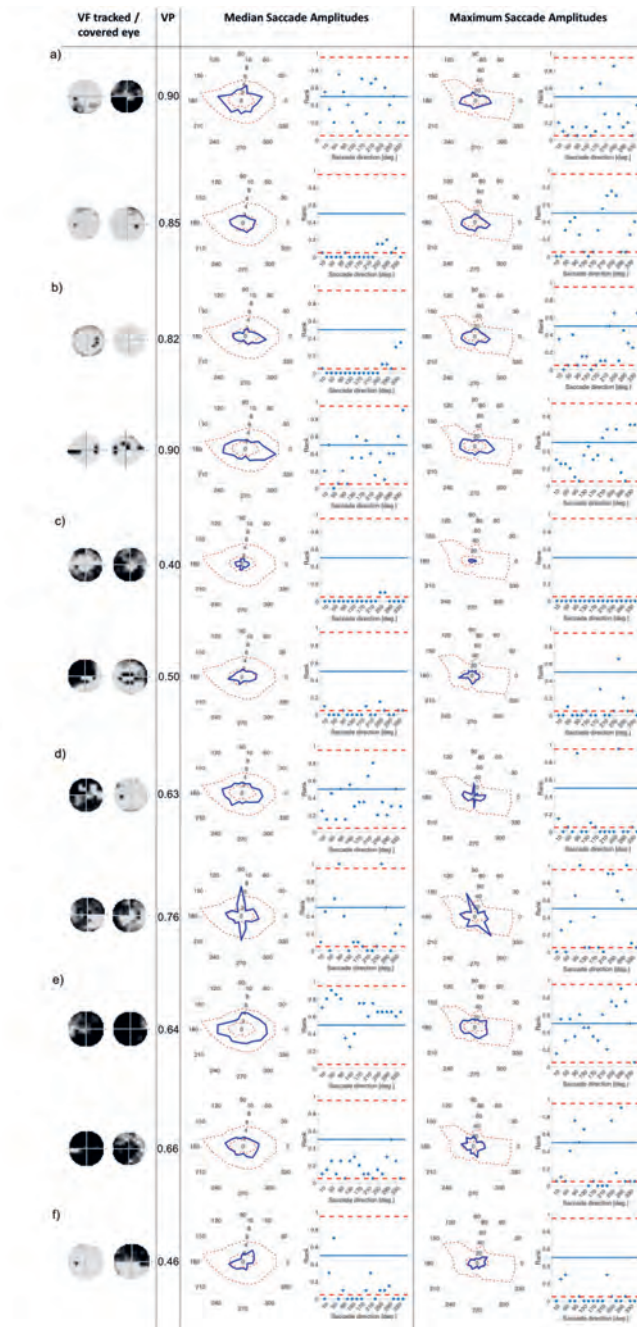
The patients with tunnel vision in the tracked eye, shown in panel 2c showed lower median and maximum saccade amplitudes compared to the control group in all directions.

The first patient in panel 2d, with a large VFD in the tracked eye, that also reached the center of the visual field, showed similar median saccade amplitudes to the control group, but reduced maximum saccade amplitudes. The second patient in panel 2d showed similar median and maximum saccade amplitudes as the control group, except in the vertical directions. The upwards and downwards saccade amplitudes are larger than those of the control group.

Panel 2e shows two patients, who were almost blind in their tracked eye. They showed similar median and maximum saccade amplitudes to the controls. The first one shows median saccade amplitudes above the average of the control group, while the second one shows median saccade amplitudes below the average of the control group. But both of them remain within the 95% confidence interval of the control group.

Panel 2f shows the patient who performed the experiment with their intact eye. This patient displayed slightly shorter median and maximum saccade amplitudes than the controls, especially towards the top-left and lower right quadrant of the visual field.

How free-viewing eye movements can be used to detect the presence of visual field defects in glaucoma patients



3

Figure 3.2: This figure consists of a series of panels, each for a group of patients with different VF characteristics. In each panel, the first column shows the visual fields of the patient as measured by SAP, with darker areas representing the less sensitive areas of the visual field. The second column lists the average VP of the patient. The left figure in the third column shows the median saccade amplitude in 18 different directions for individual patients (large red dot). For comparison, we plot saccade amplitudes of individual control participants (small blue dots) and the median saccade amplitude of the control group (a big blue dots). The figure on the right shows, in terms of saccade amplitude per direction, the normalized rank of the saccades of the patient amongst those of the controls. Red lines represent the 95% confidence intervals). In the fourth column, the figures show the same for the maximum saccade amplitude.

a) Patients with peripheral visual field loss in the tracked eye. The first two patients have large VFD in their covered eyes. b) Patients with a nasal arc or other small VFD, which were closer to the center than the VFD of the patients in the first group. c) Patients with VFD that approximate tunnel vision in the tracked eye. d) Patients with large VFD in various parts of the visual field. e) Patients who are almost blind. f) Patient, with an intact visual field of the tracked eye.

Viewing priority

We compared the median VP of patients and controls to test if the scan paths of the two groups differed when viewing the different video clips using a Wilcoxon Mann Whitney test. The median VP value of the control group was 0.91 (SD = 0.06) and the median VP of the glaucoma group was 0.76 (SD=0.21). The group medians in VP of the two groups are significantly different when taking the average VP over all trials ($p < 0.001$, z score = 4.34). Figure 3.3a shows these results as a boxplot. When computing the average VP per trial we found that the group median of the glaucoma patients was significantly lower ($p < 0.002$) for 22 out of 28 movie clips. Boxplots showing the range of VP values and the group medians for the control group and the glaucoma group of exemplary video clips can be seen in figure 3.3b.

While the group median VP of the patients was reduced compared to the control group, figure 3.3 also shows that there is a high variance in VP among the patients with VFD. We

correlated the average VP of the patients with VFD with measures indicating the severity of the visual field damage obtained by SAP to determine which factors could potentially influence this variability. Figure 3.4 shows the correlation of the VP values with the MD of the tracked eye, the IVF score and the difference of the MD of the two eyes. We found no correlation between the VP value averaged over all trials and the MD of the tracked eye (Pearsons $r=0.03$). We found a weak correlation between the VP values averaged over all trials and the IVF score (Pearsons $r=0.11$) and we found a moderate correlation between the VP values averaged over all trials and the difference in MD between the measured and the covered eye (Pearsons $r=0.39$).

When averaging the VP value over data of individual video clips, the correlation coefficients varied strongly between video clips. Some representative examples of data from different video clips are shown in rows 2-4 of figure 3.4.

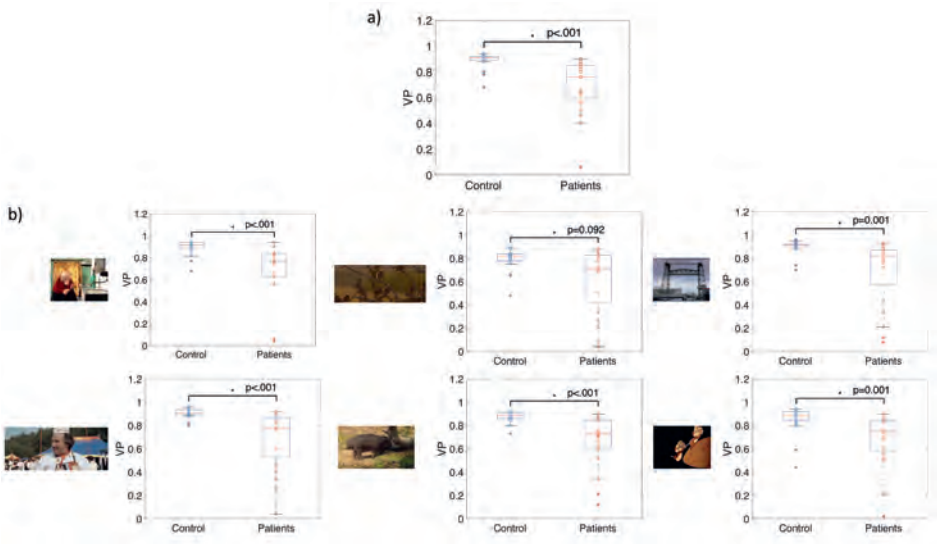


Figure 3.3: Box and whisker plots showing the median VP values of glaucoma patients and controls a) averaged over fixations of all trials and b) averaged over fixations of single video clips.

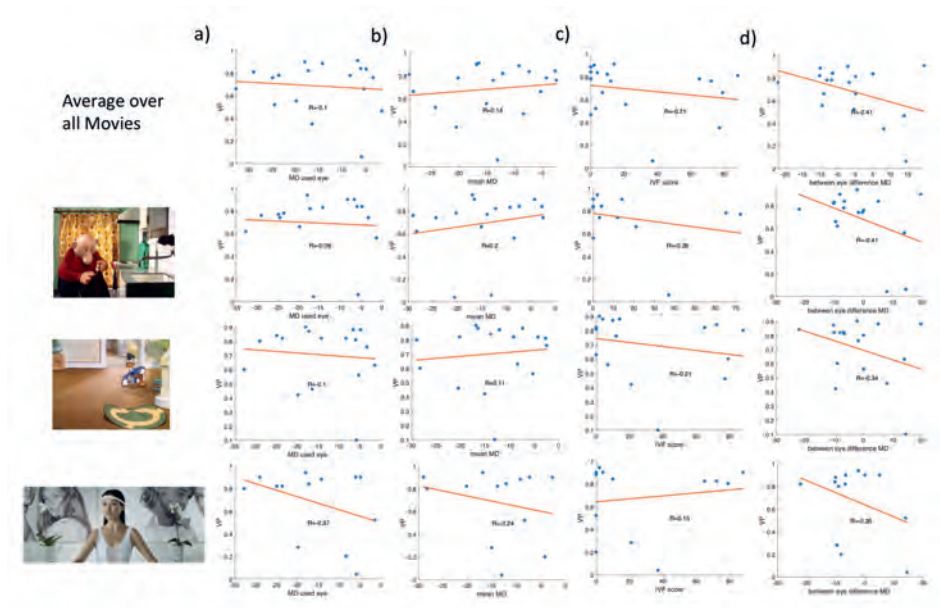


Figure 3.4: Scatter plots showing a) the correlation between the VP value and the MD value of the measured eye of the participants with VFD, b) the correlation of the IVF score and the VP, and c) the correlation of the difference between the MD value of the measure.

Spatial distribution of eye movement features in the visual field used to distinguish between patients and controls

Figure 3.5 shows the projection of the fixation maps onto the first two most significant feature axes from the kPCA using the data of all video clips and representative examples of using data from individual video clips. kPCA transforms the original data (maps of the visual field) onto a new space, in this case using the distances between individual visual field maps for the kernel matrix. If patients with VFD can be separated from controls, the two groups should form two separable clusters in this new feature space.

When performing the kPCA considering all trials of each subject, the first two significant feature axes accounted for 25% of the variance in the data. Figure 3.5 shows that the two

groups projected onto these feature axis overlaps, while more of the data points representing participants of the glaucoma group cluster on the right side of the plot, where the first feature has a positive value. The majority of the data points representing participants of the control group is located on the left side of the plot, where the first feature has a negative value. When performing the kPCA per video clip, we found that the first two feature axes together explained between 28% and 36% of the variance, depending on the video clip. The variance explained of the third feature was much lower with around 7%. Figure 3.5b shows that the two groups tend to separate along the first feature axis when we project data of individual video clips.

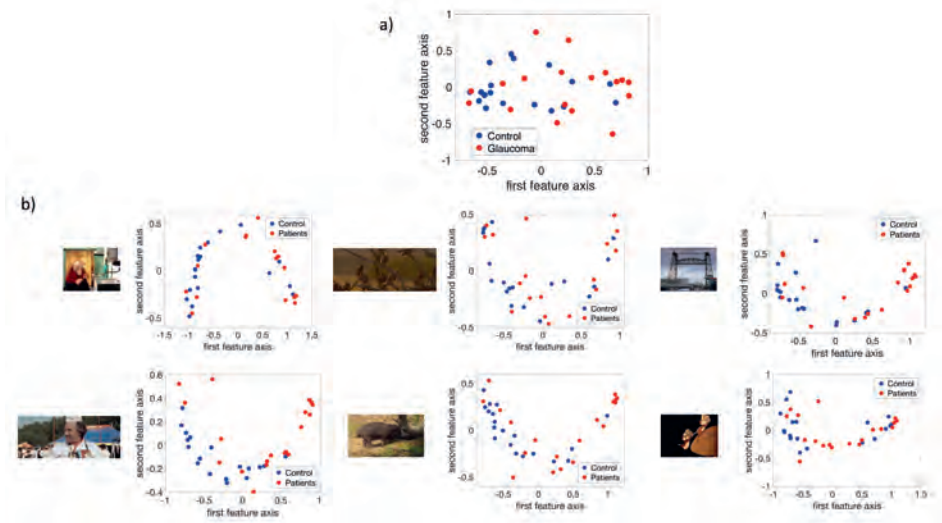


Figure 3.5: The fixation maps of each participant projected onto the two axes of the high dimensional kernel space with the highest covariance. We used a) the mean and the maximum Euclidean distance between all fixation maps of each participant for the kernel and b) the distance between fixation maps of individual video clips. These are representative examples.

Spatial distribution of eye movement features in the visual field used to reconstruct the VFD

We found that in the control group the intact visual field is correlated with an evenly distributed, high VP across the visual field. Individual glaucoma patients showed a large variability in the distribution of VP across the visual field. Both findings are shown in figure 3.6, which depicts the distribution of VP across the visual field of one representative control participant and several glaucoma patients. The distribution of the VP depended to some degree on the location and severity of the VFD. Patients with large peripheral VFD displayed a lower VP in the periphery of their visual field. In other glaucoma patients, the distribution of the VP does not correspond to their VFD. Figure 3.6b shows some representative examples.

In addition, we tested if the distribution of fixations across the visual field of glaucoma patients, differed systematically from the distribution of fixations of the control group, in such a way that it correlates with the location of the VFD. If glaucoma patients directed their gaze significantly more or less frequently towards damaged areas of the VFD, the distribution of fixation frequency could be used to localize VFD. Figure 3.7 shows that, similar to the distribution of the VP, the different glaucoma patients showed a lot of variability in the distribution of fixations across the visual field. Patients with a large peripheral VFD made significantly fewer eye movements towards the periphery than the control group, which led to a relative fixation frequency map that matched the sensitivity of their visual field. In other glaucoma patients, the relative distribution of fixations across the visual field did not correspond to the distribution of sensitivity.

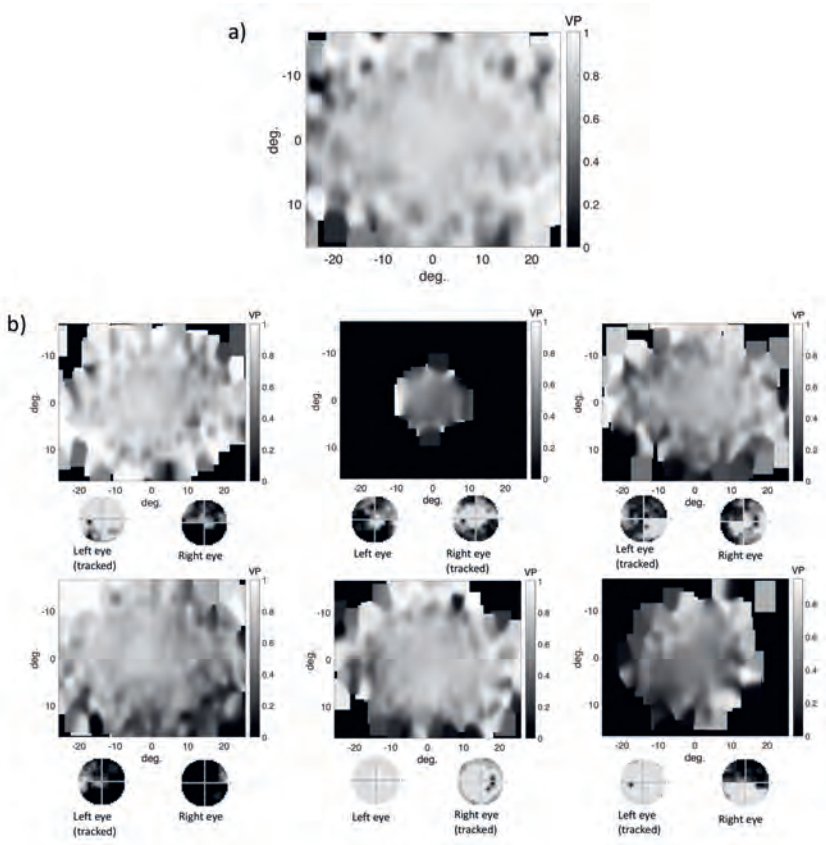


Figure 3.6: a) Representative example of the distribution of VP across the visual field of a control participant. b) Representative examples of VP maps of participants with different types of VFD. The distribution of the VP usually does not correspond to the sensitivity values of the visual field, except for the participant with tunnel vision, which is due to the fact that they never direct their gaze towards the periphery and therefore have a VP of 0 in these areas.

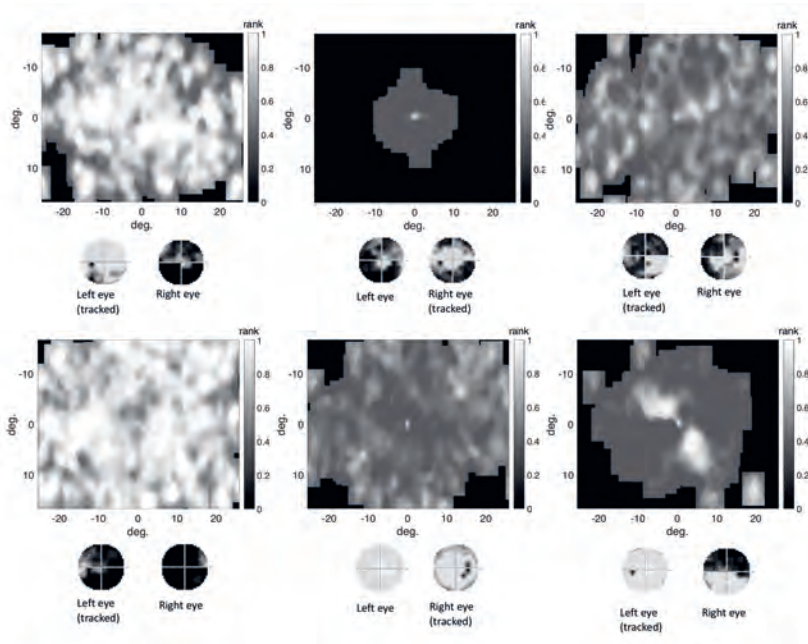


Figure 3.7: The differential fixation maps of the same patients. A value higher (lower) than 0.5 means that the patient made more (less) eye movements towards a part of the visual field than the control group.

Correlation between the measured sensitivity by the HFA

There was no correlation between the location of the VFD and the frequency in which different regions of the visual field were fixated. The mean correlation coefficient between the relative fixation frequency and the sensitivity values was: Pearson's $r=0.160$ (minimum: Pearson's $r=-0.138$, maximum: Pearson's $r=1.289$). This is also shown in figure 8, where we plotted the relative fixation frequency and the sensitivity values in discrete regions of 6 deg. over a visual field spanning 30 deg. half angle of representative example patients.1.289).

3

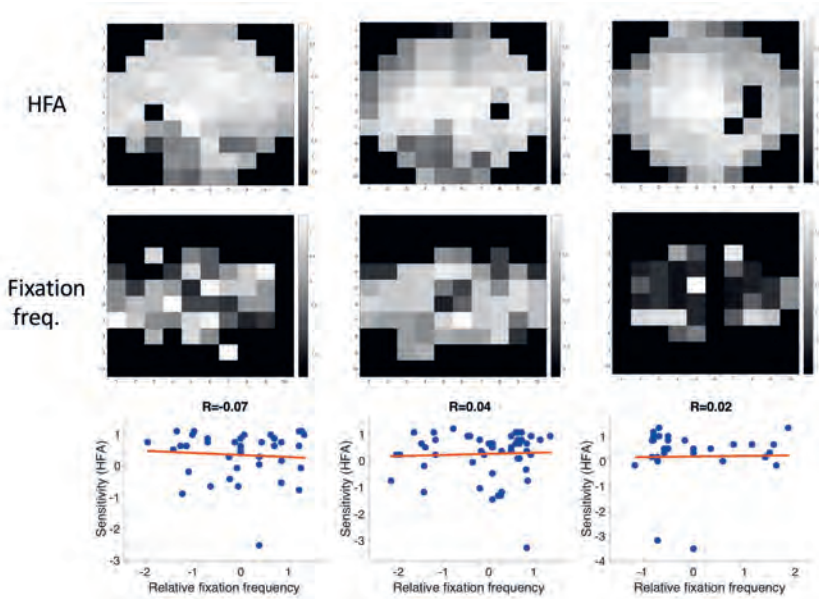


Figure 3.8: Three examples showing the correlation between sensitivity and the relative frequency of fixating in a discrete region in the visual field.

3.6 Experiment 2: binocular eye movements under free-viewing conditions of glaucoma patients compared to those of normal sighted observers

3.7 Methods

Summary

In this experiment, we analysed a data set collected at City College, London, published by Asfaw et al. (2018a) using a similar pipeline as in experiment 1. In this experiment, eye movement data was collected for glaucoma patients and age matched controls who each viewed three different video clips with both eyes.

Participants

We used the data set published by Asfaw et al.(available at <https://doi.org/10.5281/zenodo.1156863>). They had collected data of forty-four people with glaucoma recruited via the ophthalmology clinics at Moorfields Eye Hospital NHS Foundation Trust, London using an Eyelink 1000 eye tracker (SR Research Ltd., Ontario, Canada). All patients had an established clinical diagnosis of chronic open angle glaucoma (COAG) for at least two years and were between 50 and 80 years of age. They had different VFD in each eye. More details concerning the state of their visual field can be found in the publication of the data set. Thirty-two healthy people (controls), of a similar age to the patients, were recruited from the City University London Optometry Clinic. The dataset provides ophthalmic information on each participant (visual acuity, contrast sensitivity per location of each eye, and visual field loss as MD value), raw eye movement data, as well as the eye movement features (fixation locations, fixation duration, start and end points of saccades, saccade amplitude and peak velocity, pupil area) recorded while they viewed movies. We used the processed eye movement data in the following analysis.

Stimulus materials

Participants viewed three different video clips presented on a 54 cm monitor (Iiyama Vision Master PRO 514, Iiyama Corporation, Tokyo, Japan) at a resolution of 1600 by 1200 pixels (refresh rate 100 Hz). The first video clip was part of an entertainment program called Dads Army (BBC Television) 309 seconds long and covered the full screen (subtending a half-angle of 20.3 deg. by 14.9 deg.). The second film clip was taken from The History Boys (20th Century Fox) and 200 seconds long. The third clip was taken from a sports program 2010 Vancouver Winter Olympics Mens Ski Cross (BBC Television) and 436 seconds long. The last two clips were recorded at a 16:9 ratio, therefore they contained black rectangles at the top and bottom of the screen. They subtended a half-angle of 17.3 deg. by 10.6 deg.

The integrated visual field (IVF)

Participants viewed the movies with both eyes open. This means that they viewed the video clips with their integrated visual field (IVF). We computed the sensitivity value of each location in the IVF by merging the provided sensitivity values of corresponding locations in each eye. The sensitivity values had been measured with a Humphrey Field Analyzer (HFA; Carl Zeiss Meditec, CA, USA), with a standard 24-2 grid and the Swedish Interactive Testing Algorithm (SITA). We used a best location approach to determine the sensitivity of each location in the IVF, meaning that we selected the highest sensitivity value among the two eyes as the sensitivity of the IVF (Nelson-Quigg et al., 2000).

We used the IVF as the reference for visual field sensitivity. For each glaucoma patient, we calculated the integrated visual field score (IVF score) as defined by (Crabb and Viswanathan, 2005). The IVF score is a summary measure of the state of the IVF, with a higher IVF indicating more severe damage to the visual field.

Eye movement data analysis

Fixations and saccades in visual field coordinates

Analogous to experiment 1, saccades were defined using a velocity threshold of 30 deg./sec. and an acceleration threshold 8000 deg./sec.² using the Eyelinks built-in al-

gorithm. All other eye movement data was classified as a fixation. The processed eye movement data (fixation location, saccade start and end points) were provided as x-y coordinates on the screen, where the origin of the screen was the top left corner.

We defined the locations of the saccade start and end points and the fixations in the same way, as described in experiment 1 (section 3.3).

Basic eye movement features

To get a first impression of differences in eye movement behavior between the two groups, we computed the mean fixation duration, the mean saccade amplitude and the mean saccade velocity over all three video clips. We compared the two groups using a Wilcoxon-Mann-Whitney U-test. As in experiment 1, Bonferroni corrected p-value of 0.013 was regarded as significant.

Comparison of directional saccade amplitudes of glaucoma patients and controls

To compare the directional saccade amplitudes between individual patients and controls, we performed the same analysis as in experiment 1, with the small difference that we compared the saccade amplitudes to the IVF instead of the visual field of one eye. First, we computed the median and maximum saccade amplitudes of each participant in 18 different directional bins. We compared the saccade amplitudes per bin of each patient to those of the controls. To evaluate if patients with similar kinds of VFD in their IVF showed similar saccade amplitudes, we defined four different groups of patients, according to size and location of the VFD. The first one included patients with small peripheral VFD, as occur in early stages of glaucoma. The second one included patients with a VFD in the upper half of the visual field. The third group consisted of patients with large peripheral VFD (tunnel vision), as occur in late stages of the disease. The fourth group consisted of patients with a VFD in the central part of the visual field. For each patients median and maximum saccade amplitudes, we computed their ranks among the saccade amplitudes of the controls in the same directional bin and divided it by the number of control participants, so that it ranged between zero and one. Again, we did not perform any statistical inference tests, as we only had a small groups of participants with a similar type of VFD in their IVF.

Viewing priority

We extracted the fixations of each participant from the pre-processed data and computed the viewing priority (VP) for each of them (Marsman et al., 2016; Gestefeld et al., 2020). As in experiment 1, we used fixations made by the control group both as the reference and as the random set of fixations.

We averaged the VP value from all fixations of each trial for each participant and compared the two groups using a Wilcoxon-Mann-Whitney U-test. As participants had watched three video clips, in this experiment, we corrected for three repeated measures. A Bonferroni corrected p-value of 0.017 was regarded as significant. In addition, we computed the correlation coefficient of the VP and the integrated visual field score (IVF score) as defined by (Crabb and Viswanathan, 2005) of each glaucoma patient. We hypothesized that a more damaged IVF would result in a lower VP.

Comparison of the spatial distribution of eye movement features in the visual field between groups

Replication and extension of the analysis of Crabb et al. (2014):

First, we transformed all eye movement features into visual field space. Following Crabb et al. (2014), we computed saccade maps on a grid of 12 by 10 degrees half angle that was subdivided into 2x2 degree bins. The grid excluded the central four bins, thereby ignoring fixations that occurred after a very short saccade. We computed the proportion of saccades that ended in each bin. In addition to replicating their analysis, we extended it by also computing fixation distribution maps and VP maps. To compute the fixation distribution maps, we also included the proportion of fixations that followed a saccade into the central four bins. For the VP maps, we computed the average VP in each bin.

We transformed the saccade and fixation maps into a high dimensional feature space using kernel PCA with a Gaussian kernel, where the distance between any two participants i and j was determined with the following kernel:

$$k_{ij} = \exp -0.5(\text{meanDist.} + \text{maxDist.})^2 / 0.2^2 \quad (3.3)$$

For the VP maps we used the following kernel:

$$k_{ij} = \exp -0.5(\text{meanDist.} + \text{maxDist.})^2 / 2^2 \quad (3.4)$$

The Gaussian distribution has a larger variance, because the values in these maps also had a larger variance. *MeanDist* and *maxDist* were the mean and maximum of the Euclidean

distances of the respective feature maps. In addition, we again performed the kPCA on each of the trials separately, computing the Euclidean distance ($Dist$) between the fixation maps of the respective video clips, using the following kernel:

$$k_{ij} = \exp(-Dist) \quad (3.5)$$

For each movie, we visualized the first two dimensions of the transformed data in the kernel feature space. Finally, we used the first five dimensions of the projected data as input to train a naïve Bayes classifier. The classifier was trained and validated using ten-fold cross validation, training on 90% of the data and testing on the remaining 10%.

Application of the method used in experiment 1:

In experiment 1, we had used a grid that included 95% of the saccade end points. To achieve the same on this data set, we calculated the mean saccade amplitude plus two standard deviations in the horizontal (left and right) and vertical directions (up and down) in the control group. To create a symmetric grid, the maximum value of these four values was used. This resulted in a 8 x 10 bin grid of 16 by 20 deg. of visual angle, with bin size set to 2 deg. horizontally and vertically. We then computed the number of fixations that fell into each bin per video clip and divided it by the maximum value in the grid. To compare this approach to the analysis in experiment 1, we applied the kPCA and visualized the first two feature axes in kernel space. We performed kPCA using the same kernels as in experiment 1. We first computed the Euclidean distances between their fixation maps and used the mean distance ($mean\ Dist$) and the maximum distance ($max.\ Dist.$) between their fixation maps to construct the following kernel between the participants i and j :

$$k_{ij} = \exp(-0.5(meanDist. + maxDist.)) \quad (3.6)$$

In addition, we applied the kPCA to the fixation maps of each video clip individually by first computing the Euclidean distance between the fixation maps of the respective video clip. Two participants i and j were then separated using the following kernel:

$$k_{ij} = \exp(-Dist.) \quad (3.7)$$

Reconstructing the VFD based on the spatial distribution of eye movement features in the visual field

We tested whether we could use the spatial distribution of the VP and the relative fixation frequency to reconstruct the VFD in the IVF of the patients. To be able to compare the two eye movement features to the sensitivity of the IVF, as measured by the combination of the 24-2 visual fields of the two eyes, we computed VP maps of the central 24 deg. of the visual field, divided into 6 x 6 deg. bins. To construct VP maps, we computed the average VP of all fixations that fell into a bin.

To construct the maps depicting the relative frequency of fixations, for each participant we summed up all fixations that occurred in one bin and divided them by the total number of fixations. We then compared the proportion of fixations that fell into each bin of one glaucoma patient to the proportions of fixations that fell into the same bin of each of the control participants. We counted how many controls had a smaller proportion of fixations in the same location of the visual field than the respective patient and divided this number by the number of control participants. This resulted in the proportion of fixations per location of that patient being depicted as a rank, ranging between 0 and 1. A value close to 1 meaning that they fixated this area more frequently than the controls.

3.8 Results

Basic eye movement features

Figure 3.9 shows that the group medians did not differ significantly on any of the basic eye movement features we investigated. The median fixation duration of the control group was 266 ms. (SD = 44.92ms.) and 281.75 ms. (SD = 45.48 ms.) for the patients with VFD. The Wilcoxon-Mann-Whitney test did not show a significant difference in fixation duration between the two groups ($p=0.113$, $z\text{-score}=-1.584$) The median saccade amplitudes of the control group was 2.41 deg. (SD=0.57 deg.) and 2.48 deg. (SD = 0.58 deg.) for the patients with VFD. The Wilcoxon-Mann-Whitney test did not show a significant difference in saccade amplitude between the two groups ($p=0.793$, $z\text{-score}=-0.263$). The median saccade velocity of the control group was 212 deg./sec. (SD = 60.07 deg./sec.) and 202.25 deg./min. (SD = 47.77 deg./min.) for the patients with VFD. The Wilcoxon-Mann-Whitney test did not show a significant difference in saccade velocity between the two groups ($p=0.511$, $z\text{-score}=0.658$).

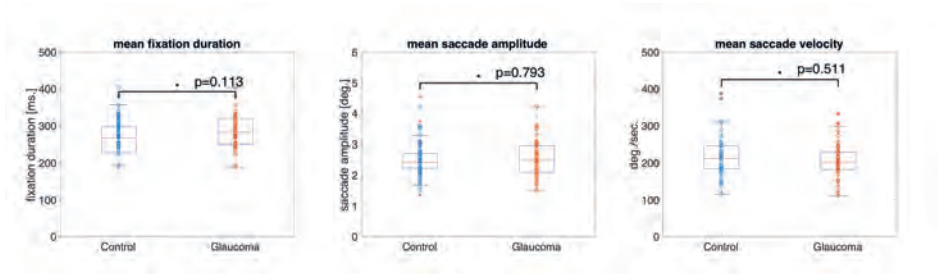


Figure 3.9: Box and whisker plots showing the mean and variance of three different eye movement features for the control and glaucoma groups. The circles represent the values of the individual participants. The group means did not differ significantly.

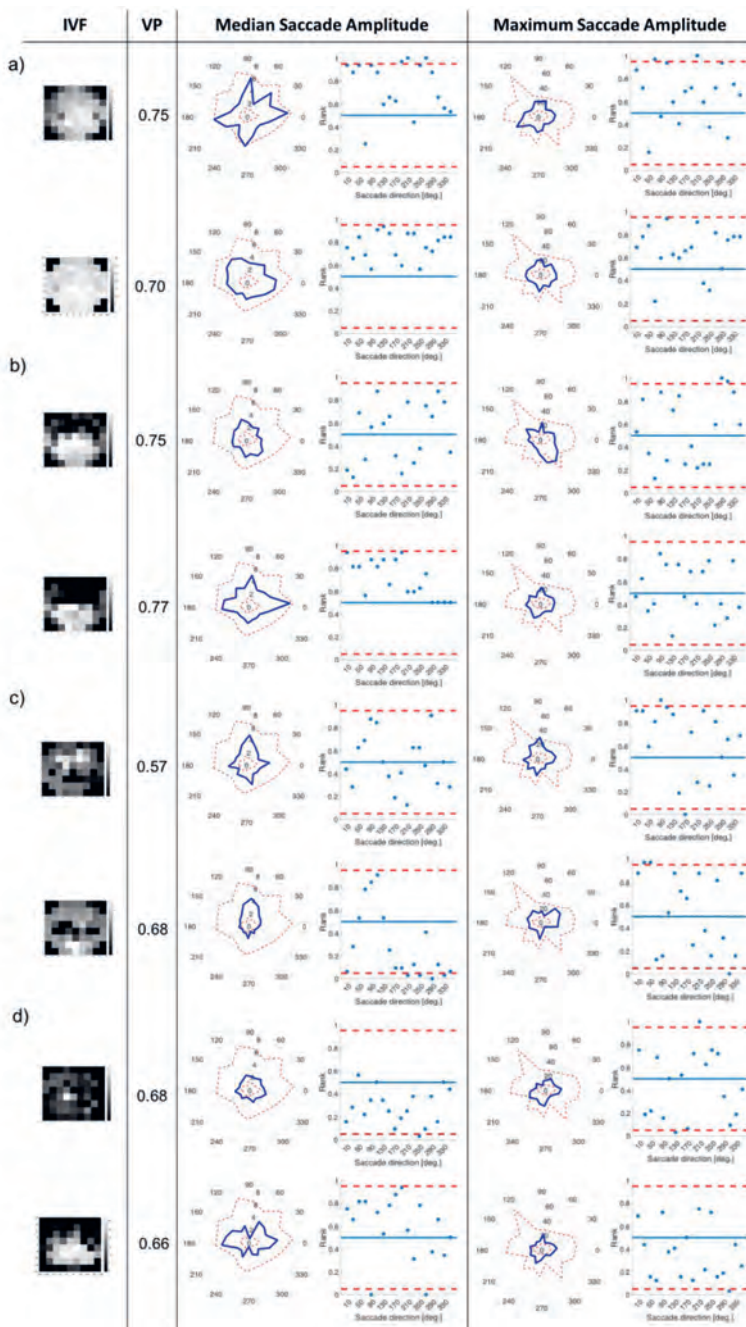
Comparison of directional saccade amplitudes between patients and controls

If the directional saccade amplitudes of a patient are influenced by the location of the VFD, we should find that the median and maximum saccade amplitudes, in directions where a VFD is located, deviate from those of the control group.

Overall, the large majority of the patients median and maximum saccade amplitudes remained within the range of those of the control group, as can be seen in figure 3.10. Examining individual patients in more detail, participants shown in figure 10a, showed high median saccade amplitudes compared to the control group, in some directions higher than 95% of the participants in the control group. They also showed maximum saccade amplitudes which were higher than those of most of the participants in the control group in some directions. Panel 10b shows examples of patients with a VFD in the upper part of the visual field. They made similar saccade amplitudes compared to the control group. Panel 10c shows patients with a VFD covering the central part of the visual field. Their median upwards saccade amplitudes were larger than their downwards or sideways median saccade amplitudes.

Panel 10d shows two patients with big VFD in the periphery. They showed median and maximum saccade amplitudes outside the 95% confidence interval in some directions.

How free-viewing eye movements can be used to detect the presence of visual field defects in glaucoma patients



3

Figure 3.10: The first column in this figure shows the state of the IVF of each patient, with darker areas representing the less sensitive areas of the visual field. The second column shows the VP of this patient averaged across all trials that they performed. The third column shows the median saccade amplitudes in 18 directional bins of each patient, represented by the blue line. The range of the saccade amplitudes by the control group is represented by the scattered red line, showing the minimum and the maximum of the saccade amplitudes of the control group, per direction. The second figure in this column shows the normalized rank that the saccade amplitude of the patient occupies among the saccade amplitudes of the controls per direction, with the red lines representing borders at which the rank is above or below the upper and lower 2.5% of the control group. The fourth column shows the same as the third column for the maximum saccade amplitudes

a) Examples of median and maximum saccade amplitudes of four different patients, who had peripheral VFD in their IVF. b) Examples of patients with VFD in the upper part of the visual field. c) Patients with a VFD which also reached the central part of the visual field. d) Examples of patients with large VFD in the periphery of the visual field. While the first and third patient in this panel showed median and maximum saccade amplitudes which were close to those of the controls, the second one showed high median saccade amplitudes towards the most intact, but also towards the most damaged area of the visual field.

Viewing priority

A significant difference in VP between the two groups would indicate that their fixation locations while viewing the same scene often differ. The median VP value of the control groups was 0.87 (SD = 0.06) and of the glaucoma patients was 0.83 (SD = 0.08). The Wilcoxon-Mann-Whitney test did not show a significant difference ($p=0.085$, $z\text{-score}=-1.723$). When calculating the average VP values per movie clip, we found that the median VP value of the control group was 0.9 (SD = 0.07) and of the glaucoma patients was 0.87 (SD = 0.13) for the movie clip Dads Army. The median VP value of the control group was 0.87 (SD = 0.09) and of the glaucoma patients was 0.83 (SD = 0.11) for the movie clip History Boys. The median VP value of the control group was 0.87 (SD = 0.09) and of the glaucoma patients was 0.83 (SD = 0.08) for the movie clip Ski Cross.

We did not find a significant difference in the group medians of patients and controls in VP, when averaging over the data collected during the video clips Dads Army ($p=0.028$, $zscore = -2.914$), History Boys ($p=0.209$, $z-score=-1.257$) and Ski Cross ($p=0.558$, $z-score=-0.586$).

Figure 3.12 shows the IVF score plotted against the median VP of each glaucoma patient. As the IVF score increases with a more severely damaged visual field, we would observe a negative correlation of VP and IVF score if the VP value decreased with disease severity. When we compare the IVF score against the median VP of each patient from the video clip Dads Army we find no correlation (Pearsons $r = 0.04$). We find a very small negative correlation when we compare the patients IVF against the VP from the video clips History Boys (Pearsons $r=-0.18$) and Ski Cross (Pearsons $r= -0.17$).

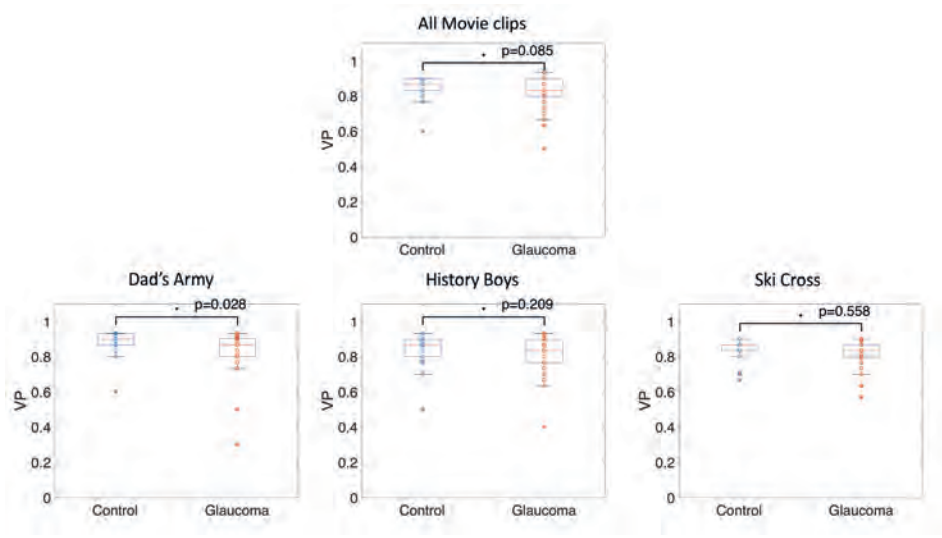


Figure 3.11: Box and whisker plots showing the group means of VP per movie clip. The circles represent the VP value of each participant.

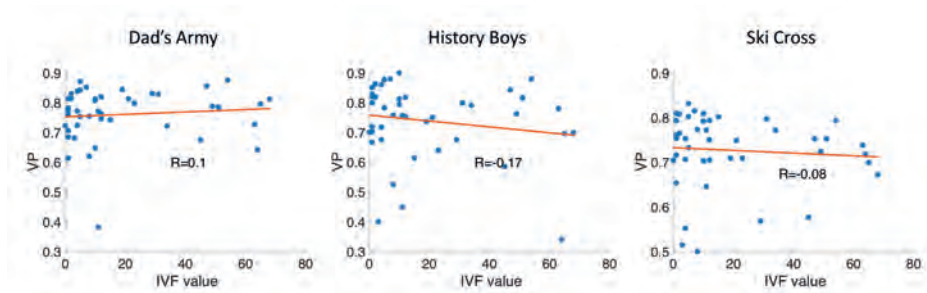


Figure 3.12: Scatter plots showing the correlation between the VP and the sensitivity of the integrated visual field (IVF score) of each participant. R is the correlation coefficient.

Spatial distribution of eye movement features in the visual field used to distinguish between patients and controls

1. Replication and extension of the analysis of Crabb et al. (2014):

If the two groups formed separable clusters in the kernel space, it would be an indicator that they could be separated in this high dimensional feature space. We found that the two groups do not separate very well along the first two feature axes as can be seen in figure 3.13, which shows the data of the saccade maps projected onto the first two significant feature axes of the kPCA. We found that the first five dimensions in kernel space explain 25% of the variance in the data for the saccade maps if we use all three video clips. When performing the same analysis with the fixation and VP maps, the transformation of the data into the feature space leads to similar results (see figure 13b and c). Table 3.3 shows the classification accuracies of the naive Bayes classifier using the first 5 significant feature axes after 10-fold cross validation.

2. Application of the method used in experiment 1

In addition, we projected the 8 by 10 bins fixation maps onto the first two principal components using kPCA on the data of all trials as well as on the data of each trial separately. In all four cases the data points of the two groups overlap in the kernel space, as can be seen in figure 3.14.

Eye movement feature	All trials	Dads Army	History Boys	Ski Cross
Saccade map	54.7% (36.8%-63.2%)	50.0(31.6%-63.2%)	46.3% (26.3%-63.2%)	50.0% (36.8%-63.2%)
Fixation map	57.9% (47.4%-73.7%)	54.2% (42.1%-68.4%)	62.6% (47.4%-79.0%)	50.5% (31.6%-68.4%)
VP map	52.6% (31.6% - 68.4%)	48.4% (36.8% - 57.9%)	47.4% (31.6% - 57.9%)	49.5% (26.3% - 68.4%)

Table 3.3: Accuracy of the naïve Bayes classifier for each of the maps. Using data of all three trials or each trial separately. In brackets, we show the minimum and maximum accuracy achieved in the 10-fold cross validation.

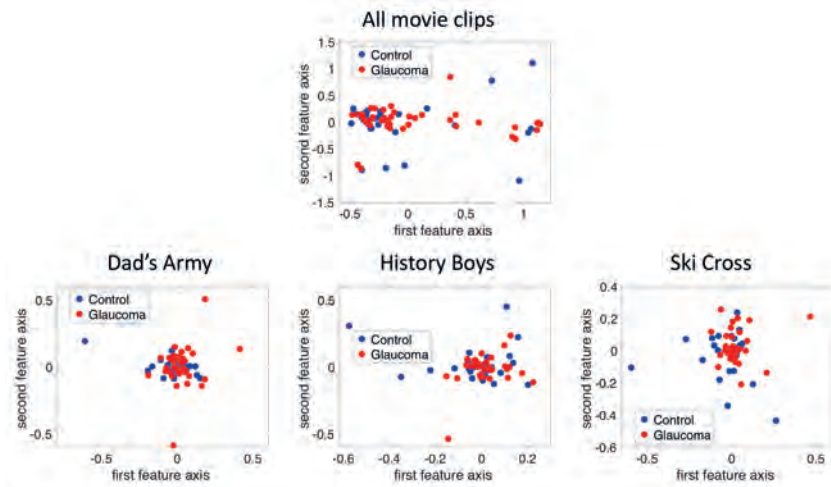


Figure 3.13: Projection of the 12 by 10 bin saccade maps onto the first two principal axes in the kernel space using the combined data of all three trials and the data of each trial separately.

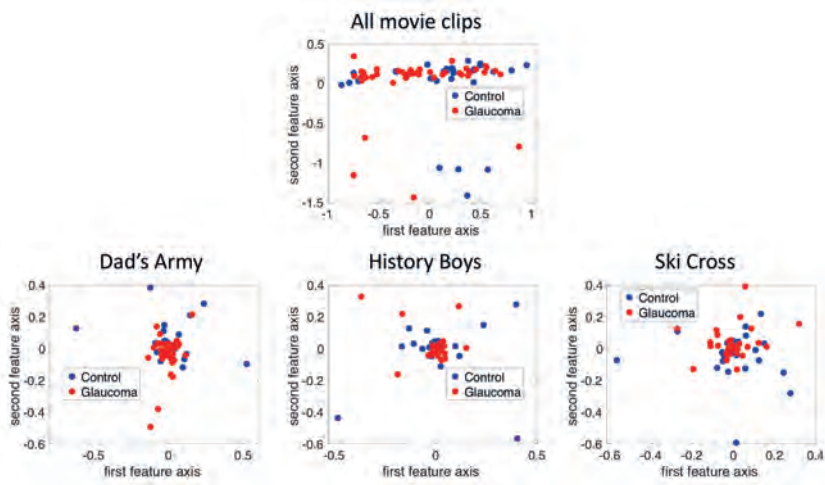


Figure 3.14: Projection of the 8 by 10 bin fixation maps onto the first two principal axes in the kernel space using the combined data of all three trials and the data of each trial separately.

Spatial distribution of eye movement features in the visual field used to reconstruct the VFD

We could reconstruct the location of the VFD, if the VP was reduced in the damaged part of the visual field or if the frequency of fixations differed significantly from normal in those areas. Figure 3.15 shows examples of the distribution of VP and maps of patients with different severity and location of the VFD. As these representative examples show, there was a lot of variability between correlation coefficients of individual glaucoma patients. When taking the group average, the sensitivity per location of the IVF of the glaucoma patients was weakly correlated with the VP per location, with an average Pearson's correlation coefficient of $r=0.127$. They however ranged between being weakly anti-correlated to being moderately correlated between individual patients (minimum: Pearson's $r=-0.270$, maximum: Pearson's $r=0.600$).

Figure 3.15b shows the differential fixation maps of the same patients. Again, they represent the variability in correlation coefficients within the group. On the group level, the differential fixation maps were weakly anti-correlated with the sensitivity indifferent locations of the IVF, with an average correlation coefficient of Pearson's $r=-0.040$. They ranged from moderately anti-correlated to moderately correlated (minimum: Pearson's $r=-0.502$, maximum: Pearson's $r=0.410$).

3.9 Discussion

The main conclusion of this study is that monocular eye movements made by glaucoma patients differ substantially from those of normal-sighted controls. Based on this, we conclude that screening patients for VFD in glaucoma patients based on their free-viewing eye-movements is possible in principle.

The viewing conditions and the video clip content influence the ability to separate patients and controls. The differences in monocular viewing behavior between the two groups, becomes apparent in the significant difference in VP between the two groups, as well as the differences in directional saccade amplitudes between individual glaucoma patients and the control group. In addition, after transforming the data using kPCA, we found that participants with glaucoma and controls tend to form separate clusters in the new features space. The binocular viewing behavior, however did not lead to significant differences in the aforementioned features. Apart from the (binocular vs. monocular) viewing conditions, the second factor that influences if the two groups show differences

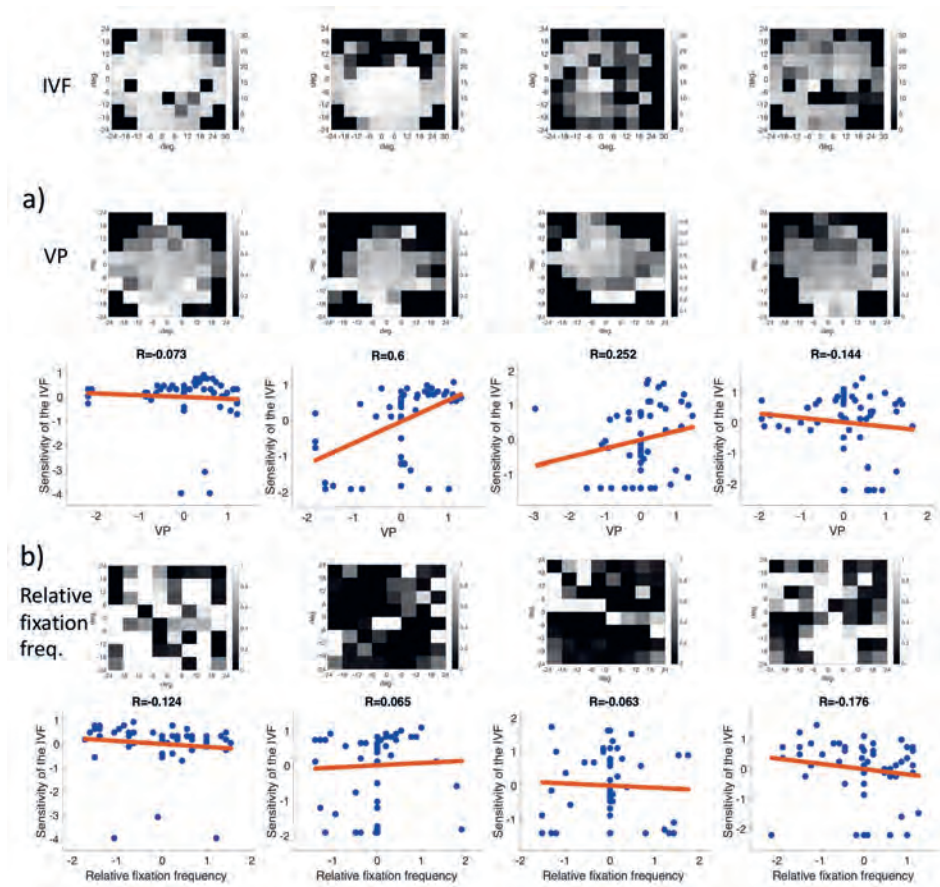


Figure 3.15: Representative examples of a) the correlation of the VP and the sensitivity of the IVF and b) the correlation of the relative fixation frequency and the sensitivity of the IVF. The discrete locations in which the VP and relative fixation frequency were binned matched the 24-2 SITA test locations of the HFA. Both panels show the same patients. Their IVF is shown in the top row. Neither the VP nor the relative fixation frequency is consistently correlated with the IVF over all patients.

in viewing behavior is the content of the video clips. Videos that contain highly dynamic content (such as comics) and that result in consistent viewing behavior in controls are

the most suitable as these result in a good separation of the two groups. However, this success in detecting the presence of a VFD does not automatically translate into its reliable reconstruction. With any of the evaluated methods, reconstruction of the location of the VFD was only possible in a few patients, specifically in those with a large peripheral VFD and in the single patient with HH that we assessed. We will discuss these results below in more detail, including how compensatory viewing strategies of glaucoma patients may have prevented us from localizing their VFD.

Detecting VFD requires monocular viewing

We analyzed the viewing behavior of glaucoma patients and controls in two comparable experiments with rather distinct, yet informative, outcomes. In experiment 1, we found significant differences in average saccade amplitude between patients and controls, a significant difference in VP after collecting data during 1-minute video clips in 27 of the 28 video clips, differences in directional saccade amplitudes of the patients from the controls and potentially separable clusters after performing kPCA on the fixation maps. In experiment 2 we only found a significant difference in VP for one of the three video clips, which lasted 5:15 minutes and differences in directional saccade amplitudes compared to controls.

Why did we only find differences in eye movement behavior between patients and controls in experiment 1, where our participants viewed movies monocularly and not in experiment 2 where participants viewed these binocularly? To answer this question, we will first consider that due to glaucoma being a gradually progressing disease, many glaucoma patients do not notice their VFD until at a late stage during the disease. Moreover, they likely have adapted their viewing behavior to their VFD. In glaucoma, the VFD is caused by damage to the optic nerve. This results in defects at different locations and of different degrees of severity which may also be different for the two eyes. This was also the case for the glaucoma patients who participated in our present experiments. In experiment 1, this meant that from the moment we covered one eye, the state of a patient's visual field changed abruptly. Presumably, in the relatively brief time of the experiment, patients did not have sufficient time to adapt to this change. This means that during the experiment, their viewing experience differed from that in their daily life, analogous to what participants with simulated VFD experience. Indeed, after the experiment, some

participants spontaneously mentioned that they had more difficulties watching the video clips monocularly, in comparison to watching television at home with both eyes.

We also found that patients who viewed the video clips with their worse eye usually showed a lower VP than those who performed the experiment with their better eye. This could be an indicator that if patients experience an instantaneous deterioration of the visual field, they become more aware of the presence of the VFD, and it reduces their ability to perform their customary viewing behavior. These findings are in line with previous studies that found differences in monocular viewing behavior of patients and controls. For example, a study where glaucoma patients viewed static images with one eye also found differences in the patterns of saccade amplitudes in different directions in patients compared to control, similar to our own findings (Wiecek et al., 2012).

Asfaw et al. (2018a) showed that the same patient displays differences in viewing behavior depending on with which eye they performed a free viewing task. The spread of fixation locations was smaller in the worse eye of glaucoma patients compared to the better eye (Asfaw et al., 2018a). This supports our finding that patients who viewed movies with their worse eye showed a less normal viewing behavior (as indicated by a lower VP) than patients who viewed the movies with their better eye.

Comparing the results of our two experiments, we conclude that glaucoma patients with asymmetric visual field loss, only show different eye movement behavior compared to normal-sighted controls, when they watch videos under viewing conditions that differ from the ones they experience in their daily life. When allowed to use both eyes, as in daily life, they seem to be able to view the videos as well as normal-sighted participants. Moreover, the presence of a VFD can be detected more easily in the worse eye. In patients with symmetric visual field loss, it may be irrelevant for their viewing behavior whether they view the video clips monocularly or binocularly.

Detecting a VFD under free-viewing conditions requires appropriate content

An uncertainty concerning the findings of experiment 2, is whether we could have found differences in viewing behaviour between the two groups if participants had watched the clips with one eye. It could also be the case that the content of the video clips did not lead to a good separation of the two groups. An indication of the videos shown not be-

ing suitable to separate the two groups, could be the low average VP of the controls in experiment 2 in comparison to the VP of the controls in experiment 1, indicating more inconsistent viewing behaviour of normal-sighted observers when watching the three video clips of experiment 2.

We found that ideal video clips should guide the attention of the (normal-sighted) observer, so that their viewing behaviour is very consistent providing a clear picture of where the salient region in a scene should be located. In addition, the salient region should change location on the screen quickly to trigger long saccades, as this is the kind of viewing behaviour that is difficult to perform for glaucoma patients. Previous studies have shown that other types of experimental paradigms, besides free-viewing, that are successful at separating glaucoma patients from controls, also when they are tested binocularly, are those that require the participants to perform saccades. Najjar et al. (2017), reported that glaucoma patients showed a reduced saccade velocity and amplitude in pro-saccade tasks, compared to the controls. The reduced amplitude means that the saccades were hypometric on average. In addition, glaucoma patients made more anti-saccade errors than controls. In a tracking test, where different patients were asked to follow a dot with their gaze, Soans et al. (2021) were able to differentiate glaucoma patients from controls and patients with other types of visual field defects, due to their inability to follow the dot when it made a sudden jump towards the periphery of the visual field, i.e. when a saccade was required. They were, however, able to follow the dot, when it moved around slowly, i.e. when smooth pursuit eye movements were required. With the free-viewing paradigm, it is difficult to trigger a sufficient number of long saccades, as we do not want to specifically instruct participants to, for example, also look towards the corners of the screen. When watching a video, the implicit task is of course to follow the storyline, which leads to quite consistent eye movements, as we showed in this study. We could select an appropriate video by trying to determine if the center of gaze of our observers would shift often and rapidly, based on the bottom-up features. We know that motion has a stronger effect on eye movements, than other features, such as color, orientation or intensity, but the sum of all features is the best predictor for gaze location (Itti, 2005). However, gaze behaviour cannot be explained by bottom-up features, as it is also guided by cognitive goals (Hayhoe and Ballard, 2005). In the case of video clips, gaze will also be influenced by the storyline of the characters in the scene. Furthermore, eye movements will usually not be directed towards the most salient location,

but towards the location from which the brain can extract the most relevant information (Najemnik and Geisler, 2005).

Practically, we can use VP to test which types of video clips lead to a good separation between the two groups. More specifically, we can select videos in which the controls have a high VP while that of the patients is significantly lower. In experiment 1, we found that comics or feature films that contain a lot of movement and active scenes usually result in rather different scan paths in patients and controls. On the other hand, the nature documentaries that we used contain mostly scenes or landscapes having relatively low color contrasts and depicting slowly moving herds of animals. Consequently, slow motion is spread out over the entire scene. These types of movies neither contain a spatially narrow and salient area of interest, an obvious story line with a main character that should be followed. This results in much more inconsistent viewing behaviour of the control group, that is quantifiable by a lower group average VP with a larger variance. In turn, this inconsistency in the viewing behaviour of the controls makes it more difficult to detect deviations in the eye movement behaviour of patients.

Usability of current eye-tracking technology in elderly and clinical populations

In experiment 1 we were unable to acquire good quality eye movement data in approximately one third of the patients with VFD and the controls. If eye tracking technology is to be used in (clinical) practice with an elderly demographic, the technology needs to be adapted accordingly.

For many participants, it took us a long time to modify the setup, adjusting the position of the eyes in the camera image of the tracker, trying to minimize reflections from the participants' glasses to be able to start the calibration. With most participants we had to perform the 9-point calibration several times, adjusting the setup in between. As the eye trackers that we used did not work with multifocal glasses, we used the trial lenses that are used to test patients' optimal correction at eye clinics. With all the necessary adjustments, in some participants it could take up to 25 minutes until we could collect data. With the goal in mind of using eye-tracking in clinical practice, either as a diagnostic tool or as support during vision rehabilitation, the time it takes to prepare for data collection needs to be reduced drastically. This could be achieved by using an eye tracker

which does not need to be calibrated for every participant separately, provided these trackers manage to maintain stable gaze tracking (e.g., the stereo-eyetracker described in Barsingerhorn et al. (2018); the Pupil Invisible (Pupil Labs) (Kassner, 2014), or the BulbiCam (Bulbitech, Trondheim)).

Using virtual reality and mobile eye tracking during daily life activities instead of a (small) screen could improve the separability of patients and controls

A particular challenge, also with established methods, is to detect glaucoma at an early stage, as it usually starts by affecting the periphery. In both parts of this study, all participants showed a strong center bias, which meant that the periphery of the visual field was extremely undersampled. This problem may be reduced by selecting content in which the salient stimuli also occur around the edges of the screen and have a sudden onset. However, a remaining complication is that observers show a tendency to look towards the center of a screen irrespective of the presented content (Bindemann, 2010). Even when shifting image features away from it, people still tend to look towards the center of the screen (Tatler, 2007). So, it is questionable whether a regular display is the best device to present stimuli for the purpose of detecting VFD. With advances in virtual reality (VR) technology that allow to combine VR and eye-tracking, presenting stimuli using a VR headset with a larger field of view and less obvious borders could be a more suitable alternative. This kind of display would potentially lead to even more natural viewing behaviour and larger saccade amplitudes. Imaoka et al. (2020) found that the HTC Vive Pro Eye VR headset could potentially be used to measure saccadic eye movements. Another interesting approach could be to record eye movements during daily life activities with a mobile eye tracker. Having data of daily life eye movements could also help to reveal how much a certain VFD diminishes functional vision in different tasks. In turn, his knowledge could be practically applied in vision rehabilitation therapy.

VP may correlate more strongly with functional vision than the severity of the VFD defined by the MD value

3

While directly linking eye movement behavior to the patients difficulties in daily life functioning lies outside the scope of this study, we can look for indicators of compensatory eye movement behavior. There are two explanations for why it was possible to detect the presence of a VFD based on eye movements. First, patients with VFD may have altered their eye movement behavior, due to the fact that they did not detect certain stimuli or interesting objects in the periphery. Consequently, they may have directed their overt attention less frequently towards damaged parts of their visual field. In other words, the viewing behavior of the patients would mainly have been altered due to bottom-up influences. Secondly, patients with VFD may employ viewing strategies with which they compensate for their VFD by directing their gaze more frequently towards certain (damaged) parts of the visual field. This strategy may either be used in a conscious or unconscious manner. If so, this would imply that their eye movement behavior would mainly have been altered by top-down mechanisms.

Importantly, if eye movements would be driven primarily by bottom-up influences, we would have expected a strong correlation between the severity of the VFD (MD or IVF score) and the VP value. In addition, when looking at the distribution of fixations across the visual field, we should have found that patients fixate damaged parts of the VF much less frequently. However, we find that this is only the case in patients with severe peripheral VFD. Other patients frequently look towards damaged parts of their visual field, which could reflect a compensatory strategy. Interestingly, patients with similar VFD nevertheless showed markedly different average VP, also depending on whether they viewed the video clips with their better or worse eye. We speculate that VP could be a predictor for the ability of individuals to cope with their VFD in daily life. Given a similar VFD, the patient with the higher VP has a better compensatory eye movement strategy. When glaucoma patients watched the videos binocularly, they exhibited a very similar viewing behaviour as the normal-sighted controls, not only showing a similar VP, but also similar saccade amplitudes and fixation distributions across the visual field. This suggests that for the task of binocularly watching videos, they may have already found mechanisms to cope with their VFD.

Future studies

Future studies could use the knowledge gained in this study to optimize the presented stimuli, as well as the stimulus display. With a larger data set it would also be possible to apply machine learning to predict the state of the visual field based on eye movement data. Based on the results of this study, the input features for a machine learning classifier should represent the spatial distribution of eye movements across the visual field.

Besides using eye movements to screen for the presence of a VFD, these could also be used to monitor the effects of vision rehabilitation training. One could test if free-viewing eye movement behavior changes over the course of different stages of vision rehabilitation. If it changed in a systematic fashion, we could conclude that the patient internalizes a certain compensatory eye movement strategy. In fact, we think it is appropriate to conclude that the degree to which a patient with a VFD could use and profit from a compensatory strategy in this experiment, depends on the size and the location of their VFD and the semantics and content of a specific video clip. This implies a potential trade-off to be made between precisely targeted, yet boring stimuli (such as a Gaussian blob), or more engaging but somewhat less accurate natural stimuli such as movies. Moreover, note that the above further implies that movies could be used to determine deviant viewing behavior (which is also evident from our saccade analyses) and potentially be used to quantify compensatory viewing behavior.

In addition, eye movement behavior during movie viewing could be used to predict how well patients can perform different daily life tasks. To answer this question, the quality of life and task performance in different daily life tasks should be assessed together with the eye movements.

Conclusion

A VFD results in specific viewing behavior during video viewing that can be used to distinguish a glaucoma patient from control observers and which could form the basis of a simple screening approach. Distinguishing requires monocular viewing and considering the spatial distribution of eye movement features, such as fixation locations and saccade amplitudes. Moreover, we conclude that while individual glaucoma patients not only have different VFD, they also appear to differ in their ability to cope with it.

Acknowledgements

We want to thank Joost Heutink for mediating access to the Psychology student pool.

Funding: This project has received funding from the European Unions Horizon 2020 research and innovation program under the Marie Skłodowska-Curie grant agreement No. 641805(EGRET) and No. 641805 (NextGenVis) and the Graduate School of Medical Sciences (GSMS), of the University Medical Center Groningen, University of Groningen. The funding organizations had no role in the design, conduct, analysis, or publication of this research.

References

- Asfaw, D. S., Jones, P. R., Mönter, V. M., Smith, N. D., and Crabb, D. P. (2018a). Does glaucoma alter eye movements when viewing images of natural scenes? a between-eye study. *Investigative Ophthalmology and Visual Science*, 59(8):31893198.
- Asfaw, D. S., Jones, P. R., Smith, N. D., and Crabb, D. P. (2018b). Data in brief data on eye movements in people with glaucoma and peers with normal vision. *Data in Brief*, 19:12661273.
- Barsingerhorn, A. D., Boonstra, F. N., and Goossens, J. (2018). Development and validation of a high-speed stereoscopic eyetracker. *Behavior Research Methods*, page 118.
- Bindemann, M. (2010). Scene and screen center bias early eye movements in scene viewing. *Vision Research*, page 25772587.
- Brainard, D. (1997). The psychophysics toolbox. *Spatial Vision*, 10:433–436.
- Carvalho, J., Renken, R., and Cornelissen, F. (2019). Predictive masking is associated with a system-wide reconfiguration of neural populations in the human visual cortex. *bioRxiv*.
- Cello, K. E., Nelson-Quigg, J. M., and Johnson, C. A. (2000). Frequency doubling technology perimetry for detection of glaucomatous visual field loss. *American Journal of Ophthalmology*, Volume 129(Issue 3).
- Cornelissen, F., Bruin, K., and Kooijman, A. (2005). The influence of artificial scotomas on eye movements during visual search. *Optom Vis Sci*, 82(1):27–35.

- Cornelissen, F., Peters, E., and Palmer, J. (2002). The eyelink toolbox: Eye tracking with matlab and the psychophysics toolbox. *Behavior Research Methods, Instruments and Computers*(34):613–617.
- Crabb, D. P., Smith, N. D., and Zhu, H. (2014). Whats on tv? detecting age-related neurodegenerative eye disease using eye movement scanpaths. *Frontiers in Aging Neuroscience*, 6(NOV):110.
- Crabb, D. P. and Viswanathan, A. C. (2005). Integrated visual fields: A new approach to measuring the binocular field of view and visual disability. *Graefes Archive for Clinical and Experimental Ophthalmology*, 243(3):210216.
- David, E. J., Lebranchu, P., Da Silva, M., and Le Callet, P. (2019). Predicting artificial visual field losses: A gaze-based inference study. *Journal of Vision*, 19(14):22.
- de Haan, G. A., Melis-Dankers, B. J. M., Brouwer, W. H., Tucha, O., and Heutink, J. (2015). The effects of compensatory scanning training on mobility in patients with homonymous visual field defects: A randomized controlled trial. *Plos One*, 10(8).
- Gestefeld, B., Grillini, A., Marsman, J. B. C., and Cornelissen, F. W. (2020). Using natural viewing behavior to screen for and reconstruct visual field defects. *Journal of Vision*, 20(9):116.
- Glen, F. C., Smith, N. D., and Crabb, D. P. (2013). Saccadic eye movements and face recognition performance in patients with central glaucomatous visual field defects. *Vision Research*, 82:4251.
- Hayhoe, M. and Ballard, D. (2005). Eye movements in natural behavior. *Trends in Cognitive Sciences*, 9(4):188194.
- Imaoka, Y., Flury, A., and de Bruin, E. D. (2020). Assessing saccadic eye movements with head-mounted display virtual reality technology. *Frontiers in Psychiatry*, 11(September):119.
- Itti, L. (2005). Quantifying the contribution of low-level saliency to human eye movements in dynamic scenes. *Visual Cognition*, 12(6):10931123.

- Kassner, M. and William Patera, A. B. (2014). Pupil: An open source platform for pervasive eye tracking and mobile gaze-based interaction. *Proceedings of the 2014 ACM International Joint Conference on Pervasive and Ubiquitous Computing: Adjunct Publication*, page 11511160.
- Katz, J. and Sommer, A. (1990). Reliability of automated perimetric tests. *Archives of Ophthalmology*, 108(6):777778.
- Kleiner, M., Brainard, D., Pelli, D., Ingling, A., Murray, R., Broussard, C., and Cornelissen, F. (2007). What's new in psychtoolbox-3? *Cognitive and Computational Psychophysics*.
- Marsman, J.-B. C., Cornelissen, F. W., Dorr, M., Vig, E., Barth, E., and Renken, R. J. (2016). A novel measure to determine viewing priority and its neural correlates in the human brain. *Journal of Vision*, 16(6):3.
- Mazumdar, D., Pel, J., Panday, M., Asokan, R., Vijaya, L., Shantha, B., George, R., and Van Der Steen, J. (2014). Comparison of saccadic reaction time between normal and glaucoma using an eye movement perimeter. *Indian Journal of Ophthalmology*, 62(1):55-9.
- Mendieta, N., Suárez, J., Barriga, N., Herrero, R., Barrios, B., and Guarro, M. (2021). How do patients feel about visual field testing? analysis of subjective perception of standard automated perimetry. *Seminars in Ophthalmology*.
- Morales, J. and Brown, S. (2001). The feasibility of short automated static perimetry in children. *Ophthalmology*, 108 (1):157–162.
- Najemnik, J. and Geisler, W. S. (2005). Optimal eye movement strategies in visual search. *Letters to Nature*, 434(7031):387391.
- Najjar, R. P., Sharma, S., Drouet, M., Leruez, S., Baskaran, M., Nongpiur, M. E., and Milea, D. (2017). Disrupted eye movements in preperimetric primary open-angle glaucoma. *Investigative Ophthalmology and Visual Science*, 58(4):24302437.
- Nasreddine, Z., Phillips, N., Bédirian, V., Charbonneau, S., Whitehead, V., Collin, I., Cummings, J. L., and H., C. (2005). The montreal cognitive assessment, moca: a brief screening tool for mild cognitive impairment. *J Am Geriatr Soc.*, 53(4).

- Nelson-Quigg, J. M., Cello, K., and Johnson, C. A. (2000). Predicting binocular visual field sensitivity from monocular visual field results. *Investigative Ophthalmology and Visual Science*, 41(8):2212-2221.
- Smith, N. D., Crabb, D. P., and Garway-Heath, D. F. (2011). An exploratory study of visual search performance in glaucoma. *Ophthalmic Physiol Opt.*, 31:225-232.
- Soans, R., Grillini, A., Saxena, R., Renken, R., Gandhi, T., and Cornelissen, F. (2021). Eye-movementbased assessment of the perceptual consequences of glaucomatous and neuro-ophthalmological visual field defects. *Trans Vis Sci Tech*.
- Tatler, B. W. (2007). The central fixation bias in scene viewing: Selecting an optimal viewing position independently of motor biases and image feature distributions. *Journal of Vision*, 7(14)(4).
- Wall M., Woodward K. R., B. C. F. (2004). The effect of attention on conventional automated perimetry and luminance size threshold perimetry. *Invest. Ophthalmol. Vis. Sci*, 45(1):342-350.
- Wiecek, E., Pasquale, L. R., Fiser, J., Dakin, S., and Bex, P. J. (2012). Effects of peripheral visual field loss on eye movements during visual search. *Frontiers in Psychology*, 3(NOV):113.

3.10 Supplementary Material

Example of a hemianopia patient, who can be distinguished from controls and whose VFD can be reconstructed using free-viewing eye movements

Apart from the glaucoma patients, we also collected and analysed data of one hemianopia patient. In this section we will present and discuss some of the results and compare them to those of the glaucoma patients, as well as to the findings with simulated HH in Geste-feld et al. (2020).

Results

Saccade amplitudes in different directions

The hemianopia patient showed similar median and maximum saccade amplitudes to the control group as shown in Figure 3.16.

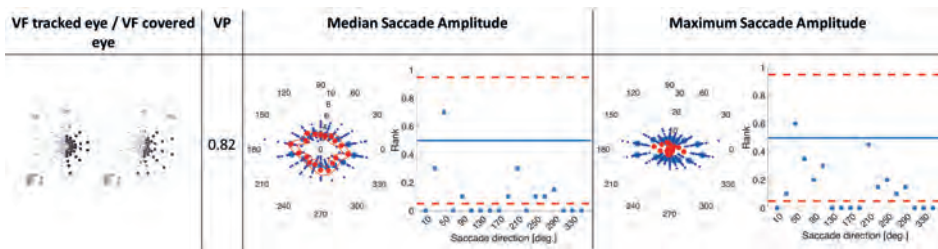


Figure 3.16: Data for a single HH patient compared to controls: the median and maximum saccade amplitudes in different directions.

Spatial distribution of eye movement features to localize the VFD

The VP of fixations made after eye movements towards the right side of the visual field is lower than that of fixations made after saccades towards the left side of the visual field, as shown in figure 3.17. The average VP over all trials of this patient was 0.78.

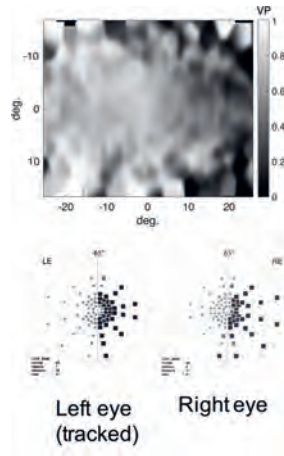


Figure 3.17: Data for a single HH patient: the distribution of VP across the visual field (left panel) and the sensitivity values of the two eyes as measured by SAP (right panel).

Conclusions

When only taking the saccade amplitudes into account, the hemianopia patient does not seem to deviate in viewing behaviour from the controls, making relatively large saccades towards the blind hemifield. When looking at the VP however, we find that the VP of fixations made after saccades towards the blind hemifield are not directed at salient locations. Due to the size and severity of the VFD, which means effectively blindness in the right hemifield, it is impossible to anticipate where precisely relevant parts of the scenery are located. The long saccades towards the right hemifield can be interpreted as a compensatory strategy to view larger parts of the screen using the intact left side of the visual field. In fact, making long saccades towards the blind hemifield is a compensatory strategy that is also being taught in vision rehabilitation therapy (de Haan et al., 2015).

Eye tracking and virtual reality in the rehabilitation of mobility of hemianopia patients: a user experience study

this chapter is based on: Gestefeld, B., Koopman, J., Vrijling, A., Cornelissen, F., de Haan, G. (2020). Eye tracking and virtual reality in the rehabilitation of mobility of hemianopia patients: a user experience study. *Vision Rehabilitation International*. 11. 10.21307/vri-2020-002.

4.1 Abstract

Purpose: To test the usability of eye tracking and virtual reality during vision rehabilitation training of hemianopia patients.

Methods: 13 individuals with hemianopia and 4 normal-sighted controls performed various exercises that are commonly used in vision rehabilitation for mobility, while wearing a head-mounted eye tracker or a head-mounted virtual reality (VR) display. 4 occupational therapists guided them through the exercises. All participants (including therapists) filled out a questionnaire, assessing their experience with the used device by giving a score between 1 and 4 for different criteria. A higher score indicated a better fulfilment of the criteria. Individuals with hemianopia were split into three groups according to their stage in vision rehabilitation therapy and performed 1 (beginner), 2 (intermediate) or 3 (advanced) different exercises.

Results: Individuals with hemianopia rated the mobile eye tracker with a score of 3.97 +/- 0.5 points (beginner), 3.8 +/- 0.5 points (intermediate) and 4 +/- 0 points (advanced) the corresponding occupational therapists with a score of 3.6 +/- 0.6, 3.4 +/- 0.9 and 3.87 +/- 0.6 points (out of a maximum of 4 points). The VR headset was rated with 3.9 +/- 0.5 points by individuals with hemianopia, 3.8 +/- 0.5 points by normal-sighted controls and 2.5 +/- 1.4 points by the occupational therapist in a virtual hallway scenario. In a street-crossing scenario, it was rated with 3.7 +/- 0.5 points by individuals with hemianopia, 3.7 +/- 0.8 points by controls and 2.8 +/- 1.2 by occupational therapists. In a walking along a pavement scenario the individual with hemianopia gave 4 +/- 0 points and the controls 3.8 +/- 0.4 points on average.

Conclusions: Both devices were seen as useful additions to vision rehabilitation therapy, as they enable better feedback to patients and the opportunity to do different exercises at different levels of difficulty.

4.2 Introduction

Patients with hemianopia are blind in one half of their visual field, due to damage to the visual system posterior to the optic chiasm. This large visual field defect may lead to difficulties in different daily life situations, such as mobility related activities. There is however a large variability in how severely different individuals are impacted by their visual field loss. A crucial factor that determines if an individual can successfully adapt to visual field loss is the development of compensatory strategies, such as certain eye movement patterns (Howard and Rowe, 2018). While some hemianopia patients are able to spontaneously develop compensatory strategies for their visual field loss, others retain difficulties, in particular with detecting objects in the periphery in situations when they are moving, e.g. during walking (Iorizzo et al., 2011). These patients can enter vision rehabilitation to learn compensatory eye movement strategies (for an overview see Pollock et al. (2019)). In one type of compensatory scanning training, InSight-Hemianopia Compensatory Scanning Training (IH-CST), these patients learn to make horizontal scanning eye-movements (de Haan et al., 2015) in order to compensate for the field defect during mobility-related activities. In IH-CST training, hemianopia patients learn to repetitively perform a triad of saccades including an initial large saccade made towards the blind hemifield. Training hemianopia patients in making this type of scanning patterns improves their detection of peripheral stimuli and their avoidance of obstacles while walking (de Haan et al., 2015). IH-CST consists of the following exercises:

1. Creating awareness of the extent of visual field loss. The therapist presents objects in different parts of the visual field (while patients keep their gaze fixated on a single location).
2. Learning the scanning pattern. The patient is taught to systematically make the eye movement pattern, being seated and fixating objects in the desired gaze locations at different distances. The occupational therapist observes the eye movements of the patient.
3. Further practice to automate the scanning pattern in a static condition. The patient has to call out numbers presented on a screen. If numbers are named correctly and quickly, it is assumed that the scanning pattern is also performed correctly.

4. Applying the scanning pattern in indoor mobility conditions. Again, the therapist observes the patients eye movements.
5. Applying the scanning pattern in outdoor mobility conditions. The scanning pattern is practised in different traffic situations outside the therapy centre with increasing complexity. Patients walk, cycle or drive a mobility scooter, depending on their needs.

4

Studies investigating the effect of eye movement compensatory strategies, so far, have only compared the performance of participants in certain tasks, such as visual scanning or detecting obstacles while walking, before and after compensatory scanning training (Nelles et al., 2001; de Haan et al., 2015). They did not evaluate whether participants had correctly performed the scanning pattern during the training exercises. In the practical application of IH-CST at Royal Dutch Visio, there is also no objective measure of the eye movements during rehabilitation training. Instead, therapists attempt to gauge the approximate gaze direction of the patient or judge whether the scanning pattern was correctly applied based on the behaviour of the patient. As this procedure is rather subjective and error-prone, adding eye tracking in the IH-CST training would provide the patient and the therapist with better insights into the actual scanning patterns made during the different exercises. These insights will then be the basis for better feedback to the patients, which should in turn improve their progress in visual rehabilitation. Secondly, the change in difficulty when transitioning from one step to the next in the training procedure can be too large for some people, as it is difficult to transfer learned perceptual skills to a new task (Ellison and Walsh, 1998). At present, the training environment transitions from a rather simple, static and predictable situation (step 3) to a dynamic environment (step 4 and 5). Therefore, having intermediate levels of difficulty, complexity and predictability would ease the transition between these steps. A possible way to achieve this is by using virtual reality (VR). In VR it is possible to create environments with increasing complexity, which can be controlled by the occupational therapist and are safe by nature (Rizzo, 2005).

An important aspect for successful integration of eye tracking and VR is that individuals with hemianopia and occupational therapists need to be willing and able to use the devices without external help. We therefore want to assess the user experience of individuals with hemianopia, normal-sighted controls and the occupational therapists with a

mobile eye tracker (study 1) and a VR headset (study 2) during different exercises for mobility training. The devices were tested in exercises that were part of the current IH-CST protocol. We established a list of requirements, which should be fulfilled by the tested devices, based on the expertise of occupational therapists, technical staff of Royal Dutch Visio and the authors of the study. Given this list of requirements we designed a questionnaire to assess the usability of the devices (Appendix A and B). The goals of this study are to find out whether the overall user experience of participants is sufficiently positive to continue working with these devices. In addition we want to establish which criteria still need improvement based on the feedback of our participants to make the integration into IH-CST training possible.

4.3 Methods

Questionnaire for both studies

The first part of the questionnaire (part A) consisted of questions for individuals with hemianopia and normal-sighted control subjects. The second part (part B) consisted of the questions for occupational therapists. Each question could be answered by ticking one of four boxes, which stood for the options: strongly disagree, somewhat disagree, somewhat agree and strongly agree. For the analysis, the answers were then converted to a score. This ranged from 1 to 4 if a positive answer to the question meant that the requirement was fulfilled. The score ranged from 4 to 1, if a negative answer to the question meant that the requirement was fulfilled. In addition, participants could comment on each question in an additional box giving them the opportunity to explain their answer and provide details about problems that occurred.

Study 1) Eye tracking

Participants

Seven individuals with hemianopia (mean age: 53 years, SD 17), who were enrolled in the vision rehabilitation program at Royal Dutch Visio in Amsterdam, and three occupational therapists tested the head mounted eye tracker. We did not include normal-sighted controls in the first study, as the device is intended for usage with individuals with hemianopia. As the exercises that were performed in this study were already established as

part of IH-CST training, we knew the effect of exposing our participants to these exercises. Detailed information about the individuals with hemianopia who participated in study 1 is provided in table 4.1. All occupational therapists had received the standard education for their profession in the Netherlands had several years of professional experience in visual rehabilitation and they were trained and highly experienced in providing the IH-CST.

Visual field	Age	Category	Gender	Glasses/Lenses
Hemianopia on left side	63	beginner	m	OD: S +0.50, OS: S +0.50
Hemianopia on left side	20	beginner	f	OD: S -0.5, OS: S -1
Hemianopia on left side	70	intermediate	m	OD: S-6.25, OS: S-5.25
Hemianopia on right side	41	intermediate	m	OD: S-4.25, OS: S-4.50
Hemianopia on right side	65	intermediate	m	OD: S-2.75, OS: S 0
Quadrantanopia upper left	53	advanced	m	OD: S +1.50, OS: S +1.25
Hemianopia on right side	52	advanced	m	No glasses

Table 4.1: Information on participants (individuals with hemianopia) in the eye tracker study.

Materials

We used a head mounted eye tracker (Pupil Labs: Pupil Core) (Kassner et al., 2014), which has a wide angle world camera (30 Hz) for recording the environment in a 100 degree field of view horizontally and two eye cameras recording the eye movements at a sampling rate of 200 Hz. The eye tracker was connected to a laptop, which had the Pupil Labs software installed (Pupil Labs, Berlin; <https://github.com/pupil-labs/pupil>).

The Pupil Labs software provides an interface through which the eye tracker can be calibrated, the data can be recorded, and the recordings can be replayed on top of the video recordings from the world camera.

Procedure

Study 1 was performed at Royal Dutch Visio in Amsterdam. The study was approved by the Ethical Committee of the Psychology department of the University of Groningen and all participants provided informed consent. Each participant completed one, two or three exercises from the IH-CST protocol while their eye movements were tracked with a head mounted eye tracker. Some exercises were repeated several times during a training session and eye movements were recorded each time. Participants were instructed to perform the scan pattern that they had already learned in previous steps of IH-CST training. As participants with hemianopia were clients of Royal Dutch Visio, who were at different stages of their rehabilitation, they only performed exercises that were suitable for their current training stage. They could be split into three groups: beginners (2 participants), intermediate (3 participants) and advanced (2 participants). Beginners only performed exercise 1, intermediates performed exercise 1 and 2, and advanced participants performed exercise 1, 2 and 3. Table 4.1 shows which participant performed which exercises. The eye movement data sheet and the movie of the eye movements projected onto the visual field of the participant were saved. Individuals with hemianopia and their occupational therapist watched the video recordings of the eye movements directly after each exercise, with one exception where the video recording was discussed about a week later. The occupational therapists assessed whether the required scanning pattern had been performed correctly based on the video recordings and gave feedback to the individuals accordingly. Individuals with hemianopia filled out part A and the occupational therapist, who accompanied them, filled out part B of the questionnaire after a test session. This means that beginners rated the eye tracker based on their experience in exercise 1, intermediates based on their experience in exercise 1 and 2, and advanced participants based on their experience in all exercises. This is the same for the therapists who accompanied them. We determined the average score over one questionnaire of each participant, as well as the average score over all questionnaires of each participant group (beginners, intermediates, advanced and their

corresponding occupational therapists). A score of above 2 out of 4 points indicates an overall positive user experience. We also collected the comments that were made by all participants about a certain criterion to illustrate which specific aspects need to be changed to improve the usability of the mobile eye tracker.

Exercise 1: *Applying the scanning pattern in a static condition*

Participants had to call out 30 or 60 numbers presented on a large screen (2x2 m, viewing distance: 85 cm, height of the numbers: 3 cm). They initially fixate a cross in the centre. Then numbers were displayed at different locations on the screen. The patient needed to use the learned scan pattern (without head movements) to see all numbers. Each exercise took about 1-3 minutes, the exact time depending on the reaction times of the participant. Participants wore the head mounted eye tracker while performing exercise 1, seated in a chair with the laptop, to which the eye tracker was connected, outside their field of view.

Exercise 2: *Applying the scanning pattern in a simple indoor environment with static obstacles.*

Individuals with hemianopia walked along a hallway of 17 m length and 1.5 to 3 m widths in the therapy centre, while performing the learned scanning pattern. This exercise can be varied, by introducing obstacles and targets on the walls, that the participant needs to see. In this study participants performed the exercise with coloured cards pinned to the walls, of which they have to report the colour to the therapist. Individuals with hemianopia performed this exercise wearing the head mounted eye tracker, while the occupational therapists accompanied them carrying the laptop, which was connected to the eye tracker. Individuals with hemianopia were instructed to perform the scanning pattern while walking, as they would usually do in this exercise during the IH-CST. This exercise takes approximately 3 min., in which the participant walks along the hallway in both directions.

Exercise 3: *Applying the scanning pattern in outdoor mobility situations.*

Individuals with hemianopia and occupational therapists crossed a road and walked down a footpath, while the individuals with hemianopia were wearing the head mounted eye tracker and a backpack with the laptop it was connected to. The individual with hemianopia was instructed to perform the learned scanning pattern while walking.

All participants crossed the same road and walked along the same footpaths. As this exercise was performed in public space, the traffic conditions were not the same for all participants. Crossing a road once took about 1 min and walking along a footpath was recorded for 1:40 min per recording.

Study 2: Virtual reality

Participants

Six individuals with hemianopia, four normal-sighted controls (3 male, 1 female, mean age: 48 years, SD: 22 years) tested the VR headset. One occupational therapist guided them while performing the exercises. The therapist explained the virtual environment, which task to perform and guaranteed the safety of the person wearing the headset, while they moved within the setup. Detailed information on the individuals with hemianopia can be found in table 4.2. Normal-sighted controls were included to test the effect of a visual field defect on the experience of virtual environments. This way we could control for the possibility that individuals with hemianopia had a negative experience with VR due to the presence of their visual field defect. The occupational therapist had received the standard education for their profession in the Netherlands, had several years of professional experience in visual rehabilitation, and was trained and highly experienced in providing the IH-CST. Individuals with hemianopia were enrolled in the vision rehabilitation program at Royal Dutch Visio in Haren. They had completed different stages of IH-CST training at the time of the experiment. All participants were naïve to using a VR headset. The occupational therapist was involved in planning the tests and therefore had about 4 months time to familiarize with the technology.

Visual field	Age	Gender	Glasses/Lenses
Hemianopia on right side	46	m	multifocal, +1,2
Hemianopia on right side	70	m	multifocal, +0,8
Hemianopia on right side, sparing at 20 degrees	65	m	multifocal, +1
Hemianopia on right side	58	m	multifocal, +1.25
Hemianopia on left side with sparing (intact vision in the foveal region of the visual field)	56	f	+0.8
Bottom right quadrantanopia	65	f	multifocal +1
Intact	65	m	Glasses (no further specification)
Intact	27	m	Glasses (no further specification)
Intact	30	m	No glasses or lenses
Intact	70	f	Glasses (no further specification)

Table 4.2: Information on participants (individuals with hemianopia) in the eye tracker study.

Materials

The exercises in virtual reality were presented with a HTC Vive (Manufacturer, City; horizontal visual field size: 110 degrees, refresh rate: 90 Hz, resolution: 1080 x 1200

pixels per eye). Two motion sensors (called Vive base stations) tracked the position of the headset in space by creating infrared pulses that are detected by the headset. The range of motion, which can be tracked, is determined by the distance between the two sensors. They are therefore placed at opposite ends of the setup. We used two different setups of the hardware. The first setup was used while developing the virtual environments. The second one was used in the final experimental session with our participants.

Setup 1: The VR headset was connected to a laptop that was placed on a table, with a cable of 4 m length. The maximum range of movement of the person wearing the headset walking in a straight line was about 4 m. due to the size of the room in which the experiment was performed. The motion sensors were placed at either end of the setup, meaning that they were approximately 4 m. apart.

Setup 2: The VR headset was connected to a PC that was placed on a cart. The motion sensors were placed about 5.5 m. apart. The therapist moved the cart with the PC so that the range of movement for the participant was 5.5 m. Virtual environments were developed by the The Virtual Dutch Men (<https://thevirtualdutchmen.com>) using Unity.

Procedure

Study 2 was performed at Royal Dutch Visio in Haren. The study was approved by the Ethical Committee of the Psychology department of the University of Groningen and all participants provided informed consent. We first met with our VR developers for two development sessions, where they presented a first version of the requested virtual environments for three different exercises. These first versions were tested by one individual with hemianopia, an age matched control and authors of the study. Two of these exercises were further developed into their final versions and tested in an experimental session by the participants mentioned in the participants section above. For completeness we will describe all three exercises, including the first version of exercise 3, which was performed by one individual with hemianopia (70 years) and 3 controls (mean age 43). Individuals with hemianopia and normal-sighted controls filled out a questionnaire after each exercise. The occupational therapist filled out one questionnaire for each exercise at the end of the experimental session. We computed the average score that was given for exercises 1 and 2 of each participant group (individuals with hemianopia, normal-sighted controls and the occupational therapist) in their final versions. We also computed the

score that was given by the individual with hemianopia and each of the controls given to exercise 3. In addition, we collected the comments that were made by each participant about each exercise to evaluate how we can improve the exercises in the future.

Exercise 1: Walking along a virtual hallway

Normal-sighted controls and individuals with hemianopia started walking at one end of the virtual hallway and had to walk to the other end. The view for the participant when starting this exercise is shown in figure 4.1. Figure 4.2 shows the entire hallway from above to get an overview over the full trajectory (not shown to the participant). The position of the headset was tracked in space so that participants perceived motion in VR in synchrony with their actual motion in the setup.. As the range of motion, that our final setup allowed, was too short to complete a walk along the entire trajectory of the hallway, participants turned around after 5.5 m. While turning around, a black screen was shown and the virtual environment was turned 180 deg., so that the participants continued to walk along a new part of the hallway.

Three different versions and six scenarios (differing in the amount of obstacles in the hallway) of a virtual hallway scenario were developed. Details about these versions and scenarios can be found in table 4.3. Participants tested several scenarios of this exercise, depending on how long completing a certain scenario took. The number of scenarios tested differed between participants.

Exercise 2: Crossing a virtual street

The exercise started with the participant standing on a pavement facing a two-lane road. The virtual environment was scaled in such a way that the participant walked the same distance in the virtual scenario as in the real world setup. This means that they stood on one end of the setup and walked in a straight line to the other end of the setup to cross the virtual street, completely.

Two scenarios of this exercise were implemented. Crossing the street with or without traffic (see 4.3). Figure 4.3 shows the scenario with traffic from above to give an impression of the virtual environment and the relative sizes of the objects in it. *Exercise 3:*

Walking along a pavement

Participants were placed on a pavement, which was surrounded by houses. The pavement was partly blocked by a construction site. Participants were instructed to walk past the construction site. Figure 4.4 shows this environment from the initial perspective of the participants.

Exercise	Scenarios
Walking along a virtual hallway	1: empty hallway with open and closed doors 2: hallway with traffic cones 3: hallway with more traffic cones than in scenario 2 4: hallway with traffic cones, windows and doors 5: different obstacles, like plants, cupboards, bins and traffic cones 6: with people, other hallways on the side, windows and doors
Crossing a road	1: Without traffic or pedestrians 2: With traffic and pedestrians
Walking along a pavement	1: with construction site

Table 4.3: Versions, setups and scenarios per exercise used in virtual reality.



Figure 4.1: Initial view of the participant in exercise 1 (walking along a hallway) of version 5 of the exercise showing different obstacles, as well as doors, windows and avatars.



Figure 4.2: View from above in exercise 1 (walking along a hallway) of version of the exercise. This figure shows the whole trajectory the participants have to walk along, while having to turn around every 5 m. within the setup.



Figure 4.3: View from above in exercise 2 (crossing a street) of version 1 of this exercise with traffic, showing an overview over this environment.



Figure 4.4: Initial view of the participant in exercise 3 (walking along a pavement) showing the pavement with construction site and surrounding buildings.

4.4 Results

Study 1: Eye tracking

All exercises

The overall feedback for the head mounted eye tracker was very positive with a mean score of 3.7 +/- 0.5 given by the beginners, a mean score of 3.8 +/- 0.5 given by the intermediates and a mean score of 4 +/- 0 given by the advanced individuals with hemianopia. The corresponding therapist questionnaires gave an average score of 3.6 +/- 0.6, 3.4 +/- 0.9 and 3.8 +/- 0.6. Figure 4.5 shows the average score and standard deviations of each participant. We identified four main criteria that were most important for the user experience, based on the comments mentioning them:

1. Usability in mobile situations and outside
2. Usability with glasses
3. Improvement of feedback
4. Being easy to use (no disruption of regular procedure of therapy session).

Table 4.4 provides an overview of the comments made by individuals with hemianopia and occupational therapists.

Criterion	Comments patients (# comments)	Comments therapists (# comments)
Usability in mobile situations and outside	Would be more comfortable without the cable (1)	Would be better to do the exercise with tablet (1) Laptop carried in backpack (2) Calibration can be difficult under varying luminance conditions(1)
Usability with glasses	Uncomfortable to wear with own pair of glasses (1)	Calibration can be difficult with glasses/lenses (2)
Improvement of feedback	Watching the eye movements to give feedback is a good addition to the performed exercises (1)	Watching the eye movements to give feedback is a good addition to the performed exercises (1) Confirmation that the client is actually doing the scan rhythm (1) Have not watched the recording, but expect it to be good material to reflect on exercise(1)

<p>Easy to use/ no disruption of regular procedure of therapy session</p>	<p>Eye cameras in the field of view, could be corrected (3)</p>	<p>Need practice to perform setup of device (1) Eye cameras in the field of view, could be corrected (1) Laptop cannot be closed; that would stop recording (1) Battery of the laptop was empty before end of session (1) In exercise 1 (calling out numbers presented on a large screen) it is not possible to watch eye movements and screen at the same time (1)</p>
---	---	---

Table 4.4: Score and comments for the head mounted eye tracker for each criterion evaluated by patients and therapists.

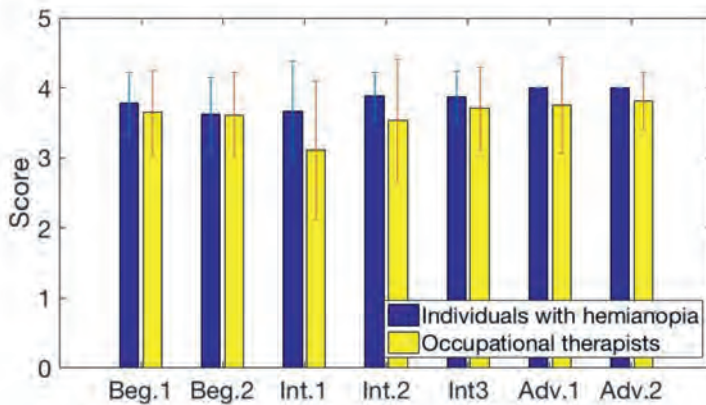


Figure 4.5: Average score given to the head-mounted eye tracker by each participant and their corresponding occupational therapist. The error bars represent the standard deviation.

Study 2) Virtual reality

Exercise 1: Walking along a virtual hallway

The feedback of individuals with hemianopia and normal-sighted controls was more positive than the feedback from the occupational therapist for this exercise. Individuals with hemianopia rated this exercise with an average score of 3.9 ± 0.5 , controls with an average score of 3.8 ± 0.5 and the occupational therapist with an average score of 2.5 ± 1.4 . Figure 4.6 shows the score given by each participant. The most important challenge in this exercise was to simulate the movement of the participant over a distance of several meters in the virtual environment, which is much longer than the range of movement in exercise 2. The current setup of the hardware did not allow for a large enough range of movement to walk all the way to the other end of the hallway, although using setup 2 improved it. Our approach of letting the participants turn around before continuing along the next section of the hallway, was not a good solution as it led to a feeling of insecurity by participants, when they had to turn around without visual input. This comment was made in several questionnaires. An overview over the comments, which were specifically relevant for this exercise, is shown in table 4.5.

Criterion	Comments patients	Comments therapist
Large range of mobility	Turning around a lot is irritating, would prefer to continue walking (2) Cables are in the way when turning therefore I have to remember which way to turn (2)	Range of mobility too short for this exercise (1) Cable in the setup make it harder to move in VR (1)
Safety	Scenery going blank when turning leads to problems with balance (1)	Higher risk of injury than when exercise is done in actual hallway (1)

Table 4.5: Score and comments on criteria that are specifically important to use the VR headset for walking along a virtual hallway.

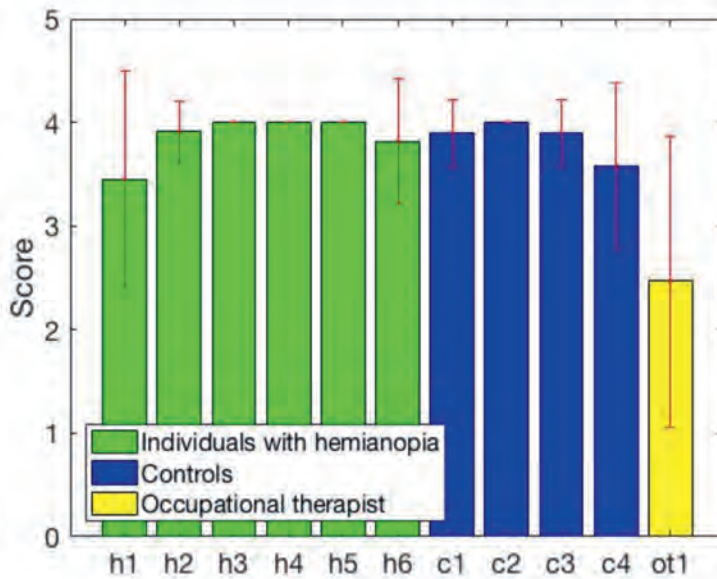


Figure 4.6: Average score given to the virtual hallway scenario by individuals with hemianopia, normal sighted controls and the occupational therapist. The error bars represent the standard deviation.

Exercise 2: Crossing the street

This exercise was rated with 3.9 +/- 0.5 points by individuals with hemianopia and 3.7 +/- 0.8 points by normal-sighted controls. The occupational therapist gave this exercise a mean score of 2.8 +/- 1.2 points . Figure 4.7 shows the score and standard deviation of each participant. An overview over the comments made about this exercise are shown in table 4.6. The range of motion was sufficient to cross the road entirely. Several participants (individuals with hemianopia and normal-sighted controls) commented that they did not like the aesthetics of the virtual environment. The occupational therapist rated the range of motion as not sufficient in this exercise.

Criterion	Comments patients	Comments healthy controls
Immersive and pleasant virtual environment	Did not feel as safe as when walking in the hallway: cars were too close to me (1) Avatars were walking through me (2) Stood too close to the street (2) Blue line that marks end of mobility range irritating (1) Cars are too close, too large (1) Pavement needs to be wider (2)	Adding sound would be helpful; horn before collision with car (1) Blue line that marks end of mobility range irritating (1) Cars show up too late in scene (1) Faces of people do not look realistic (1)

Table 4.6: Comment on criteria that are specifically important to use the VR headset for crossing a street. The occupational therapist who tested this exercise did not make any comments that were specific only to this exercise.

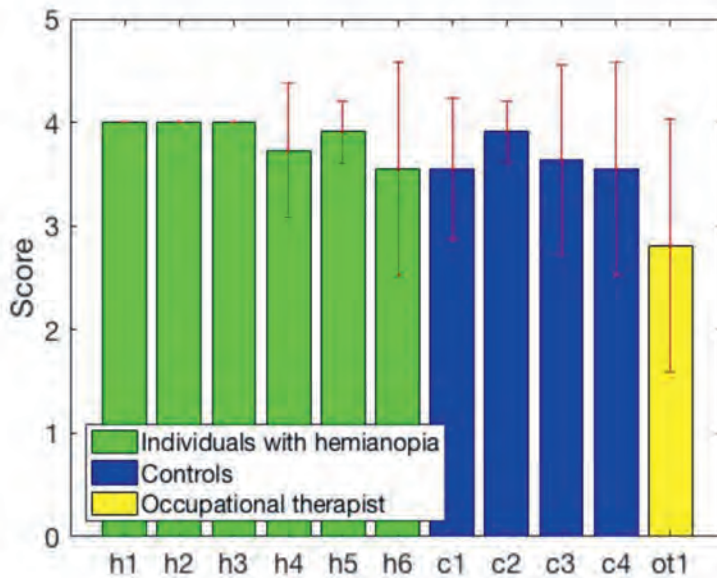


Figure 4.7: Average score given to the virtual street-crossing scenario by individuals with hemianopia, normal sighted controls and the occupational therapist. The error bars represent the standard deviation.

Exercise 3: Walking along a pavement Table 4.7 shows the comments that were made about this exercise. Participants had a positive opinion about this virtual environment. The individual with hemianopia rated it with a score of 4 ± 0 points and the normal sighted controls with a score of 3.8 ± 0.4 points.

Criterion	Comments individuals with hemianopia (# comments)	Comments healthy controls (# comments)
Immersive and pleasant virtual environment	/	Scenery was a bit too crowded (1)/
Avoid motion sickness	/	Scenery stopped moving due to an error. This led to dizziness (1)
Moving in VR	Range of movement too short (1)	/

Table 4.7: Comments on criteria that are specifically important to use the VR headset for walking along a pavement.

4.5 Discussion

The main finding of this study is that the user experience of individuals with hemianopia and normal-sighted controls was generally positive for both tested devices. While the occupational therapists, who evaluated the head mounted eye tracker, also reported a positive user experience the occupational therapist, who evaluated the virtual reality setup, reported a more negative experience. Below, we describe our findings, conclusions and these experiences in more detail.

Providing feedback by showing replay of eye movements improves the user experience of individuals with hemianopia and therapists in mobility training

A positive aspect, noted by individuals with hemianopia and therapists, of using the head mounted eye tracker during the therapy sessions was that it offers the possibility to replay the eye movements to give feedback to the participant. This was seen as a way to improve therapy progress, as individuals with hemianopia are able to reflect on their own viewing behaviour. Moreover, it helps the therapists to explain the (need for) compensatory strategies. All participants and therapists saw the recording of the eye movements during the four exercises as a beneficial addition to the training.

The device fulfilled most of the requirements of individuals with hemianopia and therapists. A problematic aspect was the usability with glasses, as the eye tracker was less precise in tracking the pupil when participants were wearing their glasses, especially under varying luminance conditions. This is a common problem for eye trackers, as glasses and contact lenses and changes in luminance distort the image of the eye that is captured by the eye tracker (Dahlberg, 2010; Fuhl, 2016). The Pupil Labs eye tracker provides a confidence interval of the recorded data, which can be used to judge the reliability of the recorded eye tracking data.

VR scenarios

All participants (individuals with hemianopia and normal-sighted controls) reported a preference for lively and realistic scenarios in virtual reality. Most participants thought that adding exercises in virtual reality would benefit vision rehabilitation therapy. They also think that if we can add the possibility to replay a recording of the exercise from the point of view of the participant, which also shows the eye movement behaviour, this will improve feedback.

These findings are in line with a study by Ishoel and Kanstad (2017), who tested different head mounted VR displays and concluded that VR is a promising method for vision rehabilitation therapy. While Ishoel and Kanstad developed a mini game, which is supposed to support therapy progress, we attempted to make the current virtual reality scenario resemble the real world exercise as much as possible by letting our participants walk within the setup. This approach makes it easy for participants to understand the task and, especially for individuals with hemianopia, to understand the objective of the exercise and transfer learned skills. It has previously been shown that using VR to train patients with unilateral spatial neglect can improve their visual spatial performance, as well as their ability to cross a real street (Katz et al., 2005). However, the setup described by Katz et al. was not immersive and did not require the participants to move. In a study by Iorizzo et al. (2011) individuals with hemianopia and normal-sighted controls were presented with an immersive virtual environment in which they had to detect basketballs that were presented in the periphery. This task was performed seated as well as while walking in an L-shaped path. They found that individuals with hemianopia had more difficulty detecting targets in the periphery when walking than the control group. This

finding emphasizes that it is necessary for individuals with hemianopia to practice eye movements while walking. Under ideal circumstances, the immersive VR environment that we created can be used while a large space is available in which the participants can safely move the required distances. To walk through the complete virtual hallway at once, the available real walking distance should be long enough, for example the same length as the actual hallway, in which the exercise is performed. Preferably, it would be even larger to allow for directional errors. At present, this was technically not feasible as it would also require that the sensors of the VR headset had to be placed much further than 5.5 meters apart, which would have made tracking of the headset impossible. In the first version of this exercise, we tested two options to compensate for this. The first idea was that one step in reality corresponded to several steps in the virtual world. The second idea was to let the participant continue along a new part of the hall virtual hallway when they turn around at the end of the setup. The participant could continue to walk along the virtual hallway by walking back to the other side of the room. As the first caused dizziness and insecurity when walking, the second idea was implemented in the following sessions. Our solution to let participants turn around after a few meters however interrupted the flow of the task and this was experienced as irritating by the participants, both the normal-sighted controls and the individuals with hemianopia. Another problem of our current setup 2 was that the cart with the computer had to be dragged along next to the participant. In our setup, the power cable for the computer was often in the way causing problems to move the cart. Therefore the occupational therapist was assisted by two people to move the cart, which is an undesirable solution in an actual therapy sessions. When turning around at the end of the setup, the cable of the VR headset was also often in the way and participants had to be instructed such that they would only turn around in one direction.

Therefore, to be able to perform these exercises within a regular training session, the setup will need to change fundamentally. Despite these difficulties, the participants and the therapist were of the opinion that adding VR exercises to the regular training sessions will be beneficial. Instead of using a larger space, which can be costly or simply not available, the space issue may also be solved by adding an all-directional treadmill to the VR setup that will enable walking longer distances in all directions (e.g. <https://www.virtuix.com>). A further way to improve future setups is to add eye tracking to the VR exercises, which is technically feasible by now (e.g. [4](https://pupil-</p></div><div data-bbox=)

labs.com/products/vr-ar/).

Limitations

In this study, not all of our participants completed and evaluated the same exercises. This has some practical reasons. In study 1 the eye tracker was tested during regular training sessions of the participants. Therefore they only performed exercises that were suitable for their current training stage. VR exercise 3 was not included in the final test session, due to time constraints, meaning that there was too little time for the developers to continue developing this exercise and there would also not have been enough time on the day of testing to let all participants perform another exercise. We still decided to report the results of the questionnaire for this exercise here, as the participants liked the virtual environment and we therefore plan to continue its development in the future.

This study does not evaluate the benefit in terms of training progress of adding eye tracking and VR to the current protocol. This will be the topic of a follow up study. The results of this study represent the subjective experiences of our participants. In our opinion a positive user experience is an important aspect for the successful integration of these devices in the IH-CST training.

Conclusion

This study shows that integrating eye tracking and VR technologies into vision rehabilitation therapy may positively impact training outcomes. Individuals with hemianopia are able to use these technologies and they consider these helpful additions to the existing training exercises. Therapists welcome the additional objective information provided, but indicate that VR setups first need to allow for a larger range of mobility. Moreover, integrating eye tracking into the setup could further increase the value of VR.

Acknowledgements

We want to thank Birgit van Iddekinge and Christiaan Pinkster for supporting the project, providing knowledge on vision rehabilitation therapy and technical aids. We want to thank the 'The Virtual Dutch Men' for developing the virtual environments.

This project was funded by Stichting Novum. Additional support was provided by Royal Dutch Visio, the European Unions Horizon 2020 research and innovation programme

under the Marie Skłodowska-Curie grant agreement No. 661883 (EGRET-cofound), and the Graduate School of Medical Sciences (GSMS), University of Groningen, The Netherlands. The funding organizations had no role in the design, conduct, analysis, or publication of this research.

References

- Dahlberg, J. (2010). Eye tracking with eye glasses. Master's thesis, Umea University.
- de Haan, G., Melis-Dankers, B. J. M., Brouwer, W. H., Tucha, O., and Heutink, J. (2015). The effects of compensatory scanning training on mobility in patients with homonymous visual field defects: A randomized controlled trial. *PLOS ONE*, page 129.
- Fuhl, W. (2016). Pupil detection for head-mounted eye tracking in the wild: an evaluation of the state of the art. *Machine Vision and Applications*, 27(8):12751288. Springer Berlin Heidelberg.
- Howard, C. and Rowe, F. J. (2018). Adaptation to poststroke visual field loss: A systematic review. *Brain and Behavior*, 8(8):121.
- Iorizzo, D. B., Riley, M. E., M., H., and Huxlin, K. R. (2011). Differential impact of partial cortical blindness on gaze strategies when sitting and walking an immersive virtual reality study. *Vision Research*, 51(10):11731184.
- Ishoel, M. and Kanstad, I. M. (2017). *Virtual reality based vision therapy For stroke patients with homonymous visual field deficits*. PhD thesis, Norwegian University of Science and Technology.
- Kassner, M., Patera, W., and Bulling, A. (2014). Pupil: An open source platform for pervasive eye tracking and mobile gaze-based interaction. *Proceedings of the 2014 ACM International Joint Conference on Pervasive and Ubiquitous Computing: Adjunct Publication*, page 11511160.
- Katz, N., Naveh, Y., and Weiss, P. (2005). Interactive virtual environment training for safe street crossing of right hemisphere stroke patients with unilateral spatial neglect. *Disability and Rehabilitation*, 27(20):12351243.

Nelles, G., Esser, J., Eckstein, A., Tiede, A., Gerhard, H., and Diener, H. (2001). Compensatory visual field training for patients with hemianopia after stroke. *Neuroscience Letters*, 306(3):189–192.

Pollock, A., Hazelton, C., Rowe, F., Jonuscheit, S., Kernohan, A., Angilley, J., Henderson, C., Langhorne, P., and Campbell, P. (2019). Interventions for visual field defects in people with stroke. *Cochrane Database of Systematic Reviews*, Issue 5.

Rizzo, A. S. (2005). A swot analysis of the field of virtual reality rehabilitation. *Presence*, 14(2):119146.

Appendix A

Evaluation usage of method

Scangedrag bij Hemianopsie

Version 19 september 2018

A. Participant

Technique (*circle around the used method*): VR / AR / mobiele eye tracker

Exercise (take number from list):

Date:

Location:

Client number:

Age:

Please make a cross at every statement in how far you agree (2 pages)?

1 = totally disagree

2 = somewhat disagree

3 = somewhat agree

4 = totally agree

		1	2	3	4	Space for remarks
1	Wearing the device was comfortable.					
2	I felt comfortable during the exercise.					
3	I did not feel dizzy during the exercise.					
4	The instructions for the exercise were easy to understand.					
5	The degree of difficulty was appropriate for me (Not too difficult or too easy).					
6	I could handle the device properly (<i>if applicable</i>).					
7	The sound was audible (<i>if applicable</i>).					

8	The image was pleasant to look at (<i>only VR and AR</i>).					
9	Parts of the device were visible and disturbed the performance of the exercise.					
10	The image resembles a real (traffic) situation (<i>only VR</i>).					
11	I had the feeling to actually be in a different environment (<i>only in VR</i>).					
12	I could talk to the therapist during the exercise when necessary.					
13	I think that this exercise is a useful addition to the training.					

What are the most important criteria to make this exercise pleasant?

Was it possible to perform the scan pattern during the exercise? If not, why was it too difficult?

Which of the versions you tested today were the best and the worst in your opinion? Why?

Do you have other remarks?

5

General Discussion

5

In this thesis, I investigated two main research questions. Can we develop more simple and comfortable screening tests for visual field defect (VFD) using free-viewing eye movements recorded during movie viewing? And can we use eye-tracking and virtual reality (VR) to improve vision rehabilitation therapy of patients with VFD? In the following sections, I summarize the findings and discuss possible interpretations as well as implications for future research or practical applications.

5.1 Summary of the results

Can we use free viewing eye-movements to detect and reconstruct VFD?

Simulated VFD

Chapter 2 described a proof of principle study showing that simulating various types of glaucomatous and hemianopic VFD in healthy participants while they viewed movie clips without explicit task instructions leads to changes in their viewing behavior. To summarize, we found that the key to separating participants with various VFD from those without lies in the difference in the spatial distribution of the eye movement features between the groups of participants.

Based on the distribution of fixation locations across the visual field after one minute of data collection, it was possible to predict whether a participant had viewed a movie clip with a simulated VFD and which type of VFD had been simulated. Using the data of at least 22 trials, we could reconstruct the hemianopic and glaucomatous VFD using two different methods. We found that the side of hemianopic VFD correlated with the distribution of viewing priority (VP) across the visual field. In contrast, the location of the glaucomatous VFD correlated with the relative distribution of fixations across the visual field.

Real VFD (of glaucoma patients)

In Chapter 3, we applied the methods of Chapter 2, as well as those used in a study by Crabb et al. (Crabb et al., 2014) to distinguish between glaucoma patients and normal-sighted controls on the basis of eye-movements. In this chapter, we also identified two factors in the experimental paradigm that strongly influence the applicability of this approach as a potential diagnostic tool. Specifically, we found that it was only possible to

distinguish between glaucoma patients and controls on the basis of their scan paths, if the movie clips had been viewed with one eye covered. Moreover, another factor that greatly influenced the ability to distinguish between the two groups was the content of the movie clips. Movie clips which are dynamic and guide the viewer's attention, like comics or feature films with interacting main characters, are more suitable to distinguish between patients and controls than scenes that display landscapes and are less dynamic, as they occur in nature documentaries.

It was not possible to replicate the previously published results by Crabb et al., where maps of saccade end points across the visual field were used to predict whether a participant was a glaucoma patient or a normal-sighted control. This could be the case because Machine learning approaches usually require large data sets and we analysed a relatively small one with 76 participants. In addition, Crabb et al. applied kPCA before classifying the data with a kernel specifically tailored to the specific data set. A small deviance in applying the method during our analysis may have caused different results. In future research, when applying machine learning approaches, larger data sets and more generalisable pipelines could lead to results that are easier to replicate.

In summary, the answer to the question is confirmatory. It is possible to differentiate between glaucoma patients and controls using eye-movements recorded during movie viewing without task instructions, provided that the presented movie clips lead to consistent viewing behaviour of normal sighted observers and trigger saccades towards the periphery of the visual field, and that the movies were viewed monocularly.

Can eye tracking and VR contribute to improving rehabilitation?

In Chapter 4, we conducted a study to test whether introducing a head mounted eye tracker and a VR headset into vision rehabilitation training exercises is regarded as beneficial by patients with homonymous hemianopia (HH) and their occupational therapists. We called this study a usability study, although it could also be called an acceptability study, as was only a first step towards using these technologies in vision rehabilitation. There is a need for follow-up studies that collect more in depth knowledge of how we could integrate eye tracking and VR into the current procedures to improve the quality of vision rehabilitation therapy for patients with HH, who learn compensatory eye movement strategies in mobility related situations. There are two problems with the

current training procedure, namely that the eye movements of the patients are not objectively measured during training and that the difficulty level between different exercises increases too fast. These problems could be solved using eye-tracking and VR. As a first step, it was necessary to determine if patients and occupational therapists were capable of using the devices and regarded the added information or possibility to perform exercises in VR as a useful addition to the current procedure. We found that this was the case. However, when combining VR and eye tracking it was necessary to connect the headset to a computer via cable, which meant that an additional person had to assist the occupational therapist during the experimental training session, which would be impossible during a regular training session. With an improved setup both devices could be beneficial for vision rehabilitation of patients with HH.

In summary, eye tracking and VR can meaningfully contribute to therapy success by providing an objective measure of eye movements during the exercises. The technology can enable better feedback based on eye movement recordings and the opportunity to practice mobility related situations, such as crossing a street in a safe environment. To successfully use these devices tested in our study in practice, they need to fulfil additional criteria. Both the eye-tracker and the VR headset should be operated wirelessly during exercises that require mobility. It should be possible to use them with glasses and to calibrate the eye-tracker under different luminance conditions.

5.2 Discussion

In the following sections, I will discuss my answers to the main research questions, as well as uncertainties and implications of my findings for future research or clinical applications.

Assessing the spatial distribution of eye movements is essential to distinguish glaucoma patients from controls

From the findings of Chapters 2 and 3, I conclude that the differences in viewing behaviour of patients with VFD and controls are subtle, which means that the two groups cannot be distinguished very well based on basic eye movements, such as the number of fixations or the average saccade amplitudes irrespective of direction. It is more informative to directly compare the spatial properties, taking the presented scene of the movie clip into account using the VP. A reduced VP in patients with VFD indicated that par-

ticipants with VFD do not direct their gaze towards the most salient region of the visual field as often as the controls. In free-viewing paradigms, without task instructions that could control the viewing behaviour of participants in a top-down manner, the VP of the control group viewing a certain movie clip indicates how well their viewing behaviour is guided by the content of the movie clip. It can therefore be used to select movie clips, where the control group shows a consistent viewing behaviour, before testing whether the patient group shows a different viewing behaviour.

In the context of measuring the eye movements of clinical populations, VP can also be considered an indicator of the ability to perform a certain visual task, like watching a movie. In our experimental chapters, we found that not only the severity of the VFD, but also its location influenced the ability of participants with simulated or actual VFD to direct their gaze towards the most salient parts of the visual scene.

In addition to showing different scan paths when watching the same content, we found that participants with VFD showed a different distribution of fixation locations across the visual field compared to the controls. We also found that in glaucoma patients, the saccade amplitudes differed from those of the controls, depending on their direction. The pattern of these directional saccade amplitudes depends on the size and location of the VFD.

The importance of considering the spatial distribution of eye movements corroborates several previous studies. For example, (David et al., 2019) found that the angle between consecutive saccades in combination with the saccade amplitude and peak velocity were the features which best predicted the presence of a simulated scotoma. Similarly, a study by Wiecek et al. (2012) showed that directional saccade amplitudes differed between glaucoma patients and controls during a visual search task.

Another study that our findings corroborate showed that the spread of fixations of glaucoma patients viewing natural images is correlated with the severity of their VFD, with a lower MD leading to a smaller spread in fixations (Asfaw et al., 2018).

Experiments using simulated VFD help to establish a blueprint for an analysis approach

It is fairly obvious that experiments with simulated VFD cannot replace experiments with actual patients. Yet, the findings from chapter 2 provided us with a good guideline for

how to approach our studies in actual patients. An advantage of using simulated VFD is that we know exactly which parts of the visual field were affected by the VFD. So, when using simulated VFD, we actually have a ground truth of the state of the visual field against which we can compare our eye movement data analysis, while we need to treat the results of the SAP with some caution.

In chapter 2, we found that the two different pathologies (glaucoma and HH), which we simulated, led to fundamentally different viewing behaviors. In chapter 3, we primarily investigated the viewing behavior of glaucoma patients. However, in part 3a we also included one patient with HH. Although we cannot generalize our findings having measured only one patient with HH, we found that this patient showed differences in viewing behavior from the glaucoma patients. More importantly, their viewing behaviour is actually more similar to that of the participants with simulated HH studied in chapter 2. In both the patient and the simulations, the distribution of VP across the visual field indicated the vision intact and deprived parts. In glaucoma, the viewing behavior of the patients differed substantially from that of the participants with simulated glaucomatous VFD. This can partly be explained by the fact that the simulated VFD bears more resemblance to the way patients with HH experience their VFD. In HH, the VFD occurs instantaneously and patients lose sight in one hemisphere completely, as opposed to the more gradual reduction of sensitivity experienced by glaucoma patients over the course of their disease. Also, we simulated the two types of VFD that occur in HH, a right sided or left sided damage. Glaucoma patients, on the other hand, can experience a variety of different types of VFD and we only simulated three possible types. Glaucoma patients, whose VFD was similar to the ones that we had simulated, namely nasal arcs and tunnel vision, also showed a similar viewing behavior similar to the participants with the respective simulated VFD. This shows, that simulated VFD elicit similar viewing behaviour as real VFD, provided that they are similar in shape and size.

Interpreting results in a free-viewing paradigm with an ecologically valid stimulus

The interpretation of the results of a free-viewing paradigm is, in a way, more difficult than interpreting the results of a task-based paradigm. For example, in visual search or visual pursuit, eye movement behavior can be related to task success. Performance and

search time indicate the difficulty that a participant has with a task. If the error rate or search time is correlated with the number of fixations, we may infer that the change in eye movement behavior is in response to the participant not seeing all the dots or the target stimulus (Coeckelbergh et al., 2002). Similarly, in the visual pursuit task described by Grillini et al. (2018), the spatial and temporal error when following the dot are caused by missing bottom-up information, i.e. the participant not seeing the dot. In these tasks, top-down guidance of the eye movements is required. In contrast, in a free-viewing paradigm, the influence of voluntary behavior is larger, which also makes it harder for classical saliency models to predict gaze locations. This is why classical saliency models, which focus on bottom-up features only, do not perform well predicting gaze locations (Koehler et al., 2014). Using VP solves this problem by using the fixation locations of the control group as the predictor for normal gaze behavior. In addition, the stimuli that were used in the studies described in chapters 2 and 3 are relatively complex. A movie clip tells a story and contains emotional content that may attract attention. Therefore, we defined the salient region in a scene the other way around compared to classical models. Instead of using the stimulus properties and trying to model top-down factors, VP defines salient regions in an implicit, experimental way, utilizing the variability of the viewing behavior among observers, also taking into account task independent biases, such as the center bias. As in free-viewing there is no task performance that could be evaluated, we could use VP to evaluate how well or normally a patient with a VFD performed the task of movie viewing. In this way, we could, however, not detect patients who used a good compensatory strategy for their specific VFD. In future research, asking the participants questions concerning the content of the movie clips could help to identify patients with a good compensatory strategy. The patients with a good compensatory strategy would be those with a low VP, who nevertheless were able to follow the movie clip.

Usability of current eye-tracking and VR technology in (elderly) clinical populations

The study described in chapter 4.4 was aimed at testing the usability of an eye tracker and a VR headset. However, we also found out a lot about the usability of modern day eye-tracking technology in an elderly population including patients with VFD.

The practical application of eye-tracking and VR technology as screening tools or sup-

5

port for vision rehabilitation depends largely on further development of those technologies. Eye tracking in natural environments with elderly participants is rather challenging and often results in a large amount of data that cannot be used (Kasneci et al., 2017). Under laboratory conditions and using the Eyelink 1000 or the Eyelink duo, we experienced similar issues when collecting eye-movement data in elderly participants with and without VFD. In chapter 3a, we had to exclude many participants, because we could not accurately calibrate the eye tracker or it would not track continuously. For many participants, it took us a long time to modify the setup, adjusting the position of the eyes in the camera image of the tracker, trying to minimize reflections from the participants glasses to be able to start the calibration. With most participants we had to perform the 9-point calibration several times, adjusting the setup in between. As the eye trackers that we used did not work with multifocal glasses, we used the trial lenses that are used to test patients optimal correction at eye clinics. With all the necessary adjustments, in some participants it could take up to 25 minutes until we could collect data. With the goal in mind of using eye-tracking in clinical practice, as a diagnostic tool or as support during vision rehabilitation, the time it takes to prepare for data collection needs to be reduced drastically. This could be achieved by using an eye tracker, which does not need to be calibrated for every participant separately if these trackers manage to maintain stable gaze tracking ((Barsingerhorn et al., 2018), Pupil Invisible Pupil Pro, (Kassner et al., 2014), BulbiCam, Bulbitech).

When using VR and eye tracking in mobility related exercises for vision rehabilitation, state of the art technology had its limitations. In our set up, it was only possible to collect eye tracking data via a cable, which was either connected to a laptop (in the case of the eye tracker) or a desktop PC (in the case of the VR headset). This was perceived as a major limitation by the occupational therapists as they were not able to operate the equipment and guide the patients through the exercises at the same time. Moreover, they were concerned that the patients could fall over the cable. Luckily, such limitations may soon no longer hinder application. We can expect that many of the difficulties we faced when conducting the experiments described in this thesis will be solved through technological advances. For example, a recent eye-tracker, the Pupil Invisible by Pupil Labs, has software that runs on a smartphone instead of a laptop. There is also the Dikablis Mobile eye tracker, which can be used with glasses and without being connected to a computer (Kasneci et al., 2017).

Such types of eye-tracker enable patients to freely perform their exercises. To improve the quality of eye-tracking data obtained in elderly participants and visually impaired people, it would be necessary for manufacturers of eye-tracking hardware and software to make their products suitable for these participant groups.

5.3 Clinical applications

Towards using free-viewing eye movements to monitor therapy progress

We know from chapter 4 that both patients and occupational therapists appreciate the possibility to receive and provide better feedback concerning the patients' scan paths based on the eye tracking. The next step towards introducing these technologies into vision rehabilitation therapy would also require better analyses of the data. For example, the analyses developed in chapters 2 and 3 could be used to assess the eye movements performed during the training sessions. The results could be used to objectively monitor therapy progress. In current IH-CST training, there is an emphasis on making long saccades into the blind hemifield. Whether patients actually do this is easy to monitor but it is harder to monitor the effect on their visual abilities. Using our methods, we could actually assess whether making this long saccade results in a functionally larger visual field. This should become apparent from an increase in VP in the blind hemifield over the course of the therapy. Such an increase would indicate that the visual information on the blind side receives more overt attention.

Towards using free-viewing eye movements to establish suitable models of compensatory eye movement strategies for vision rehabilitation

We could also assess the scan paths of patients who perform well and those who perform poorly in a specific task and determine whether these differ in a systematic manner. If so, this would indicate that the scan path of the good performers is more optimally geared towards a task. In turn, this suggests that such a suitable compensatory eye movement strategy could serve as a model for other patients with the same type of VFD. It could also be feasible to provide patients with a simple eye tracker to take home and perform exercises on their own. Future research could aim at developing software to automatically analyse the eye movement data, so that they can get instant feedback and

guidance through the software.

In the future, it seems useful to have VR exercises that get adjusted automatically in level of difficulty depending on the performance of the patient. It is also possible to add auditory aids or other kinds of stimulation to help to trigger certain eye movement behaviors. These advances could also reduce the workload for the occupational therapist. Another advantage of VR technology in combination with eye tracking is the possibility to simulate VFDs. This could be used to give the family members or caretakers better insights into the condition of the patient. In summary, eye tracking and VR may enable a future vision rehabilitation that is tailored to the needs of the individual patient. In my thesis, I primarily investigated whether eye tracking and VR could be used for vision rehabilitation of patients with HH. In my view, these techniques could also benefit the rehabilitation of patients with glaucoma. In fact, they may benefit even more from the possibility of a personalized rehabilitation than patients with HH, as their visual field loss shows much more individual variability. This is also a reason why there is no standardized vision rehabilitation program for glaucoma patients as of today (Livengood and Baker, 2015). If we could identify an optimal eye movement strategy for individual glaucoma patients, we could provide them with more effective vision rehabilitation training. The approach indicated above, of comparing naturally good and bad performers, could be a first step towards achieving this goal.

Concluding Remarks

The overall conclusions from the work presented in this thesis is that free-viewing eye movements during movie viewing could be used to distinguish between patients with VFD and normal-sighted controls. Another conclusion of this thesis is that eye tracking and VR should get introduced into vision rehabilitation therapy, as they are seen as beneficial for therapy progress by patients and occupational therapists. Combining these two conclusions, the next step in this line of research could be to find ways to assess and improve patients functional vision using the tools and procedures presented in this thesis.

References

- Asfaw, D. S., Jones, P. R., Mönter, V. M., Smith, N. D., and Crabb, D. P. (2018). Does glaucoma alter eye movements when viewing images of natural scenes? a between-eye study. *Investigative Ophthalmology and Visual Science*, 59(8):31893198.
- Barsingerhorn, A. D., Boonstra, F. N., and Goossens, J. (2018). Development and validation of a high-speed stereoscopic eyetracker. *Behavior Research Methods*, page 118.
- Coeckelbergh, T. R. M., Cornelissen, F. W., Brouwer, W. H., and Kooijman, A. C. (2002). The effect of visual field defects on eye movements and practical fitness to drive. *Vision Research*, 42(5):669677.
- Crabb, D. P., Smith, N. D., and Zhu, H. (2014). Whats on tv? detecting age-related neurodegenerative eye disease using eye movement scanpaths. *Frontiers in Aging Neuroscience*, 6(NOV):110.
- David, E. J., Lebranchu, P., Perreira Da Silva, M., and Le Callet, P. (2019). Predicting artificial visual field losses: A gaze-based inference study. *Journal of Vision*, 19(14)(22).
- Grillini, A., Ombelet, D., Soans, R. S., and Cornelissen, F. W. (2018). Towards using the spatio-temporal properties of eye movements to classify visual field defects. *Eye Tracking Research and Applications Symposium (ETRA)*.
- Kasneci, E., Black, A. A., and Wood, J. M. (2017). Eye-tracking as a tool to evaluate functional ability in everyday tasks in glaucoma. *Journal of Ophthalmology*.
- Kassner, M., W., P., and A., B. (2014). Pupil: An open source platform for pervasive eye tracking and mobile gaze-based interaction. Technical report, Cornell University.
- Koehler, K. L., Guo, F., Zhang, S., and Eckstein, M. P. (2014). What do saliency models predict? *Journal of Vision*, 14(3):127.
- Livengood, H. M. and Baker, N. A. (2015). The role of occupational therapy in vision rehabilitation of individuals with glaucoma. *Disability and Rehabilitation*, 37(13):12021208.

Wiecek, E., Pasquale, L. R., Fiser, J., Dakin, S., and Bex, P. J. (2012). Effects of peripheral visual field loss on eye movements during visual search. *Frontiers in Psychology*, 3(NOV):113.

Thesis Summary

Intact peripheral vision is needed to direct our visual attention and subsequently our eye movements to relevant parts of the visual environment. People with a visual field defect (VFD) suffer from reduced sensitivity or even complete blindness in parts of the visual field. Two common causes of VFD are glaucoma, a neurodegenerative disease in which peripheral vision slowly declines due to damage to the optic nerve, and homonymous hemianopia (HH), blindness in one half of the visual field, which is caused by damage to the visual pathways after the optic chiasm. In this thesis I explored two questions. The first question was whether we can detect VFD based on eye movements? This could potentially lead to simpler methods of performing visual field assessments.

To answer that question, I firstly conducted a study in which participants with and without simulated VFD watched short movie clips while their eye movements were measured. Using machine learning and statistical methods, I determined the spatial distribution of eye movements across the presentation screen and the field of view. With these methods, I was able to accurately predict whether a video clip had been viewed by someone with a simulated VFD or ordinary vision. I was also able to reconstruct the size and location of the simulated VFD. I then examined whether the same methods were suitable for doing this in participants with a real VFD. In addition, I investigated the influence of viewing with one or two eyes and the content of the film clips on the ability to separate participants with and without a VFD. When the movie clips were viewed with one eye, I found important differences in the viewing behavior of participants with and without a real VFD. This was not the case when the participants viewed the movie clips with two eyes. In that case, they seemed able to compensate for their VFD and watched the movies

in a similar way as the control participants without a real VFD. In addition, I found that the content of the video clips influenced the difference in viewing behavior between the two groups.

My second question was whether we can use virtual reality and eye tracking to support people with a VFD during their rehabilitation? This could improve rehabilitation.

In vision rehabilitation therapy, people with a visual field defect learn to compensate for their visual field defect by performing a certain eye movement scan pattern. Participants who tried a VR headset or a mobile (head-mounted) eye tracker during various mobility exercises had a positive experience and saw benefits from using these technologies. The same was true for the occupational therapists.

For example, by using eye tracking, the occupational therapist can show a client videos of their viewing behavior during an exercise, which makes it easier to give feedback.

In summary, I have found that eye movements can be used to determine the presence of a visual field defect in a very simple way. In addition, they can also be used to compensate for a visual field defect. In rehabilitation, recordings of the eye movements can help teach correct compensatory scanning patterns.

Samenvatting

Intact perifeer zicht is nodig om onze visuele aandacht en vervolgens ons oogbewegingen naar relevante delen van de visuele omgeving te leiden. Mensen met een gezichtsvelddefect hebben last van verminderde gevoeligheid of zelfs volledige blindheid in delen van het gezichtsveld. Twee veelvoorkomende oorzaken voor gezichtsvelddefecten zijn glaucoom, een neurodegeneratieve ziekte waarbij het perifere zicht langzaam afneemt als gevolg van schade aan de oogzenuw, en homonieme hemianopie (HH), blindheid in één helft van het gezichtsveld, hetgeen veroorzaakt wordt door schade aan de visuele banen na het optisch chiasma. In dit proefschrift heb ik twee vragen onderzocht. De eerste vraag was of we gezichtsvelddefecten kunnen detecteren op basis van oogbewegingen? Dit kan mogelijk leiden tot eenvoudigere methoden om gezichtsveldmetingen uit te voeren.

Om die vraag te beantwoorden deed ik als eerste een onderzoek waarbij deelnemers met en zonder gesimuleerde gezichtsvelddefecten naar korte filmclips keken terwijl hun oogbewegingen werden gemeten. Met behulp van machine learning en statistische methodes heb ik bepaald hoe de ruimtelijke verdeling van de oogbewegingen over het presentatiescherm en het gezichtsveld was. Met deze methoden kon ik goed voorspellen of een videoclip was bekeken door iemand met een gesimuleerd gezichtsvelddefect of gewoon zicht. Ik kon er ook goed de grootte en plaats van het gesimuleerde gezichtsvelddefect mee reconstrueren. Vervolgens ben ik nagegaan of dezelfde methoden geschikt waren om dit ook te doen bij deelnemers met een echt gezichtsvelddefect. Daarbij onderzocht ik ook de invloed van het kijken met een of twee ogen en de inhoud van de filmclips op de mogelijkheid om deelnemers met en zonder een gezichtsvelddefect van elkaar te

scheiden. Als de filmclips met een oog werden bekeken vond ik belangrijke verschillen in het kijkgedrag van deelnemers met en zonder een echt gezichtsvelddefect. Dit was niet zo als de deelnemers de filmclips met twee ogen bekeken. In dat geval leken ze in staat om voor hun gezichtsvelddefect te compenseren en keken ze op een vergelijkbare manier naar de filmpjes als de controle deelnemers zonder een echt gezichtsvelddefect. Daarnaast vond ik dat de inhoud van de videoclips invloed had op het verschil in kijkgedrag tussen de twee groepen.

Mijn tweede vraag was of we virtual reality en eye-tracking kunnen gebruiken om mensen met een gezichtsvelddefect tijdens hun revalidatie te ondersteunen? Dit zou de revalidatie namelijk kunnen verbeteren.

Mensen met een gezichtsvelddefect leren in de revalidatie om voor hun gezichtsvelddefect te compenseren door het maken van een bepaalde kijkritme. Deelnemers die een VR-headset of een mobiele (op het hoofd gemonteerde) eyetracker uitprobeerden tijdens verschillende mobiliteitsoefeningen hadden een positieve ervaring en zagen voordelen van het gebruik van deze technologieën. Dat gold ook zo voor de ergotherapeuten.

Door bijvoorbeeld eye-tracking te gebruiken, kan de ergotherapeut video's van het kijkgedrag gemaakt tijdens een oefening aan een cliënt laten zien, wat het makkelijker maakt om feedback te geven.

Samenvattend heb ik gevonden dat oogbewegingen gebruikt kunnen worden om op een heel eenvoudige manier de aanwezigheid van een gezichtsvelddefect vast te stellen. Daarnaast kunnen ze ook worden gebruikt om voor een gezichtsvelddefect te compenseren. In de revalidatie kunnen opnames van de oogbewegingen helpen bij het aanleren van juiste compenserende scanpatronen.

Zusammenfassung

Ein intaktes peripheres Sehen ist erforderlich, um unsere visuelle Aufmerksamkeit und anschlieSSend unsere Augenbewegungen auf relevante Teile der visuellen Umgebung zu lenken. Menschen mit einem Gesichtsfelddefekt leiden unter verminderter Sensibilität oder sogar vollständiger Erblindung in Teilen des Gesichtsfeldes. Zwei häufige Ursachen für Gesichtsfeldausfälle sind das Glaukom, eine neurodegenerative Erkrankung, bei der das periphere Sehen aufgrund einer Schädigung des Sehnervs langsam nachlässt, und die homonyme Hemianopsie (HH), Blindheit in einer Hälfte des Gesichtsfeldes, die durch eine Schädigung des Sehnervs verursacht wird Sehbahnen nach dem Chiasma opticum. In dieser Arbeit bin ich zwei Fragen nachgegangen. Die erste Frage war, ob wir Gesichtsfelddefekte anhand von Augenbewegungen erkennen können. Dies könnte möglicherweise zu einfacheren Verfahren zum Durchführen von Gesichtsfeldmessungen führen.

Um diese Frage zu beantworten, führte ich als erster eine Studie durch, in der Teilnehmer mit und ohne simulierten Gesichtsfelddefekten kurze Filmclips sahen, während ihre Augenbewegungen gemessen wurden. Mit maschinellem Lernen und statistischen Methoden habe ich die räumliche Verteilung der Augenbewegungen über den Präsentationsbildschirm und das Sichtfeld bestimmt. Mit diesen Methoden konnte ich genau vorhersagen, ob ein Videoclip von jemandem mit simuliertem Gesichtsfelddefekten oder normalem Sehvermögen angesehen wurde. Auch die GröSSe und Lage des simulierten Gesichtsfelddefekts konnte ich rekonstruieren. Ich habe dann untersucht, ob die gleichen Methoden dafür geeignet sind, dies bei Teilnehmern mit einem echten Gesichtsfelddefekt zu tun. Darüber hinaus habe ich auch den Einfluss des ein- oder zweiäugigen Sehens

und des Inhalts der Filmausschnitte auf die Trennbarkeit von Teilnehmern mit und ohne Gesichtsfelddefekte untersucht. Beim Betrachten der Filmsequenzen mit einem Auge fand ich fundamentale Unterschiede im Sehverhalten von Teilnehmern mit und ohne Gesichtsfelddefekt. Dies war nicht der Fall, wenn die Teilnehmer die Filmausschnitte mit zwei Augen betrachteten. In diesem Fall schienen sie ihren Gesichtsfelddefekt kompensieren zu können und sahen sich die Filme ähnlich wie die Kontrollteilnehmer ohne Gesichtsfelddefekt an. AuSSerdem stellte ich fest, dass der Inhalt der Videoclips den Unterschied im Sehverhalten zwischen den beiden Gruppen beeinflusst.

Meine zweite Frage war, ob wir Menschen mit Gesichtsfelddefekten mit Virtual Reality und Eyetracking bei ihrer Rehabilitation unterstützen können, da dies die Rehabilitation verbessern könnte. Menschen mit einem Gesichtsfelddefekt lernen in der Rehabilitation, ihren Gesichtsfelddefekt durch einen bestimmte Augenbewegungsmuster auszugleichen. Teilnehmer, die bei verschiedenen Mobilitätsübungen ein VR-Headset oder einen mobilen (am Kopf angebrachten) Eyetracker ausprobierten, empfanden diese Erfahrung positiv und sahen den Nutzen des Einsatzes dieser Technologien. Gleiches galt für die Ergotherapeuten.

Durch Eyetracking kann der Ergotherapeut beispielsweise einem Klienten Videos des Sehverhaltens zeigen, die er während einer Übung aufgenommen hat, was die Rückmeldung erleichtert.

Zusammenfassend habe ich festgestellt, dass durch Augenbewegungen auf sehr einfache Weise das Vorliegen eines Gesichtsfelddefekts festgestellt werden kann. Darüber hinaus können sie auch zum Ausgleich eines Gesichtsfelddefekts verwendet werden. In der Rehabilitation können Aufzeichnungen der Augenbewegungen helfen, korrekte kompensatorische Augenbewegungsmuster zu lernen.

Acknowledgements

I am extremely grateful for all the people, who supported me during this journey towards a PhD thesis.

First of all I would like to thank my supervisors for their guidance, support and encouragement. Frans, you supervised the process of my PhD research with a lot of patience and gave me a lot of freedom to explore different ideas, which was great to become an independent researcher. Apart from that, this thesis would never have been finished without your knowledge in visual and computational neuroscience and your help with manuscript writing.

Jan-Bernard, thank you for helping to transform vague ideas into concrete analysis steps and eventually Matlab code. You always inspired me to try new methods and helped me find solutions whenever I got stuck.

Nomdo, I learned a lot about ophthalmology in general, and glaucoma and visual field defects in particular from you. Thank you for providing the clinical perspective for this thesis.

A special thanks to all the participants, who took part in the different studies and showed a lot of patience during data collection.

I would like to thank the reading committee Prof. Joost Heutink, Prof. Peter Koenig, Prof. David Crabb for their helpful comments and their time.

The colleagues at the NIC for a friendly work environment, excursions to the bouldering

hall and Christmas celebrations. A special thanks to my colleagues at the experimental ophthalmology lab (Azzura, Shereif, Ale, Joana, Hinke, Rijul, Sang Yi, Sandra, Barbara). It was a pleasure to work with you! Remco, thank you for finding time to meet in your very busy schedule. Your comments and questions always helped a lot.

Many thanks to all the EGRETErs! It was a special privilege to have such a great network of people with different expertise, sharing knowledge and inspiring each other, as a PhD student. A special thanks to all the EGRET fellows in Groningen (Anna, Allison, Asterios, Catarina Georgia, Iris, Konstantinos, Lorenzo, Nigus, Sina, Tuomas, Valeria) and abroad (Stephen, Daniel Gokul, Jaqueline, Jeferson, Khaldoon, Phillip, Sandra, Vincenzo). I am sure my PhD experience would have been quite dull without the conferences, parties and excursions that we shared.

Hinke and Kim thank you for preventing us from running around like headless chickens and the organization of the amazing workshops. Kim, thank you for providing assistance with ophthalmological testing at the clinic and taking calls from participants.

Thank you to the people I got to work with during my internships at Koninklijke Visio in Haren and the Donders Institute in Nijmegen. Birgit, thanks to you I learned about vision rehabilitation therapy and practical applications for my research, that I was completely unaware of before my internship at Visio. Christian, thank you for contributing the technical expertise. Gera, Anne and Jan, it was great to have you as my research collaborators and to write a paper with you.

Jeroen, thank you for being such a dedicated supervisor, explaining the eye tracker and searching for bugs in my code. Annemiek, I was impressed by your work of building an eye tracker from scratch.

Muddi und Vaddi, danke dass ihr mich immer unterstuetzt habt und mich ermutigt habt, meinen Weg zu gehen. Maddin, es freut mich dass du dir an mir ein Vorbild nimmst. Tim, zonder jouw was het laatste jaar van mijn PhD waarschijnlijk ook mijn zwaarste tijd in Groningen geweest. Maar met jou was het de leukste tijd. Dank je voor je steun en optimisme in elke situatie.

Curriculum Vitae

Birte Gestefeld was born on December 10, 1988 in Bremen, Germany. In 2009 she started studying Cognitive Science at the University of Osnabrueck. During her Bachelor she did an internship at the University of Vienna developing a Psychophysics experiment for an automated testing device for pigeons. During her Masters she specialized in computational and visual Neuroscience and performed research for her Master thesis at Monash University in Melbourne. At Monash she researched how high gamma power modulations in intracranial EEG data reflect the perceptual state of humans during a continuous flash suppression experiment.

In 2016 she started her PhD in Experimental Ophthalmology at the University Medical Center Groningen under the supervision of Prof. Frans Cornelissen and Prof. Nomdo Jansonius. In March 2021 Birte joined the Neuro-Cognitive Psychology group at the University of Bielefeld as post-doctoral researcher. She is working on the KogniEye project aiming to use different eye movement tasks to differentiate between patients with neurological problems from controls.